

# Variational Study of Fermionic and Bosonic Systems with Non-Gaussian States: Theory and Applications

Tao Shi<sup>1</sup>, Eugene Demler<sup>2</sup>, and J. Ignacio Cirac<sup>1</sup>

<sup>1</sup>*Max-Planck-Institut für Quantenoptik, Hans-Kopfermann-Strasse. 1, 85748 Garching, Germany*

<sup>2</sup>*Department of Physics, Harvard University, 17 Oxford st., Cambridge, MA 02138*

(Dated: July 20, 2017)

We present a new variational method for investigating the ground state and out of equilibrium dynamics of quantum many-body bosonic and fermionic systems. Our approach is based on constructing variational wavefunctions which extend Gaussian states by including generalized canonical transformations between the fields. The key advantage of such states compared to simple Gaussian states is presence of non-factorizable correlations and the possibility of describing states with strong entanglement between particles. In contrast to the commonly used canonical transformations, such as the polaron or Lang-Firsov transformations, we allow parameters of the transformations to be time dependent, which extends their regions of applicability. We derive equations of motion for the parameters characterizing the states both in real and imaginary time using the differential structure of the variational manifold. The ground state can be found by following the imaginary time evolution until it converges to a steady state. Collective excitations in the system can be obtained by linearizing the real-time equations of motion in the vicinity of the imaginary time steady-state solution. Our formalism allows us not only to determine the energy spectrum of quasiparticles and their lifetime, but to obtain the complete spectral functions and to explore far out of equilibrium dynamics such as coherent evolution following a quantum quench. We illustrate and benchmark this framework with several examples: a single polaron in the Holstein and Su-Schrieffer-Heeger models, non-equilibrium dynamics in the spin-boson and Kondo models, the superconducting to charge density wave phase transitions in the Holstein model.

## I. INTRODUCTION

Many areas of physics face their greatest challenges in understanding quantum many-body systems in and out of equilibrium. This includes quark confinement in QCD, non-equilibrium superfluidity in neutron stars, and strongly correlated electron systems in condensed matter physics. Many powerful techniques have been developed to analyze strongly correlated many-body systems, including path integral approach and Feynman diagrams, effective field theories, large- $N$  expansion, and renormalization group approach. These methods have been successfully applied to a broad range of problems, but in many cases the mathematical complexity of the theoretical techniques makes it difficult to see clearly the underlying physical phenomena. Hence variational solutions, which allow to unveil fundamental physical mechanisms with relatively simple wavefunctions, have always been considered particularly valuable. Variational wavefunctions have been successfully applied to understand such important physical phenomena as Bose-Einstein condensation (BEC) [1, 2], Superconductivity (SC) [3], Superfluidity [4], Quantum Magnetism [89], and the Integer [5] and Fractional [6, 7] Quantum Hall effect (IQHE and FQHE). Remarkably variational wavefunctions made it possible to understand not only the ground state properties of these systems but in many cases also their out of equilibrium dynamics. Choosing appropriate variational states is a delicate issue however: on the one hand, they should be sufficiently general to reveal fundamental physical properties, on the other hand, their structure should be simple enough that one can efficiently perform many-

body computations. This last point strongly restricts the set of states one can use, as in general the determination of physical properties starting from a wavefunction requires resources (computation time / memory) that increase exponentially with the number of constituents.

Gaussian states [8] constitute one of the most successful variational families. They are given by the exponentials of quadratic functionals of creation and annihilation operators of the original fields, and are defined for both bosonic and fermionic systems. They are characterized by  $O(N^2)$  parameters, where  $N$  is the number of modes, although in the presence of symmetries (e.g. translational invariance) this number can be dramatically reduced. For Gaussian states the expectation values of physical observables can be efficiently computed as they obey Wick's theorem [9], which allows one to reexpress expectation values of an arbitrary product of mode operators in terms of products of pairs. The Gross-Pitaevski equation [1, 2, 10] describing BEC and the dynamics of the condensate is based on a Gaussian wavefunction that is an exponential of linear functions of mode operators. Gaussian states form the basis of the BCS theory of SC and have been applied not only to describe the ground state but also to understand the nature of the phase transition into the broken symmetry phase as well as the non-equilibrium dynamics of the order parameter [12–14]. Gaussian variational techniques can be applied to spin models by transforming them to bosonic or fermionic systems using Holstein-Primakoff [15], Jordan-Wigner (Schwinger) [16, 17], or the slave boson (fermion) transformation [18]. This makes it possible to investigate phenomena such as (anti-) ferromagnetism, para-

and dia-magnetism. Furthermore, the linearization of time-dependent equations of motion around the Gaussian state approximating the BCS ground state gives rise to the Bogoliubov-de Gennes theory for the low energy excitations, which can be used to describe a large variety of phenomena in superconductors.

While the Gaussian approach has been successful in describing a broad range of problems, it also has some important limitations. For example, starting with a model of interacting electrons and phonons it is not possible to use directly a Gaussian state of electrons and phonons to describe the BCS type superconducting state. The Gaussian state is factorizable between the electron and phonon degrees of freedom and can not describe correlations between electrons and phonons, crucial for understanding phonon induced attraction between electrons. Only after integrating out the phonons to obtain a model with explicit electron-electron attraction one can introduce a familiar BCS type wavefunction. Another important class of systems which can not be described directly with Gaussian states are Luttinger liquids of interacting fermions in one dimension. One needs to perform a bosonization, which can be understood as introducing collective bosonic degrees of freedom, which then makes it possible to represent the ground state as a bosonic Gaussian state. The list of important beyond-Gaussian states goes much longer and includes FQHE systems, the Kondo model and spin-boson systems [19], and ultracold fermions close to unitarity in the BCS-BEC crossover regime [20–23]. In all these cases, Gaussian states can not be used directly to describe these paradigmatic many-body systems because they do not contain sufficient entanglement between constituent particles. This is particularly striking in the case of boson-fermion mixtures (either in cold atoms or in the context of electron-phonon systems), where the Gaussian state is a product of bosonic and fermionic wavefunctions.

The primary goal of the current paper is to introduce a broad class of variational wavefunctions, which exhibit strong entanglement between different microscopic degrees of freedom, yet retain most of the simplicity of Gaussian wavefunctions. In short, the idea of our approach is to perform generalized canonical transformations, which introduce correlations and entanglement between particles. The nature of the appropriate transformations depends on the system at hand, but the general form is inspired by canonical transformations in condensed matter physics, including polaron transformations in electron-phonon systems and flux attachment in FQHE. After performing the transformation we introduce generalized Gaussian states. An important new feature of our wavefunctions, which makes them different from all earlier work, is that we treat the parameters of both the original unitary transformation and the Gaussian wavefunction as variational. This gives them sufficient flexibility to describe a variety of strongly correlated many-body systems ranging from quantum impurity problems, over to electron-phonon models, and to FQHE systems. Our variational wavefunctions are well

suited to find accurate approximations to ground states, determine collective excitations, and to describe out of equilibrium dynamics for certain problems. The simple form of our variational wavefunctions makes them easy to apply to real problems. We derive the equations of motion of the variational parameters in imaginary time for calculating the ground state, and in real time for describing out of equilibrium dynamics. Expectation values of physical observables can also be easily computed. We demonstrate the viability of our approach by applying it to several concrete examples. We analyze the single-polaron problem in electron-phonon systems described by the Holstein and Su-Schrieffer-Heeger (SSH) models, and show that the ansatz accurately describes all of the known physical phenomena. We analyze the spin-boson model (which is directly related to the Kondo model), and show that our ansatz provides an improvement over methods that have been previously used in the literature [24–26]. In particular we describe the non-equilibrium quench dynamics of the Kondo impurity spin in the ferromagnetic regime with easy plane anisotropy. We demonstrate the existence of finite time crossovers in the dynamics which are consistent with the equilibrium renormalization group flow. To our knowledge, non equilibrium dynamics of the Kondo problem in this regime has not been studied previously. Compared to the usual antiferromagnetic or SU(2) symmetric ferromagnetic cases this regime requires analyzing the coherent evolution over longer times, which makes it very challenging to conventional numerical techniques such as the numerical renormalization group (NRG) calculation [27]. Finally, we analyze the SC-charge density wave (CDW) phase transition in the Holstein model. We also comment on possible applications of our formalism to FQHE systems and Luttinger liquids.

This paper is organized as follows. We begin by presenting a general methodology for studying quantum many-body systems using variational wavefunctions in Sec. II. The key element of our method is understanding the differential structure of the variational manifold [28]. In order to describe the ground state, we derive a set of differential equations for the variational parameters. They correspond to the projection of the evolution in imaginary time onto the variational manifold, which ensures that the energy is a monotonically decreasing function of time. We use a similar technique to describe the real-time evolution, which ensures the conservation of energy (in time-independent problems) and other constants of motion. To find the ground state one needs to solve the equations of motion in imaginary time until the system reaches a fixed point. By linearizing the equations of motion around the fixed point of the imaginary time evolution, we derive a set of equations that describe the low-energy excitations of the theory projected onto the tangent plane of the variational manifold, so that response and spectral functions can be computed. This extends the standard Bogoliubov technique to the more general families of variational states.

To make the presentation more accessible, we first illustrate the method based on projected equations of motion in the simple case of Gaussian states. We then introduce canonical transformations to obtain non-Gaussian states and show how they can be analyzed using projected equations of motion. The first class of states that we consider is inspired by the flux attachment idea in the FQHE systems [29–31]. It can be used to describe composite fermions [32] in FQHE, fragmented condensates [33, 34], and entangles boson-fermion mixtures in ultracold atoms.

In Sec. III, we use a non-Gaussian family inspired by the Lee-Low-Pines (LLP) transformation [35], and benchmark the variational approach with a single polaron problem in electron-phonon interacting systems. We analyze the polaron dispersion in the SSH model using imaginary time evolution and demonstrate that our approach correctly describes the phase transition in which the minimum of the dispersion moves from zero to finite momentum [36]. We also use the real-time evolution method in combination with the Wei-Norman algebra method (Appendix G) to determine the single polaron spectral function.

In Sec. IV, we apply our method to the ground state and real-time dynamics of the spin-boson (Kondo) model. We employ two non-Gaussian families motivated by the parity conservation and polaron transformations [24, 37]. In contrast to previous approaches [24, 25] our wavefunctions are constructed using general Gaussian states, and thus include squeezing as well as displacement of the bosonic bath modes. This gives us a better value of spin magnetization in the ground state in comparison to the Silbey-type transformation approach [24]. Our results are in excellent agreement with the results of the NRG calculations [27]. Furthermore, we study the spin relaxation and the dynamics of the bath degrees of freedoms in several regimes of the Kondo model, and point out a correspondence between nonequilibrium coherent dynamics and renormalization group flows for equilibrium systems.

In Sec. V, we consider a family of non-Gaussian states inspired by the polaron transformation and apply the variational principle to study the transition between the SC and CDW phases in the Holstein model. In agreement with earlier studies we find that the transition takes place at half-filling. We determine the SC and CDW order parameters, the density distributions of the electrons, the displacements and covariances of phonon modes in both phases.

In Sec. VI, we summarize our results and discuss promising directions for future studies.

## II. NON-GAUSSIAN STATE APPROACH

In this section we develop a variational theory to describe the ground state and dynamics of a many-body system composed of bosons, fermions, or both. We

consider a system that consists of  $N_b$  bosonic and  $N_f$  fermionic modes. The modes are described in terms of creation and annihilation operators,  $b_j, b_j^\dagger$  ( $j = 1, \dots, N_b$ ) for the bosons, and  $c_j, c_j^\dagger$  ( $j = 1, \dots, N_f$ ) for the fermions. These operators fulfill canonical commutation and anti-commutation relations, respectively. We will use  $n_j^b = b_j^\dagger b_j$  and  $n_j^f = c_j^\dagger c_j$  to denote the corresponding number operators. We will find it convenient to use the quadrature operators,  $x_j = b_j + b_j^\dagger$ ,  $p_j = i(b_j^\dagger - b_j)$  for the bosons, and the Majorana operators,  $a_{1,j} = c_j^\dagger + c_j$ ,  $a_{2,j} = i(c_j^\dagger - c_j)$  for the fermions, where the (anti-) commutation relations are  $[x_i, p_j] = 2i\delta_{ij}$  and  $\{a_{\alpha,i}, a_{\beta,j}\} = 2\delta_{\alpha\beta}\delta_{ij}$ , and  $\{\dots\}$  denotes the anti-commutator. In order to shorten the notation we will collect these operators in column vectors,

$$\begin{aligned} R &= (x_1, \dots, x_{N_b}, p_1, \dots, p_{N_b})^T, \\ C &= (c_1, \dots, c_{N_f}, c_1^\dagger, \dots, c_{N_f}^\dagger)^T, \\ A &= (a_{1,1}, \dots, a_{1,N_f}, a_{2,1}, \dots, a_{2,N_f})^T, \end{aligned} \quad (1a)$$

where  $T$  denotes the transpose. We will denote by  $|0\rangle$  the vacuum state, i.e. the state that fulfills  $b_j|0\rangle = c_j|0\rangle = 0$ .

We assume that dynamics of the system is described by the Hamiltonian  $H$  and coupling to external reservoirs can be neglected. Our goal is to find variational approximations to the wavefunction and energy of the ground state of this Hamiltonian, as well as efficient description of the system dynamics. We consider a family of states,  $|\Psi(\xi)\rangle$ , where  $\xi$  is a short-hand notation for  $\xi_1, \xi_2, \dots$ , the set of variational parameters. We will assume that all the states in the family are normalized, i.e.,

$$\langle \Psi(\xi) | \Psi(\xi) \rangle = 1 \quad (2)$$

for all possible values of the variational parameters  $\xi$ . Thus, the goal is to find  $\xi_G$  or  $\xi(t)$  such that the corresponding state in the family approximates the ground state or its dynamics, respectively. In the following we will use the variational principle to derive a set of differential equations that will allow us to solve these problems. Once the approximation to the ground state is found, we can linearize the equations of motion around this state and obtain low energy excitations.

We begin by summarizing basic features of the generalized Gaussian states,  $|\Psi_{GS}\rangle$ . They are defined as states that can be written as exponentials of up to 2-degree polynomials of bosonic mode operators (note that this includes linear terms), as well as quadratic fermionic mode operators, acting on the vacuum. By construction such states are factorizable between fermions and bosons and therefore contain no correlations between the two types of particles. Furthermore, the correlation functions fulfill the conditions of Wick's theorem: all correlation functions can be reduced to combinations of the products of one- and two- point correlation functions. Intrinsic limitations of the Gaussian wavefunctions strongly constrain us in the type of states that we can describe with them.

To avoid these limitations we consider a more general family of wavefunctions

$$|\Psi_{\text{NGS}}\rangle = U_S |\Psi_{\text{GS}}\rangle, \quad (3)$$

Here  $U_S$  is a unitary operator, which we will refer to as generalized canonical transformation. This operator depends on a set of variational parameters and its primary role is to introduce entanglement between different fields, in particular between bosons and fermions. Transformation (3) allows us to construct states which are no longer constrained by the Wick's theorem. A practical consideration for the choice of  $U_S$  is that we should be able to apply variational principle on this state in an efficient way. Most importantly we want to circumvent the exponential dependence of the computational resources on the number of particles  $N_{b,f}$  present in common numerical approaches such as exact diagonalization.

This Section is divided into four subsections. In the first one we will review variational principle for both imaginary and real time dynamics. The former can be used to find the lowest energy state within a family of variational states. We discuss how to analyze fluctuations around the variational ground state, thus providing a generalization of the Bogoliubov-de Gennes theory. Section II B reviews application of this general technique in the simple case of Gaussian wavefunctions. While most of these results have been obtained in the literature before, we provide this discussion in order to make the paper self-contained and to set the stage for subsequent analysis of non-Gaussian states. In Sec. II C, we construct several families of non-Gaussian states, and show that time-dependent variational method can be efficiently applied to these states as well. In the last Section we will summarize the procedure which one needs to follow in order to apply analysis based on non-Gaussian wavefunctions to a specific problem.

### A. Time-dependent variational principle

In this subsection, we review the time-dependent variational principle [28] that will be used throughout the paper. At each infinitesimal time-step we project the evolution of the wavefunction onto the subspace tangent to the manifold defining the variational family of states. While this method is standard for describing the evolution in real time, we also consider imaginary-time evolution as a way of obtaining a variational approximation to the ground state within the family  $|\Psi(\xi)\rangle$ . At the end of the subsection we will also derive equations that approximate the low energy dynamics around the variational ground state. This procedure allows us to obtain elementary excitations around the ground state.

#### 1. Imaginary-time evolution

Here we derive a set of differential equations for finding an approximation to the ground state within the family of variational states  $|\Psi(\xi)\rangle$ . We first remind the readers that outside of variational techniques a common approach to finding the ground state is to start with some initial state  $|\varphi(0)\rangle$  and follow the imaginary time evolution according to

$$|\varphi(\tau)\rangle = \frac{e^{-H\tau} |\varphi(0)\rangle}{\sqrt{\langle\varphi(0)| e^{-2H\tau} |\varphi(0)\rangle}}. \quad (4)$$

As long as there is a non-vanishing overlap of  $|\varphi(0)\rangle$  with the ground state of  $H$  and one can accurately compute the evolution of the wavefunction  $e^{-H\tau} |\varphi(0)\rangle$ , the ground state will be obtained from Eq. (4) in the limit  $\tau \rightarrow \infty$ . We follow a similar strategy for variational states and implement the imaginary time evolution within a restricted set of states. Our goal is to find the lowest energy state in the variational ansatz that we consider. From Eq. (4) it follows that  $|\varphi(\tau)\rangle$  fulfills

$$d_\tau |\varphi(\tau)\rangle = -(H - \langle H \rangle) |\varphi(\tau)\rangle, \quad (5)$$

where  $\langle H \rangle = \langle \varphi(\tau) | H | \varphi(\tau) \rangle$ , and  $d_\tau$  is a shorthand notation for the derivative with respect to  $\tau$ .

In the variational approach we need to project Eq. (4) at every time-step onto the tangent plane (with respect to the family of states' manifold). Details of the derivation are given in Appendix A and here we only present the final result

$$d_\tau \xi_i = \sum_{j=1} \mathbf{G}_{ij}^{-1} \langle \Psi_j | \mathbf{R}_\Psi \rangle \quad (6)$$

for the variational parameters  $\xi_i$ . The Gram matrix  $\mathbf{G}$  has elements

$$\mathbf{G}_{ij} = \langle \Psi_i | \Psi_j \rangle, \quad (7)$$

where  $|\Psi_j\rangle = \partial_{\xi_j} |\Psi(\xi)\rangle$  span the tangent plane of the variational state manifold at  $\xi$ , which is a subspace of the full many-body Hilbert space. The vector  $|\mathbf{R}_\Psi\rangle = -(H - E) |\Psi(\xi)\rangle$ , where

$$E = \langle \Psi(\xi) | H | \Psi(\xi) \rangle \quad (8)$$

is the mean energy of the state  $|\Psi(\xi)\rangle$ .

In deriving Eq. (6) we assumed that the Gram matrix is invertible, namely, the vectors  $\Psi_i$  spanning the tangent plane are linearly independent. If this is not the case, one can make  $\mathbf{G}$  invertible by keeping some of the parameters fixed. In Appendix A we show that, since states in the family are normalized,

$$d_\tau E = -2 \langle \mathbf{R}_\Psi | \mathbf{P}_\xi | \mathbf{R}_\Psi \rangle \leq 0, \quad (9)$$

where  $\mathbf{P}_\xi$  is the projector onto the tangent plane. Thus, the energy  $E$  monotonically decreases and reaches a minimum in the limit  $\tau \rightarrow \infty$ . We will denote by

$$|\Psi_G\rangle = \lim_{\tau \rightarrow \infty} |\Psi(\xi(\tau))\rangle, \quad (10)$$

the variational state obtained in that limit, which we expect to approximate the ground state, and by  $\xi_G = \lim_{\tau \rightarrow \infty} \xi(\tau)$ , the corresponding variational parameters [38]. The value of  $\langle \mathbf{R}_\Psi | \mathbf{R}_\Psi \rangle$  is then the variance of the energy, which should be small if the state we reach is close to the ground state. Thus, this quantity can be used to estimate the accuracy of the variational family.

We remind the readers that the system may have several local minimum, with different basins of attractions in the imaginary time flow. They may correspond, for example, to different types of symmetry breaking. Depending on the initial choice of  $|\varphi(0)\rangle$  the long time limit of imaginary time evolution may be a local minimum, which is not the global minimum. To find the ground state one needs to compare energies of different stable points and identify the global minimum. Local minima that are not global minima of the energy may be interesting in their own right, e.g., near a first order phase transition when the system may be "stuck" in a metastable state.

### 2. Real-time evolution

We can use a similar procedure to approximate the real-time dynamics. We obtain Eq. (6), but now  $|\mathbf{R}_\Psi\rangle = -iH|\Psi(\xi)\rangle$  and the derivative is taken with respect to the real time,  $t$ , instead of  $\tau$ . It follows that

$$d_t E = \langle \Psi(\xi) | d_t H | \Psi(\xi) \rangle \equiv \langle d_t H \rangle \quad (11)$$

for  $E$  defined in Eq. (8). When  $H$  is time-independent, Eq. (11) implies energy conservation,  $d_t E = 0$ . In fact, it is well known [28] that the evolution given by this time-dependent variational principle is symplectic: for any operator  $O$  that satisfies  $[O, H] = 0$ , the expectation value  $\langle O \rangle_\xi = \langle \Psi(\xi) | O | \Psi(\xi) \rangle$  is conserved by Eq. (6), i.e.,  $d_t \langle O \rangle_\xi = 0$ . In addition, as we show in Appendix A, the real-time evolution of the variational ground state  $|\Psi_G\rangle$  given in (10) is

$$|\Psi_G(t)\rangle = e^{-iE_G t} |\Psi_G\rangle, \quad (12)$$

where  $E_G = \langle \Psi_G | H | \Psi_G \rangle$  is the ground state energy.

### 3. Fluctuations

We can use the differential Eq. (6) to study fluctuations around the variational ground state,  $|\Psi_G\rangle$ . Let us consider the evolution of the system in a state whose variational parameters are close to those of the ground state. The dynamics in this state can be described by low energy excitations in the tangent plane of  $|\Psi_G\rangle$ . In order to find the elementary excitations we linearize Eq. (6) around the equilibrium positions,  $\xi_G$ ; that is,  $\xi = \xi_G + \epsilon$ , so that (see Appendix A)

$$\mathbf{G} d_t \epsilon = -i\mathbf{M}\epsilon, \quad (13)$$

where  $\mathbf{M}_{ij} = \langle \Psi_i | H | \Psi_j \rangle$ .

The motion Eq. (13) can be solved by introducing the vector  $\eta = \mathbf{G}^{1/2}\epsilon$ , where we used that  $\mathbf{G}$  is positive-definite, and thus has a positive square-root. It defines an orthonormal basis in the tangent plane and satisfies

$$d_t \eta = -i\mathbf{L}\eta, \quad (14)$$

where the hermitian matrix  $\mathbf{L} = \mathbf{G}^{-1/2}\mathbf{M}\mathbf{G}^{-1/2}$  can be viewed as the Hamiltonian projected onto the tangent subspace,  $H_{\mathbf{P}}$ , expressed in the orthonormal basis

$$|V_k\rangle = \sum_j |\Psi_j\rangle (1/\sqrt{G})_{jk}. \quad (15)$$

The eigenvalues,  $\mu^\lambda$ , and eigenvectors,  $\eta^\lambda$ , of  $\mathbf{L}$  determine the fluctuation spectrum and the nature of the excitations. The orthonormal basis of the tangent subspace  $H_{\mathbf{P}}$  is given by

$$|\Psi_{\text{ex}}^\lambda\rangle = \sum_k \eta_k^\lambda |V_k\rangle. \quad (16)$$

When discussing states in the tangent plane,  $|V_i\rangle$ , it is important to remember that they include both collective modes and single particle excitations. For Gaussian states they are closely related to the Bogoliubov excitations. Hence, this theory may be viewed as a generalization of the Bogoliubov-de Gennes equations. Equation (13) indicates that the states  $|V_i\rangle$  themselves are not eigenstates of  $H_{\mathbf{P}}$ , and thus they will hybridize in a sense that  $|V_i\rangle \rightarrow |V_j\rangle$ , with the transition amplitude

$$\mathcal{A}_{ji}(t) = \langle V_j | e^{-iH_{\mathbf{P}}t} | V_i \rangle = \sum_\lambda \eta_j^\lambda \eta_i^{\lambda*} e^{-i\mu^\lambda t}. \quad (17)$$

The spectral function of the excitation  $|V_k\rangle$  can be defined as

$$\begin{aligned} Z_k(\omega) &= -\frac{1}{\pi} \text{Im} \left[ -i \int_0^{+\infty} \mathcal{A}_{kk}(t) e^{i\omega t} dt \right] \\ &= \sum_\lambda |\eta_k^\lambda|^2 \delta(\omega - \mu^\lambda). \end{aligned} \quad (18)$$

In the thermodynamics limit when the number of variational parameters is infinite we expect to find a continuous spectrum of excitations. Peaks in  $Z_k(\omega)$  can be interpreted as describing collective modes. Positions of the peaks in  $\omega$  correspond to the collective mode energies and their widths to the inverse of the lifetimes.

### B. Gaussian states

Mean-field theory has been one of the most successful approaches for understanding quantum many-body systems. The two most important examples of this approach are the Bogoliubov theory of superfluidity of weakly interacting bosons and the BCS theory of superconductivity. At its core the mean-field theory is a variational approach which uses a family of Gaussian states  $|\Psi_{\text{GS}}\rangle$ . In

this subsection we summarize time-dependent variational approach for general Gaussian states. We point out that time-dependent Gaussian states have been discussed before to describe a broad range of dynamical phenomena [13, 39]. While results of this section can be found in earlier literature, although with a different notation and motivation, we present them here for completeness and as a simple illustration of the general time-dependent variational theory.

### 1. Definition

Gaussian states are defined as  $|\Psi_{\text{GS}}\rangle = U_{\text{GS}}|0\rangle$ , where the operators  $U_{\text{GS}}$  describes a unitary transformation

$$U_{\text{GS}} = e^{i\theta} e^{i\frac{1}{2}R^T\sigma\Delta_R} e^{-i\frac{1}{4}R^T\xi_b R} e^{i\frac{1}{4}A^T\xi_m A}. \quad (19)$$

Here,  $\theta$  is a global phase,  $\Delta_R$  is the displacement vector of bosons, and  $\xi_b$  ( $\xi_m$ ) are (anti-) symmetric matrices, which describe correlations of the bosonic (fermionic) modes. We also used the symplectic matrix

$$\sigma = \begin{pmatrix} 0 & \mathbb{1}_{N_b} \\ -\mathbb{1}_{N_b} & 0 \end{pmatrix}, \quad (20)$$

where  $\mathbb{1}_{N_b}$  is the  $N_b \times N_b$  identity matrix.

We point out that there is a gauge degree of freedom in the definition of  $U_{\text{GS}}$ , since different Gaussian transformations  $U_{\text{GS}}$  and  $U_{\text{GS}}V_{\text{GS}} \equiv \tilde{U}_{\text{GS}}$  can describe the same Gaussian state provided that  $V_{\text{GS}}|0\rangle = |0\rangle$ . The simplest choice is  $V_{\text{GS}} = e^{ib^\dagger\chi_b b} e^{ic^\dagger\chi_f c}$ , where  $\chi_b, \chi_f$  can be constructed using any Hermitian matrices. If we show that  $\tilde{U}_{\text{GS}} = U_{\text{GS}}V_{\text{GS}}$  also has a Gaussian form given by Eq. (19), but with different values of the variational parameters, i.e.,

$$\tilde{U}_{\text{GS}} = e^{i\theta} e^{i\frac{1}{2}R^T\sigma\Delta_R} e^{-i\frac{1}{4}R^T\tilde{\xi}_b R} e^{i\frac{1}{4}A^T\tilde{\xi}_m A}, \quad (21)$$

then we establish that different  $\xi_{b/m}$  can describe the same Gaussian state. To verify Eq. (21) we check the condition that  $\tilde{U}_{\text{GS}}$  and  $U_{\text{GS}}V_{\text{GS}}$  result in the same transformations of  $\delta R$  and  $A$ , i.e.,

$$\begin{aligned} \tilde{U}_{\text{GS}}^\dagger \delta R \tilde{U}_{\text{GS}} &= V_{\text{GS}}^\dagger U_{\text{GS}}^\dagger \delta R U_{\text{GS}} V_{\text{GS}}, \\ \tilde{U}_{\text{GS}}^\dagger A \tilde{U}_{\text{GS}} &= V_{\text{GS}}^\dagger U_{\text{GS}}^\dagger A U_{\text{GS}} V_{\text{GS}}, \end{aligned} \quad (22)$$

which, Eq. (22), determines  $\tilde{\xi}_{b,m}$  by the relation

$$\begin{aligned} e^{\sigma\tilde{\xi}_b} &= \frac{1}{2} e^{\sigma\xi_b} W_b \begin{pmatrix} e^{i\chi_b} & 0 \\ 0 & e^{-i\chi_b^*} \end{pmatrix} W_b^\dagger, \\ e^{i\tilde{\xi}_m} &= \frac{1}{2} e^{i\xi_m} W_m \begin{pmatrix} e^{i\chi_f} & 0 \\ 0 & e^{-i\chi_f^*} \end{pmatrix} W_m^\dagger. \end{aligned} \quad (23)$$

Here, the matrix

$$W_b = \begin{pmatrix} \mathbb{1}_{N_b} & \mathbb{1}_{N_b} \\ -i\mathbb{1}_{N_b} & i\mathbb{1}_{N_b} \end{pmatrix} \quad (24)$$

relates  $R$  and  $B = (b_{j=1,\dots,N_b}, b_{j=1,\dots,N_b}^\dagger)^T$  by  $R = W_b B$ , and

$$W_m = \begin{pmatrix} \mathbb{1}_{N_f} & \mathbb{1}_{N_f} \\ -i\mathbb{1}_{N_f} & i\mathbb{1}_{N_f} \end{pmatrix} \quad (25)$$

relates  $A$  and  $C$  by  $A = W_m C$ .

The transformations  $U_{\text{GS}}$  and  $\tilde{U}_{\text{GS}}$  related by the unitary transformation  $V_{\text{GS}}$  define an equivalent class  $\{U_{\text{GS}}\}$ , and the transformations in each class give the same Gaussian state. As a result, there is some redundancy in the variational parameters  $\xi_{b,m}$ . Instead of using the elements  $\xi_{b,m}$  as variational parameter, it is more convenient to use the covariant matrices (defined below) instead. For each equivalent class  $\{U_{\text{GS}}\}$  the covariant matrices are uniquely defined (note that  $\Delta_R$  is also defined unambiguously).

For bosons, Gaussian states are completely characterized by the displacement vector  $\Delta_R$ , and the covariant matrix  $\Gamma_b$  for the fluctuations  $\delta R = R - \Delta_R$ , defined as

$$\Delta_{Ri} = \langle \Psi_{\text{GS}} | R_i | \Psi_{\text{GS}} \rangle, \quad (26a)$$

$$(\Gamma_b)_{ij} = \frac{1}{2} \langle \Psi_{\text{GS}} | \{\delta R_i, \delta R_j\} | \Psi_{\text{GS}} \rangle, \quad (26b)$$

where both of them take real values. Under the Gaussian state transformation  $U_{\text{GS}}$ , the quadrature transforms as  $U_{\text{GS}}^\dagger R_i U_{\text{GS}} = (\Delta_R)_i + (S_b R)_i$ , where the Baker-Campbell-Hausdorff (BCH) formula has been used, and the symplectic matrix  $S_b = e^{\sigma\xi_b}$  fulfills  $S_b \sigma S_b^T = \sigma$ . The symmetric covariance matrix  $\Gamma_b$  fulfills

$$\Gamma_b = S_b S_b^T \quad (27)$$

for pure states, as it is the case here.

In the Gaussian state  $|\Psi_{\text{GS}}\rangle$  fermions are characterized by the covariance matrix

$$(\Gamma_m)_{ij} = \frac{i}{2} \langle \Psi_{\text{GS}} | [A_i, A_j] | \Psi_{\text{GS}} \rangle. \quad (28)$$

This matrix is real and anti-symmetric, and for pure states it fulfills  $\Gamma_m^2 = -\mathbb{1}$ . By BCH formula, the Majorana operator transform as  $U_{\text{GS}}^\dagger A_i U_{\text{GS}} = (U_m A)_i$ , where  $U_m = e^{i\xi_m}$ . Since  $\xi_m$  is an anti-symmetric Hermitian matrix,  $U_m$  is an orthogonal matrix. The covariance matrix is related to  $U_m$  through  $\Gamma_m = -U_m \sigma U_m^T$ . Sometimes it is more convenient to use the original creation and annihilation operators, and define

$$\Gamma_f \equiv \langle \Psi_{\text{GS}} | C C^\dagger | \Psi_{\text{GS}} \rangle = \frac{1}{2} \mathbb{1}_{2N_f} - i \frac{1}{4} W_m^\dagger \Gamma_m W_m. \quad (29)$$

Wick's theorem can be applied to all Gaussian states, so that higher order correlations can be expressed in terms of the displacement vector and the covariant matrices. Note that Eq. (19) does not introduce any correlation between the bosons and the fermions, so that  $|\Psi_{\text{GS}}\rangle$  is a product state between bosons and fermions.

## 2. Variational principle

It is convenient to take the elements of  $\Delta_R$  and  $\Gamma_{b,m}$  as variational parameters. We do not provide a separate derivation of the equations of motion for Gaussian states but only present the final results. Readers interested in the derivation can use appendix E, in which we obtain equations of motion for a broader class of non-Gaussian states defined in Eq. (3). Gaussian states are a special case of such states with  $U_S = 1$ .

For the imaginary-time evolution we obtain

$$\begin{aligned} d_\tau \Delta_R &= -\Gamma_b h_\Delta, \\ d_\tau \Gamma_b &= \sigma^T h_b \sigma - \Gamma_b h_b \Gamma_b, \\ d_\tau \Gamma_m &= -h_m - \Gamma_m h_m \Gamma_m, \end{aligned} \quad (30)$$

and for the real-time dynamics

$$\begin{aligned} d_t \Delta_R &= \sigma h_\Delta, \\ d_t \Gamma_b &= \sigma h_b \Gamma_b - \Gamma_b h_b \sigma, \\ d_t \Gamma_m &= [h_m, \Gamma_m]. \end{aligned} \quad (31)$$

Here, the vector  $h_\Delta = 2\delta E/\delta \Delta_R$  and the matrices  $h_b = 4\delta E/\delta \Gamma_b$ ,  $h_m = 4\delta E/\delta \Gamma_m$  are determined by the functional derivatives of the mean energy,  $E = \langle H \rangle_{\text{GS}}$ , corresponding to the Gaussian state. We note that equations for  $\Gamma_m$  agree with those in Ref. [40].

Solutions of Eqs. (30) in the limit  $\tau \rightarrow \infty$  determine the Gaussian mean-field ground state. By solving Eq. (31), we can study real-time dynamics in the Gaussian state manifold. Note that in the standard mean-field (Gross-Pitaevskii) theory for bosons one uses a coherent state to describe a system in which macroscopic number of bosons occupy the same single particle state. In fact, Eq. (31) is nothing but Gross-Pitaevskii equation for the time evolution of the macroscopically occupied state. Including  $\Gamma_b$  as variational parameters one can also describe a squeezed state of bosons, which is usually introduced into the wavefunction via the Bogoliubov-de Gennes equations. Note that our approach is more general.

## 3. Fluctuations

We continue our discussion of the Gaussian states and consider fluctuations around the variational ground state. In the case of bosons, we have excitations corresponding to two different directions in the tangent plane: fluctuations obtained by taking derivatives with respect to  $\Delta_R$  and with respect to  $\Gamma_b$ . They have the form

$$|V_j^{(1)}\rangle = U_{\text{GS}} b_j^\dagger |0\rangle, \quad (32a)$$

$$|V_{ij}^{(2)}\rangle = U_{\text{GS}} b_i^\dagger b_j^\dagger |0\rangle. \quad (32b)$$

The first type describes single particle excitations, and the second one corresponds to two particle excitations.

In the case of non-interacting bosons, i.e., when the Hamiltonian  $H$  is quadratic in  $R$ , the Gram matrix  $\mathbf{G}$  in Eq. (7) does not connect the single-particle and two-particle sectors. If we denote by  $\lambda^{(1,2)}$  the eigenvalues corresponding to the two sectors and by  $\eta^{\lambda^{(1,2)}}$  the corresponding eigenvectors of the matrix  $\mathbf{L}$  [see Eq. (14)], we will have that for each  $\lambda^{(2)}$  there will exist two  $\lambda^{(1)}$  with  $\lambda_{i,j}^{(2)} = \lambda_i^{(1)} + \lambda_j^{(1)}$ , and  $\eta_{i,j}^{\lambda^{(2)}}$ , when considered as a matrix, will have just one non-trivial singular value in its singular value decomposition. This tells us that quasiparticles do not interact and the energy of two quasiparticles is the sum of individual energies. In the presence of interactions we expect that the matrix  $\mathbf{L}$  connects the two sectors, giving rise to a decay of the single particle excitations into two particles, something that can be characterized in terms of Eq. (18). For example, such process can describe a decay of one Higgs amplitude excitation in a strongly correlated superfluid state into a pair of Goldstone modes [see e.g., [41]]. The form of the eigenvectors  $\eta^{\lambda^{(2)}}$  describes the nature of interactions between the two types of fluctuations in Eqs. (32a) and (32b).

For Fermions we only have two-particle excitations

$$|V_{ij}^{(2)}\rangle = U_{\text{GS}} c_i^\dagger c_j^\dagger |0\rangle \quad (33)$$

in the tangent space. In this case, the eigenvalues and eigenvectors of  $\eta_{i,j}^\lambda$ , when considered as a matrix, will determine the two particle excitations, e.g. particle-hole excitations around the Fermi sea. For  $N_f \gg 1$  we expect to recover the standard Bogoliubov-de Gennes theory. Note that eigenmodes in Eq. (33) also contain collective modes, such as the phase (Goldstone) and amplitude modes for superconductors, spin waves for magnetically ordered states.

## C. Non-Gaussian states

As we discussed earlier, Gaussian states are not sufficiently versatile to describe many interesting situations. In this subsection, we extend simple Gaussian states to include a richer structure of entanglement and correlations between modes, in particular entanglement between the bosonic and fermionic modes. While we cannot take very general extensions, as we need a computationally tractable description of many-body systems, we will see that we can define several broad classes of interesting states. Our main requirement is that we can compute efficiently quantities that appear in Eq. (6), i.e., the Gram matrix  $\mathbf{G}$ , the energy  $E$ ,  $\langle \Psi_j | H | \Psi(\xi) \rangle$ , as well as  $\langle \Psi(\xi) | \Psi(\xi) \rangle$  to ensure the normalization.

The main idea is to consider states of the form (3), and choose  $U_S$  such that the above quantities can be expressed as expectation values of operators taken in the Gaussian state,  $|\Psi_{\text{GS}}\rangle$ . In particular operators which we need to compute in order to solve dynamically Eq. (6) will be usually of the following types: they contain polynomials of  $R$  and  $A$ , or exponentials of some of these

polynomials. As we discuss below for several useful choices of  $U_S$  such expectation values can be reduced to those in the Gaussian states, which makes it possible to compute them efficiently.

In this subsection, we will introduce five families of Non-Gaussian states  $U_{S=1,\dots,5}$  for problems dealing with fermionic systems, bosonic systems, and Bose-Fermi mixtures.

### 1. Fermionic systems

For purely fermionic systems we define

$$\begin{aligned} U_1 &= \bar{U}_{\text{GS}} U_{\text{FA}}, \\ U_{\text{FA}} &= e^{i\frac{1}{2} \sum_{ij} \omega_{ij}^f :n_i^f n_j^f:}, \end{aligned} \quad (34)$$

where  $\bar{U}_{\text{GS}} = e^{iC^\dagger \bar{\xi}_f C/2}$  and  $: \dots :$  denotes the normal ordering with respect to the vacuum state. This transformation has two types of new variational parameters:  $\omega^f$  and  $\bar{\xi}_f$ . We remind the readers that  $U_1$  acts on the Gaussian state itself [see Eq. (3)]. So these new parameters should be considered together with  $\xi_m$  introduced in Eq. (19). Unitarity requires that  $\omega^f$  is a real symmetric matrix and  $\bar{\xi}_f$  a hermitian matrix. A useful way of understanding  $\bar{U}_{\text{GS}}$  is that it provides a transformation from the original single particle basis to localized Wannier orbitals. Then  $U_{\text{FA}}$  acts locally in space. To understand the physical meaning of  $U_{\text{FA}}$  we observe that

$$U_{\text{FA}}^\dagger c_j U_{\text{FA}} = e^{i \sum_i \omega_{ij}^f n_i^f} c_j.$$

This can be understood as a particle in the orbital  $i$  contributing a phase  $\omega_{ij}^f$  to a particle in the orbital  $j$ . Taking  $\omega_{ij}^f$  of the form  $n_v \arg(z_i - z_j)$ , where  $n_v$  is an integer even number and  $z_i = x_i + iy_i$ , we observe that this is equivalent to the flux attachment procedure in which  $n_v$ -vortices are attached to every fermion. Hence transformation (34) enables the description of FQHE systems in the spirit of composite-fermions [29–31]. While the exact form of the energetically optimal functions  $\omega_{i-j}^f$  may differ, we expect that in FQHE-like systems variational parameters  $\omega_{i-j}^f$  develop branch cuts in the 2D plane, such as  $w_{ij}^f \propto n_v \text{Im} \ln(z_i - z_j)$ . This should be contrasted to  $\omega_{ij}^f$  which are analytic functions in the 2D plane, which we expect to apply to non-topological systems with time-reversal symmetry.

### 2. Bosonic systems

For purely bosonic systems, we can define a transformation

$$U_2 = \bar{U}_{\text{GS}} \exp(i\frac{1}{2} \sum_{ij} \omega_{ij}^b :n_i^b n_j^b:), \quad (35)$$

where  $\omega^b$  is a real symmetric matrix, and  $\bar{U}_{\text{GS}} = e^{iR^T \sigma \bar{\Delta}_R/2} e^{-iR^T \bar{\xi}_b R/4}$  is defined by a real vector  $\bar{\Delta}_R$  and a real symmetric matrix  $\bar{\xi}_b$ . Similar to the fermionic case, this transformation can be used to describe the flux attachment for bosons. The FQHE of bosons, i.e., the half-filled phase in the rotating BEC systems, can be investigated using this transformation.

We also introduce a non-unitary transformation

$$U_3 = \frac{1}{\sqrt{\mathcal{N}}} e^{\lambda P} \quad (36)$$

defined by the variational parameter,  $\lambda$ , the parity operator  $P = \exp(i\pi \sum_j b_j^\dagger b_j)$ , and the normalization factor  $\mathcal{N}$ . This transformation creates superposition

$$|\Psi_{\text{NGS}}\rangle = U_3 \left| \Psi_{\text{GS}}^{(+)} \right\rangle = \sum_{s=\pm} u_s \left| \Psi_{\text{GS}}^{(s)} \right\rangle \quad (37)$$

of two Gaussian states

$$\left| \Psi_{\text{GS}}^{(s)} \right\rangle = e^{i\frac{1}{2} s R^T \sigma \Delta_R} e^{-i\frac{1}{4} R^T \xi_b R} |0\rangle, \quad (38)$$

where the amplitudes  $u_{s=\pm}$  satisfy the relation  $\tanh \lambda = u_-/u_+$ . In particular, in the limits  $\lambda \rightarrow \pm\infty$  we have states with even and odd parity, something which is not possible with Gaussian states alone. They correspond to certain types of fragmented condensates, which can be constructed as superpositions of two Gaussian states but not as a single Gaussian state. For physical applications of such states we refer the readers to Refs. [33, 34].

### 3. Bose-Fermi mixtures

For bosons interacting with fermions we define two types of transformations

$$U_4 = e^{i\frac{1}{2} C^\dagger \bar{\xi}_f C} e^{i\frac{1}{2} \sum_{ij} \omega_{ij}^f :n_i^f n_j^f:} e^{i \sum_{ij} \bar{\omega}_{ij} R_i n_j^f}, \quad (39)$$

and

$$\begin{aligned} U_5 &= e^{i\frac{1}{2} C^\dagger \bar{\xi}_f C} e^{i\frac{1}{2} R^T \sigma \bar{\Delta}_R} e^{-i\frac{1}{4} R^T \bar{\xi}_b R} \\ &\times \exp[i \sum_{ij} (\frac{1}{2} \omega_{ij}^f :n_i^f n_j^f: + \frac{1}{2} \omega_{ij}^b :n_i^b n_j^b: + \omega_{ij}^{bf} n_i^b n_j^f)], \end{aligned} \quad (40)$$

where  $\bar{\omega}$  and  $\omega^{bf}$  are real matrices.

For the special case  $\bar{\omega} = 0$ , transformation  $U_4$  reduces to  $U_1$ . For the case  $\omega^f = 0$ , transformation  $U_4$  is the polaron transformation used for describing electron-phonon systems. While in the usual treatments of polaronic phenomena in electron-phonon systems variational parameters in  $\bar{\xi}_f$  are taken as time independent, we will allow all parameters of  $U_4$  and  $U_5$  to change during the imaginary or real time evolutions. Note that  $U_4$  generates entanglement between fermions and bosons. It is characterized by the non-vanishing cubic correlations  $\langle \delta R_i A_j A_k \rangle$ . In Secs.



IV and V, we will illustrate the application of this variational polaron transformation using two concrete problems: spin-relaxation in the spin-boson model and the SC-CDW phase transition in the Holstein model.

The transformation  $U_5$  can be employed to study the quantum phases of Bose-Fermi mixtures. The entanglement properties between the bosonic and fermionic modes are characterized by the non-trivial quartic correlations  $\langle \delta R_i \delta R_j \delta R_k \delta R_l \rangle$ ,  $\langle A_i A_j A_k A_l \rangle$ , and  $\langle \delta R_i \delta R_j A_k A_l \rangle$ . For the special case  $\omega^{bf} = 0$ ,  $U_5$  reduces to  $U_1 U_2$ . A physical motivation for introducing states described by  $U_5$  with  $\omega_{bf} \neq 0$  comes from the Lee-Low-Pines (LLP) transformation [35] in impurity problems. In Sec. III we will illustrate how to apply the variational principle to the family of states obtained using Eq. (40) and study the single polaron problem in both Holstein and SSH models. Our analysis goes beyond computing the dispersion of the polaron and allows us to obtain complete spectral functions. We also discuss a single-polaron phase transition in the SSH model.

In the following we will show how one can efficiently compute quantities that appear in the time evolution described by Eq. (6) for the families of non-Gaussian states introduced in this section. Since  $U_{4,5}$  already include  $U_{1,2}$  we only need to carry out this task for  $U_{3,4,5}$ . Note that all states are normalized, since all the  $U$ s are unitary except for  $U_3$ , for which we explicitly included the normalization factor in Eq. (36).

#### 4. Efficient computations for non-Gaussian states

In order to analyze the dynamics described by Eqs. (6) for the three types of non-Gaussian states,  $U_{3,4,5} |\Psi_{\text{GS}}\rangle$ , we need to be able to compute the Gram matrix and the overlap  $\langle \Psi_j | \mathbf{R}_\Psi \rangle$ . Here, we show how to compute these quantities analytically for any Hamiltonian,  $H$ , that is a polynomial  $\text{poly}(R, C)$  in terms of  $R$  and  $C$ . We will explain the main steps in this section, and in Appendices B-D we provide a more detailed derivation.

Firstly, we show that the tangent vectors  $|\Psi_j\rangle$  can be written as

$$U_S \exp[i \sum_j (\alpha_j n_j^f + \beta_j n_j^b + \gamma_j R_j)] \text{poly}(R, C) |\Psi_{\text{GS}}\rangle. \quad (41)$$

This is obtained as follows. We write

$$\partial_\tau |\Psi_{\text{NGS}}\rangle = U_S [(\partial_\tau U_{\text{GS}}) U_{\text{GS}}^{-1} + O] U_{\text{GS}} |0\rangle, \quad (42)$$

where  $O = U_S^{-1} \partial_\tau U_S$ . In Appendix B, we prove that  $(\partial_\tau U_{\text{GS}}) U_{\text{GS}}^{-1}$  only contains constant, linear, and quadratic terms in the Bose and Fermi creation and annihilation operators, and  $O$  is the sum of operators of the form

$$\exp[i \sum_j (\alpha_j n_j^f + \beta_j n_j^b + \gamma_j R_j)] \text{poly}(R, C) \quad (43)$$

for  $U_S = U_{3,4,5}$ . As a result, the tangent vectors  $\partial_{\xi_j} |\Psi_{\text{NGS}}\rangle$  are composed of terms like those appearing in Eq. (41). Note that for the special case  $\xi_{f,b} = \bar{\Delta}_R = 0$  in  $U_{4,5}$ , the tangent vectors

$$\partial_{\xi_j} |\Psi_{\text{NGS}}\rangle = U_S \text{poly}(R, C) |\Psi_{\text{GS}}\rangle, \quad (44)$$

i.e.,  $\alpha_j = \beta_j = \gamma_j = 0$  in Eq. (41).

Secondly, we notice that the right hand side of Eq. (6) is determined by  $H(R, C) |\Psi_{\text{NGS}}\rangle$ . In Appendix B, we show that for  $U_S = U_{3,4,5}$  and the Hamiltonian  $H$  with the polynomial form  $\text{poly}(R, C)$ , the state  $H(R, C) |\Psi_{\text{NGS}}\rangle$  is also composed of terms as in Eq. (41).

Finally, the Gram matrix and the overlap  $\langle \Psi_j | \mathbf{R}_\Psi \rangle$  are determined by the expectation values

$$\left\langle e^{i \sum_j (\beta_j n_j^b + \gamma_j R_j)} \text{poly}(R) \right\rangle_{\text{GS}} \left\langle e^{i \sum_j \alpha_j n_j^f} \text{poly}(C) \right\rangle_{\text{GS}} \quad (45)$$

on the Gaussian state  $|\Psi_{\text{GS}}\rangle$ . In Appendices C and D, we show how to evaluate them analytically with the help of Gaussian techniques [42–44].

As an example, in Appendices E and F, we derive the equations of motion for  $\Delta_R$  and  $\Gamma_{b,m,f}$  characterizing the Gaussian part in the non-Gaussian state  $U_{4,5} |\Psi_{\text{GS}}\rangle$  with  $\bar{\xi}_{f,b} = \bar{\Delta}_R = 0$ , where Eqs. (30) and (31) are reproduced in the Gaussian limit  $U_S = I$ .

#### 5. Fluctuations

As the non-Gaussian states introduced here are constructed on top of the Gaussian ones, they contain the latter. Thus, among the tangent vectors there will be terms of the form

$$|V_b^{(1)}\rangle = U_S U_{\text{GS}} b_j^\dagger |0\rangle, \quad (46)$$

as well as

$$\begin{aligned} |V_b^{(2)}\rangle &= U_S U_{\text{GS}} b_i^\dagger b_j^\dagger |0\rangle, \\ |V_f^{(2)}\rangle &= U_S U_{\text{GS}} c_i^\dagger c_j^\dagger |0\rangle. \end{aligned} \quad (47a)$$

They describe single-, and two-particle excitations in the rotated frame defined by the transformation  $U_S U_{\text{GS}}$ . As before, the tangent vectors do not contain states with an odd number of fermionic excitations due to the fermionic-supersselection rule, but their properties can be studied following the approach presented after equation (49b) below (see also discussion in Appendix E).

The spectrum of  $\mathbf{L}$  gives information about quasiparticles, such as their energies, quasiparticle weight, and lifetime. All information about quasiparticles is contained in the spectral function  $Z_k(\omega)$ . The non-Gaussian character of the state is reflected in the fact that the tangent space contains states with several types of excitations, i.e., the three-particle states

$$\begin{aligned} |V_b^{(3)}\rangle &= U_S U_{\text{GS}} b_i^\dagger b_j^\dagger b_k^\dagger |0\rangle, \\ |V_{bf}^{(3)}\rangle &= U_S U_{\text{GS}} b_i^\dagger f_j^\dagger f_k^\dagger |0\rangle, \end{aligned} \quad (48a)$$

and the four-particle states

$$\begin{aligned} |V_b^{(4)}\rangle &= U_S U_{GS} b_i^\dagger b_j^\dagger b_k^\dagger b_l^\dagger |0\rangle, \\ |V_{bf}^{(4)}\rangle &= U_S U_{GS} b_i^\dagger b_j^\dagger f_k^\dagger f_l^\dagger |0\rangle, \\ |V_f^{(4)}\rangle &= U_S U_{GS} f_i^\dagger f_j^\dagger f_k^\dagger f_l^\dagger |0\rangle. \end{aligned} \quad (49a)$$

Our analysis includes interactions among all of the excitations  $|V^{(1\sim 4)}\rangle$ , which appear in the tangent space. These interactions lead to the decay of quasi-particles and collective excitations.

Finally, we can use unitaries  $U_S = U_{1,2,4,5}$ , which minimize the energy within the family of Gaussian states to define a new Hamiltonian in the rotating frame as

$$\bar{H} = U_{GS}^\dagger U_S^\dagger H U_S U_{GS}. \quad (49b)$$

We can use the quadratic expansion of  $\bar{H}$  to study fermionic quasiparticles in the ground state (the procedure for calculating  $h_{b,m}$  which define an effective quadratic Hamiltonian is presented in Appendix E). We note that we could also analyze interactions between these quasiparticles perturbatively by expanding  $\bar{H}$  beyond quadratic order and using standard field theoretical techniques, such as Green's function or the renormalization approaches [37].

#### D. Summary of Section II

In this subsection, we formalized the time dependent variational theory for several families of non-Gaussian states. This approach can be used to study the ground state and real-time dynamics of many-body systems that contain both fermions and bosons. Here, we briefly summarize the procedure:

(i) Choose the appropriate transformation  $U_S$  and use physical intuition and symmetries to set some of the parameters equal to zero.

(ii) For the selected  $U_S$ , compute analytically the Gram matrix and the overlap  $\langle \Psi_j | \mathbf{R}_\Psi \rangle$  using the methods presented in Sec. II C 4 as a function of variational parameters.

(iii) Solve differential Eq. (6) until the system reaches the steady state solution  $\xi_G$ . In this fixed point compute the variance of the energy and verify that the selected family of variational states is appropriate.

(iv) To analyze elementary excitations around the ground state use the formalism of linearized equations of motion from Sec. II A 3. This means determining and diagonalizing matrix  $\mathbf{L}$ . Properties of the single and two particle excitations can be analyzed using the effective Hamiltonian obtained from Eq. (49b) and discussion in Appendix E.

(v) Use the variational ansatz to study real time dynamics. Applicability of the considered class of wavefunctions can be estimated every step by computing the norm of  $\|(1 - \mathbf{P}_\xi) | \mathbf{R}_\Psi \rangle\|^2$ .

In the next sections we illustrate the general discussion presented in this section with several concrete examples. When possible, we will provide a comparison between our results and previously published ones to benchmark the variational methods.

### III. ANALYSIS OF POLARONS IN THE HOLSTEIN AND SU-SCHRIEFFER-HEEGER MODELS

In this section, we apply the non-Gaussian state approach developed in Sec. II to investigate the problem of an individual electron interacting with a phonon bath, the so-called polaron model. Although this type of systems has been studied in condensed matter physics for more than sixty years since the pioneering papers of Landau, Pekar, and Fröhlich, there are still many interesting not fully understood questions. We focus on the paradigmatic cases of the Holstein and Su-Schrieffer-Heeger (SSH) models. We demonstrate that variational approach gives the dispersion of the polaronic quasiparticle which is in agreement with the results of earlier studies [36, 45]. In particular, we observe that a single polaron phase transition in the SSH model [36] can be described very accurately by the non-Gaussian state when combined with the LLP transformation. Furthermore we study the real time evolution of polarons starting from a state in which an electron creation operator is applied to a phonon vacuum. This analysis allows us to extract the full spectral function of the polaron, which is difficult to obtain using the Monte Carlo approach. We will present results for the time dependent mean quadratures and the squeezing of the phonons.

The general lattice model for the electron phonon system is given by

$$\begin{aligned} H &= \sum_{nm} t_{nm} c_n^\dagger c_m + \sum_q \omega_q b_q^\dagger b_q \\ &+ \sum_{nm,q} c_n^\dagger c_m [g_{nm}(q) b_q + g_{mn}^*(-q) b_{-q}^\dagger], \end{aligned} \quad (50)$$

where  $t_{nm} \equiv t_{n-m}$  is the electron hopping amplitude between sites  $n$  and  $m$ ,  $\omega_q$  is the frequency of the phonon with momentum  $q$ , and for translationally invariant systems the electron-phonon coupling  $g_{nm}(q) = e^{iq(n+m)/2} \tilde{g}_{n-m}(q)$ . Two paradigmatic cases, the Holstein and the SSH models, describe two qualitatively different cases of electron-phonon coupling. The former corresponds to phonons coupling to the on-site energy of electrons and the latter describes phonons modulating electron tunneling, i.e.,

$$\tilde{g}_l(q) = \begin{cases} \frac{q}{\sqrt{N_b}} \delta_{l0}, & \text{Holstein model,} \\ \frac{2iq}{\sqrt{N_b}} \delta_{l,\pm 1} \sin \frac{q}{2}, & \text{SSH model.} \end{cases} \quad (51)$$

The Hamiltonian (50) conserves the total electron number  $N_e = \sum_k c_k^\dagger c_k$ . In this section we concentrate on

the single electron subspace, i.e.,  $N_e = 1$ . The Hamiltonian (50) does not conserve the phonon number. Hence even though there is only one electron in the system, many phonons may be excited either in the ground state or during real-time evolution.

To understand the character of the phonon dressing of a single electron, we perform a unitary transformation of the Hamiltonian  $H_{\text{LLP}} = U_{\text{LLP}}^\dagger H U_{\text{LLP}}$  with  $U_{\text{LLP}} = e^{-iQ_b X}$ , where  $Q_b = \sum_q q b_q^\dagger b_q$  is the total momentum operator of the phonons and  $X = \sum_n n c_n^\dagger c_n$  is the coordinate operator of the electron. The LLP transformation belongs to the class  $U_5$  introduced in Sec. II. The LLP transformation accomplishes two important goals. Firstly it separates explicitly the total conserved momentum of the system. Secondly it can be understood as going to the frame co-moving with the electron. The LLP transformed Hamiltonian is

$$H_{\text{LLP}} = \sum_k c_k^\dagger c_k \sum_\delta t_\delta e^{-i(k-Q_b)\delta} + \sum_q \omega_q b_q^\dagger b_q \quad (52) \\ + \sum_k c_k^\dagger c_k \sum_{l,q} [\tilde{g}_l(q) e^{-i(k-\frac{q}{2}-Q_b)l} b_q + \text{H.c.}].$$

Note that in (52) occupation numbers  $c_k^\dagger c_k$  are integrals of motion and can be related to the conserved total momentum of the system. Hence for the polaron with momentum  $k$ , the ground state can be described by the variational state  $c_k^\dagger |0\rangle \otimes |\Psi_{\text{GS}}\rangle_b$ , where the Gaussian state

$$|\Psi_{\text{GS}}\rangle_b = e^{i\theta_0} e^{i\frac{1}{2}R^T \sigma \Delta_R} e^{-i\frac{1}{4}R^T \xi_b R} |0\rangle_b \quad (53)$$

of the phonons is the approximate ground state of the Hamiltonian

$$\bar{H}_k = \sum_q \omega_q b_q^\dagger b_q + \sum_\delta t_\delta e^{-i(k-Q_b)\delta} \\ + \sum_{l,q} e^{-i(k-\frac{q}{2}-Q_b)l} \tilde{g}_l(q) b_q + \text{H.c.} \quad (54)$$

Here  $R = (x_q, p_q)^T$  is the quadrature defined in the basis of momentum eigenstates. The real time dynamics of a state with a well defined total momentum  $k$  can also be studied using the ansatz  $c_k^\dagger |0\rangle \otimes |\Psi_{\text{GS}}(t)\rangle_b$ . We remind the readers that the factorization of the wavefunction is only present after the LLP transformation. In the “original frame”, i.e., with the bare electron and phonon operators, this state displays strong entanglement between the electron and phonons. When the initial state of the system is not an eigenstate of the total momentum, it should be expanded in momentum eigenstates and the dynamics in each  $k$ -sector should be studied separately (see e.g., [46]). The state  $|\Psi_{\text{NGS}}\rangle = U_{\text{LLP}}(c_k^\dagger |0\rangle \otimes |\Psi_{\text{GS}}\rangle_b)$  in the original representation is in the non-Gaussian state family (3), where the transformation  $U_{\text{LLP}}$  does not have any variational parameters. Hence the ground state properties and real time dynamics can be studied by Eqs. (E28) and (E29) from Appendix E.

#### A. Ground state properties and single polaron phase transitions

In this subsection, we study the ground state properties of polarons by solving Eq. (30) [or equivalently Eq. (E28) with  $O_\Delta = 0$ ,  $O_b = 0$ ], where the vector  $h_\Delta = 2\delta E_k / \delta \Delta_R$  and the matrix  $h_b = 4\delta E_k / \delta \Gamma_b$  can be obtained from the expectation value of the energy

$$E_k = \langle \bar{H}_k \rangle_{\text{GS}} = {}_b \langle \Psi_{\text{GS}} | \bar{H}_k | \Psi_{\text{GS}} \rangle_b. \quad (55)$$

A detailed calculation of the last expression for  $\bar{H}_k$  from Eq. (54) is given in Appendix C. Here we only summarize the result. We find

$$E_k = \frac{1}{4} \Delta_R^T \omega \Delta_R + \frac{1}{4} \text{tr}(\omega \Gamma_b) + \sum_\delta t_\delta e^{-ik\delta} \frac{s_0 e^{-\frac{1}{2} \Delta_R^T \tilde{\Gamma}_B^{-1} (1-f_0) \Delta_R}}{\sqrt{\det(\Gamma_B/2)}} \\ + 2\text{Re} \sum_\delta e^{-ik\delta} \frac{s_0 e^{-\frac{1}{2} \Delta_R^T \tilde{\Gamma}_B^{-1} (1-f_0) \Delta_R}}{\sqrt{\det(\Gamma_B/2)}} \Delta_R^T \tilde{\Gamma}_B^{-1} \mathbf{g} - \frac{1}{2} \sum_q \omega_q, \quad (56)$$

where, in the basis of momentum eigenstates the frequency matrix is diagonal  $\omega = \mathbb{1}_2 \otimes \text{diag}(\omega_q)$ , the matrices

$$\Gamma_B = \sqrt{1-f_0} \Gamma_b \sqrt{1-f_0} + 1 + f_0, \\ \tilde{\Gamma}_B = (1-f_0) \Gamma_b + 1 + f_0 \quad (57)$$

are determined by  $f_0 = \mathbb{1}_2 \otimes \text{diag}(e^{iq\delta})$ , and  $\mathbf{g} = (1, i)^T \otimes \tilde{g}_\delta(q) e^{iq\delta/2}$ . As shown in Appendix C, the sign  $s_0$  can be determined by the Takagi diagonalization [47] of the symmetric matrix  $\Gamma_B$ .

We can use Eq. (56) to find the vector  $h_\Delta$  and the matrix  $h_b$  that enter Eq. (31)

$$\begin{aligned}
h_\Delta &= \omega \Delta_R - 2 \sum_\delta t_\delta e^{-ik\delta} \frac{s_0 e^{-\frac{1}{2} \Delta_R^T \tilde{\Gamma}_B^{-1} (1-f_0) \Delta_R}}{\sqrt{\det(\Gamma_B/2)}} \tilde{\Gamma}_B^{-1} (1-f_0) \Delta_R \\
&\quad + 4 \text{Re} \sum_\delta e^{-ik\delta} \frac{s_0 e^{-\frac{1}{2} \Delta_R^T \tilde{\Gamma}_B^{-1} (1-f_0) \Delta_R}}{\sqrt{\det(\Gamma_B/2)}} [1 - \tilde{\Gamma}_B^{-1} (1-f_0) \Delta_R \Delta_R^T] \tilde{\Gamma}_B^{-1} \mathbf{g}
\end{aligned} \tag{58}$$

and

$$\begin{aligned}
h_b &= \omega - 2 \sum_\delta t_\delta e^{-ik\delta} \frac{s_0 e^{-\frac{1}{2} \Delta_R^T \tilde{\Gamma}_B^{-1} (1-f_0) \Delta_R}}{\sqrt{\det(\Gamma_B/2)}} W_1 \\
&\quad - 4 \text{Re} \sum_\delta e^{-ik\delta} \frac{s_0 e^{-\frac{1}{2} \Delta_R^T \tilde{\Gamma}_B^{-1} (1-f_0) \Delta_R}}{\sqrt{\det(\Gamma_B/2)}} (\Delta_R^T \tilde{\Gamma}_B^{-1} \mathbf{g} W_1 + W_2 + W_2^T)
\end{aligned} \tag{59}$$

are determined by Eqs. (E11) and (56), where

$$\begin{aligned}
W_1 &= \tilde{\Gamma}_B^{-1} (1-f_0) [1 - \Delta_R \Delta_R^T \tilde{\Gamma}_B^{-1} (1-f_0)], \\
W_2 &= \tilde{\Gamma}_B^{-1} \mathbf{g} \Delta_R^T \tilde{\Gamma}_B^{-1} (1-f_0).
\end{aligned} \tag{60}$$

By solving the equations of motion (30) with  $h_\Delta$  and  $h_b$  given by Eqs. (58) and (59), we obtain the values of  $\Delta_R$  and  $\Gamma_b$  for the Gaussian ground state  $|\Psi_{\text{GS}}\rangle_b$  in the limit  $\tau \rightarrow \infty$ . With the steady state solution, the energy (56) determines the dispersion relation  $E_k$  of the polaron with momentum  $k$ . Polaronic suppression of the quasiparticle weight is given by

$$\begin{aligned}
Z_k &= |\langle 0 | c_k | \Psi_{\text{NGS}} \rangle|^2 = |\langle 0 | \Psi_{\text{GS}} \rangle_b|^2 \\
&= \frac{e^{-\frac{1}{2} \Delta_R^T (\Gamma_b + \mathbb{1}_{2N_b})^{-1} \Delta_R}}{\sqrt{\det[(\Gamma_b + \mathbb{1}_{2N_b})/2]}}.
\end{aligned} \tag{61}$$

To understand the character of the variational solution it is useful to consider the polaron wavefunction in the original basis  $|\Psi_{\text{NGS}}\rangle = U_{\text{LLP}} (c_k^\dagger |0\rangle \otimes |\Psi_{\text{GS}}\rangle_b)$ . We note that the LLP Hamiltonian (52) does not conserve phonon momentum, hence the state  $|\Psi_{\text{GS}}\rangle_b$  is a superposition of different momentum eigenstates  $|\Psi_{\text{GS}}\rangle_b = \sum_q \phi_k(q) |\Psi_q(k)\rangle_b$ . Here  $|\Psi_q(k)\rangle_b$  is a phonon state which has net phonon momentum  $q$  (the wavefunction  $\Psi_q(k)$  depends on  $k$ , but its specific form is not important for our argument below). We recall that the LLP transformation simply shifts the electron momentum by the amount equal to the total momentum of the phonons, therefore  $|\Psi_{\text{NGS}}\rangle = \sum_q \phi_k(q) c_{k-q}^\dagger |0\rangle \otimes |\Psi_q(k)\rangle_b$ . We use  $c_{k-q}^\dagger = \frac{1}{\sqrt{N_0}} \sum_{j_0} e^{i(k-q)j_0} c_{j_0}^\dagger |0\rangle$  and  $\sum_q e^{-iqj_0} \phi_k(q) |\Psi_q(k)\rangle_b = e^{-i\hat{Q}_b j_0} |\Psi_{\text{GS}}\rangle_b$  where  $\hat{Q}_b$  is the operator of the total phonon momentum. Then we find

$$\begin{aligned}
|\Psi_{\text{NGS}}\rangle &= \frac{1}{\sqrt{N_b}} \sum_{j_0} e^{ikj_0} |\Phi_{j_0}\rangle, \\
|\Phi_{j_0}\rangle &= c_{j_0}^\dagger |0\rangle \otimes e^{-i\hat{Q}_b j_0} |\Psi_{\text{GS}}\rangle_b.
\end{aligned} \tag{62}$$

The physical interpretation of  $|\Phi_{j_0}\rangle$  is a polaron centered on site  $j_0$ . By analyzing  $e^{-i\hat{Q}_b j_0} |\Psi_{\text{GS}}\rangle_b$  we can understand the corresponding phonon configuration

$$\begin{aligned}
\tilde{\Delta}_R &= {}_b \langle \Psi_{\text{GS}} | e^{iQ_b j_0} \tilde{R} e^{-iQ_b j_0} | \Psi_{\text{GS}} \rangle_b \\
&= \frac{1}{2} W_b V_F W_b^\dagger \Delta_R
\end{aligned} \tag{63}$$

of phonon fields  $\tilde{R} = (x_j, p_j)^T$  in the coordinate space. Here,

$$V_F = \begin{pmatrix} v & 0 \\ 0 & v^* \end{pmatrix}, \tag{64}$$

the matrix  $W_b$  was defined in Eq. (24), and the Fourier transform is represented in the matrix form by  $v$  with the element  $v_{d,q} = e^{idq}/\sqrt{N_0}$ , and  $d = j - j_0$  is the distance between the electron and the local phonon mode at the position  $j$ . The covariance matrix

$$\begin{aligned}
\tilde{\Gamma}_b &= {}_b \langle \Psi_{\text{GS}} | e^{iQ_b j_0} \frac{1}{2} \{ \delta \tilde{R}, \delta \tilde{R}^T \} e^{-iQ_b j_0} | \Psi_{\text{GS}} \rangle_b \\
&= \frac{1}{4} W_b V_F W_b^\dagger \Gamma_b W_b V_F^\dagger W_b^\dagger
\end{aligned} \tag{65}$$

describes the squeezing of phonons around the electron, where the fluctuation field  $\delta \tilde{R} = \tilde{R} - \tilde{\Delta}_R$ .

In Fig. 1, we present results for polarons in the one dimensional Holstein model: the dispersion  $E_k$  and single-particle residue  $Z_k$ . Note that our analysis gives the lowest energy state for a given total momentum  $k$ , which is an integral of motion of the system. The true ground state corresponds to finding the energy minimum with respect to  $k$ . In our analysis we consider only nearest neighbor hopping of electrons, i.e.,  $t_l = -t_0 \delta_{l,\pm 1}$  and we set  $t_0 = 1$ . We also neglect the dispersion of phonons, namely, we consider Einstein phonons with frequency  $\omega_0 = 0.5t_0$ . From Fig. 1a-b we observe that an increase in the electron-phonon interaction leads to a strong flattening of the band and suppression of the quasiparticle weight  $Z_k$ . The momentum dependence of  $Z_k$  in Fig. 1b

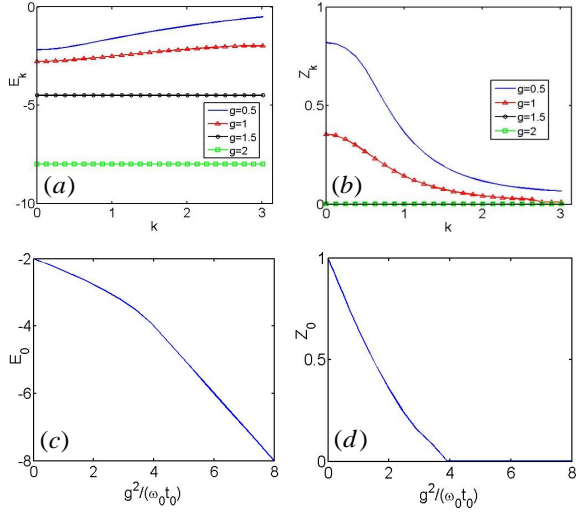


FIG. 1: The dispersion relation and single particle weight of polarons in the 1D Holstein model. Variational analysis was done in a system with 50 sites,  $\omega_0 = 0.5$ , and the hopping constant  $t_0$  taken as the unit of energy. (a)-(b) Dispersion relations and single particle weights for different coupling constants. (c)-(d) The energy and the single particle weight for the polaron with zero momentum.

indicates that polaronic dressing is enhanced at higher momenta.

The bandwidth of the polaron is primarily determined by the second term in Eq. (54). Polaronic reduction of the bandwidth (which can be understood as the effective mass becoming heavier) comes from the  $\langle e^{iQ_b \delta} \rangle_{GS}$  factor in the second term in Eq. (54).

In Figs. 1c-d, we show the energy  $E_0$  and the single particle weight  $Z_0$  for the polaron with momentum  $k = 0$ . These two properties of the Holstein polaron have been studied in earlier papers using several techniques: the self-consistent Born approximation, the Lang-Firsov (LF) approach [48], Diagrammatic Monte Carlo (DMC) calculations [49], the momentum average (MA) method [45], and the numerical minimization based on the Toyozawa ansatz (TA) [50, 51].

We emphasize that  $E_0$  and  $Z_0$  in Figs. 1c-d agree with the results from DMC and MA quantitatively [45]. In the TA, the coherent and squeezing properties of phonons around the electron in the co-moving frame can also be studied variationally, where the variational parameters are obtained by the brute-force minimization of the ground state energy. Compared with TA, the imaginary time evolution of non-Gaussian states is more efficient in finding the optimal variational parameters. Thus the general Gaussian ansatz from Eq. (19) can be used to analyze phonon squeezing at large distances from the impurity.

The figure 2 shows the spatial structure of the polaron with momenta  $k = 0$  and  $\pi/2$  when the coupling constant  $g = 1$ . We present both the displacement (63) and the

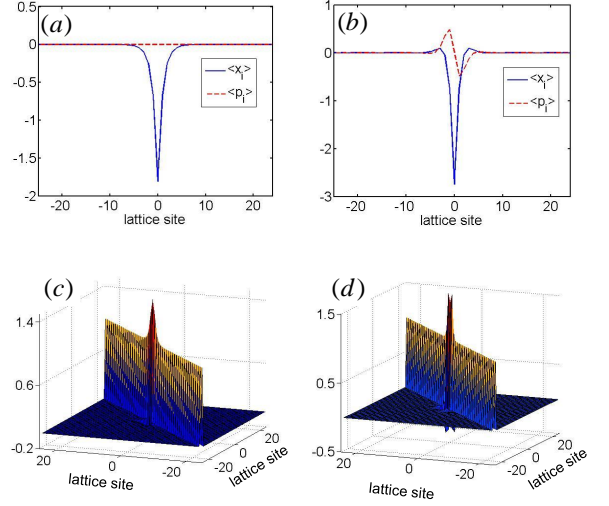


FIG. 2: The average values of quadratures and correlation functions  $\langle \delta x_i \delta x_j \rangle$  of phonons in the Holstein model with 50 sites, where  $\omega_0 = 0.5$ ,  $g = 1$ , and the hopping constant  $t_0$  is taken as the unit. (a)-(b) The average values of quadratures along the chain for  $k = 0$  and  $k = \pi/2$ . (c)-(d) The correlation functions  $\langle \delta x_i \delta x_j \rangle$  of displacements at positions  $i$  and  $j$  for  $k = 0$  and  $k = \pi/2$ .

squeezing (65) of the phonons around the electron. Note that for a given total momentum of the polaron they only depend on the distance to the electron, hence we set the electron position to be  $j_0 = 0$ . We find that the canonical phonon momentum  $\langle p \rangle$  vanishes on all sites when the total momentum of the polaron  $k = 0$ . In Figs. 2c-d, the correlation functions  $\langle \delta x_i \delta x_j \rangle$  for  $k = 0$  and  $\pi/2$  show that phonons around the electron are squeezed along the direction of the canonical momentum in the phase space, i.e.,  $\langle \delta x_j^2 \rangle > 1$  for  $j$  close to  $j_0$ .

The remarkable “single-polaron phase transition” takes place when the electron-phonon interaction depends on the momenta of the electron and the phonons, as is the case for the 1D SSH model. For the SSH model with  $t_l = -t_0 \delta_{l, \pm 1}$  and Einstein phonon frequency  $\omega_q = \omega_0 = 0.5 t_0$ , Fig. 3 displays the dispersion relation  $E_k$  and the single particle weight  $Z_k$  of the lowest polaron band. In agreement with earlier studies we find that when the interaction  $g$  exceeds a certain critical value  $g_c$ , the lowest energy state of the polaron is at a finite momentum  $k \neq 0$ .

Previously this phase transition has been studied by MA and three numerical methods [36]: DMC, exact diagonalization (ED), and bold DMC. To understand the origin of the transition using our LLP+Gaussian approach we observe that the momentum dependence of  $E_k$  in Eq. (54) comes from both the second and the third terms. The former corresponds to the polaronically dressed electron hopping and the latter comes from the electron-phonon interaction. The competition between the two terms gives rise to the polaron dispersion minimum mov-

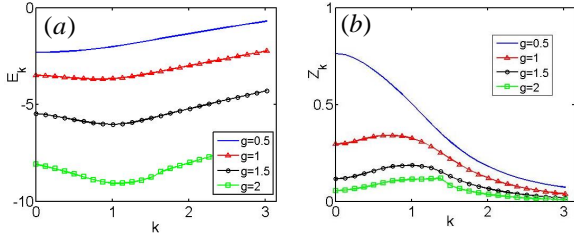


FIG. 3: The dispersion relation and single particle weight of the 1D SSH model with 50 sites, where  $\omega_0 = 0.5$  and the hopping constant  $t_0$  is taken as the unit.

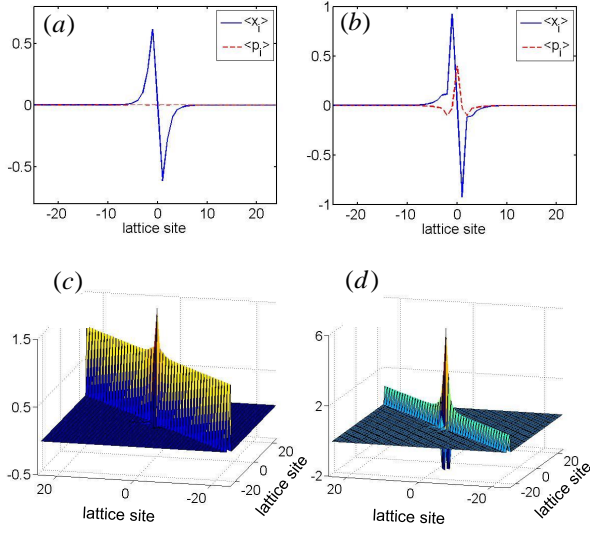


FIG. 4: The average values of quadratures and correlation functions  $\langle \delta x_i \delta x_j \rangle$  of phonons in the SSH model with 50 sites,  $\omega_0 = 0.5$  and the hopping constant  $t_0$  taken as the unit of energy. (a)-(b) The average values of quadratures in the ground states with  $k = 0$  and  $k = 0.88$  for  $g = 0.5$  and  $g = 1$ , respectively. (c)-(d) The correlation functions  $\langle \delta x_i \delta x_j \rangle$  of displacements at positions  $i$  and  $j$  in the ground states with  $k = 0$  and  $k = 0.88$  for  $g = 0.5$  and  $g = 1$ , respectively.

ing away from  $k = 0$  for large interaction strengths.

The figure 4 compares the structure of the ground state polarons at the two sides of the transition. Parts a) and c) correspond to  $g = 0.5$ ,  $\omega_0 = 0.5$ , and the momentum  $k = 0$  of the ground state at this interaction strength. Parts b) and d) correspond to the polaron for  $g = 1$ ,  $\omega_0 = 0.5$ , and the momentum  $k = 0.88$  of the ground state for this interaction strength. We show both the average value of the phonon displacements  $\bar{\Delta}_R$  and the correlation functions  $\langle \delta x_i \delta x_j \rangle$ . Phonon squeezing is significantly enhanced for larger values of the coupling constant.

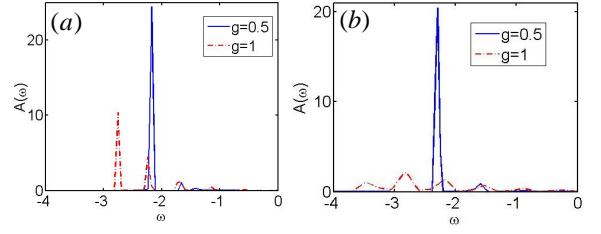


FIG. 5: The spectral functions of the 1D Holstein model and the 1D SSH model, where the system size  $N = 50$ , the phonon frequency  $\omega_0 = 0.5$ , and  $t_0$  taken as the unit of energy. (a) The polaron momentum  $k = 0$  for  $g = 0.5$  (solid blue curve) and  $g = 1$  (dashed red curve) in the Holstein model; (b) The polaron momentum  $k = 0$  for  $g = 0.5$  (solid blue curve) and  $k = 0.88$  for  $g = 1$  (dashed red curve) in the SSH model.

## B. Real time dynamics

We now discuss how to compute the polaron spectral function

$$\mathcal{A}(\omega) = -\frac{1}{\pi} \text{Im} G_R(\omega), \quad (66)$$

where  $G_R(\omega) = \int dt G(t) e^{i\omega t}$  is the Fourier transform of the retarded Green function

$$G_R(t) = -i \langle 0 | c_k e^{-iHt} c_k^\dagger | 0 \rangle \theta(t). \quad (67)$$

Applying the LLP transformation  $U_{\text{LLP}}$  to the definition of the retarded Green's function (67) we find

$$G_R(t) = -i \langle 0 | e^{-i\bar{H}_k t} | 0 \rangle \theta(t), \quad (68)$$

where  $\bar{H}_k$  is given in equation (54).

In the co-moving frame, the real-time evolution  $|\Psi(t)\rangle = e^{-iH_p t} |0\rangle$  is approximated by a Gaussian state  $|\Psi_{\text{GS}}(t)\rangle$  obeying the Schrödinger equation

$$i\partial_t |\Psi_{\text{GS}}(t)\rangle = \mathbf{P}_\xi \bar{H}_k |\Psi_{\text{GS}}(t)\rangle \quad (69)$$

projected onto the tangent space. Since  $|\Psi_{\text{GS}}(t)\rangle$  is a Gaussian state, the tangent vectors only contain  $U_{\text{GS}} |0\rangle$ ,  $U_{\text{GS}} b_q^\dagger |0\rangle$ , and  $U_{\text{GS}} b_{q_1}^\dagger b_{q_2}^\dagger |0\rangle$ . After projecting onto the tangent space (see Eqs. (E10) and (E11) for details), equation of motion (69) becomes

$$i\partial_t |\Psi_{\text{GS}}(t)\rangle = \bar{H}_{\text{MF}} |\Psi_{\text{GS}}(t)\rangle, \quad (70)$$

where the normal ordering expansion can be used to construct the mean field Hamiltonian

$$\bar{H}_{\text{MF}} = \frac{1}{4} \delta R^T h_b \delta R + \frac{1}{2} \delta R^T h_\Delta + E_k \quad (71)$$

with  $h_\Delta$  and  $h_b$  given in Eqs. (58) and (59). The first term in  $\bar{H}_{\text{MF}}$  is normal ordered with respect to the squeezed vacuum, i.e., the coherent part has been removed using  $\delta R = R - \Delta_R$ . As shown in Appendix E, the projected Schrödinger equation can be used to derive

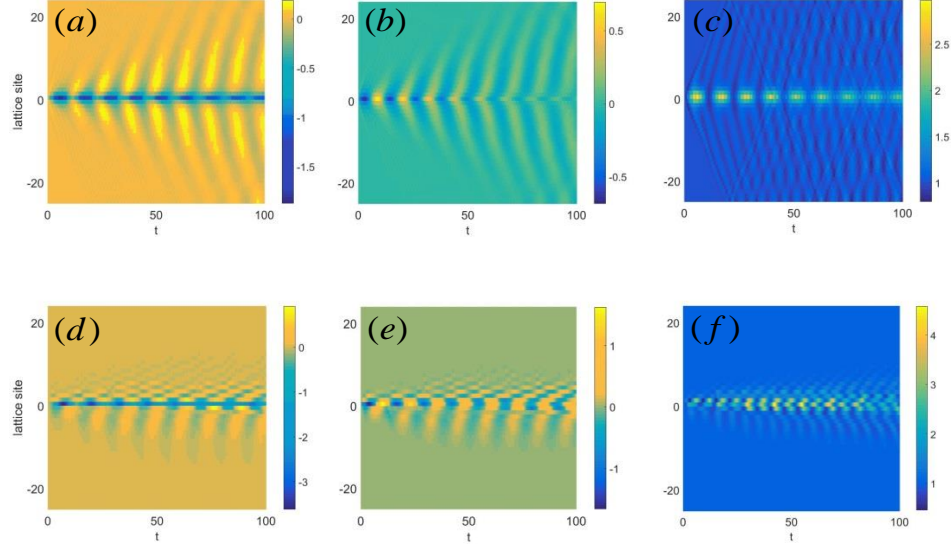


FIG. 6: The time evolution of average values  $\tilde{\Delta}_R$  and diagonal elements  $\langle \delta x_i^2 \rangle$  of  $\tilde{\Gamma}_b$  for the Holstein model, where  $\omega_0 = 0.5$ ,  $g = 1$ , and  $t_0$  is taken as the unit. (a)-(c) The average values  $\langle x_i \rangle$ ,  $\langle p_i \rangle$ , and  $\langle \delta x_i^2 \rangle$  for  $k = 0$ ; (d)-(f) The average values  $\langle x_i \rangle$ ,  $\langle p_i \rangle$ , and  $\langle \delta x_i^2 \rangle$  for  $k = \pi/2$ .

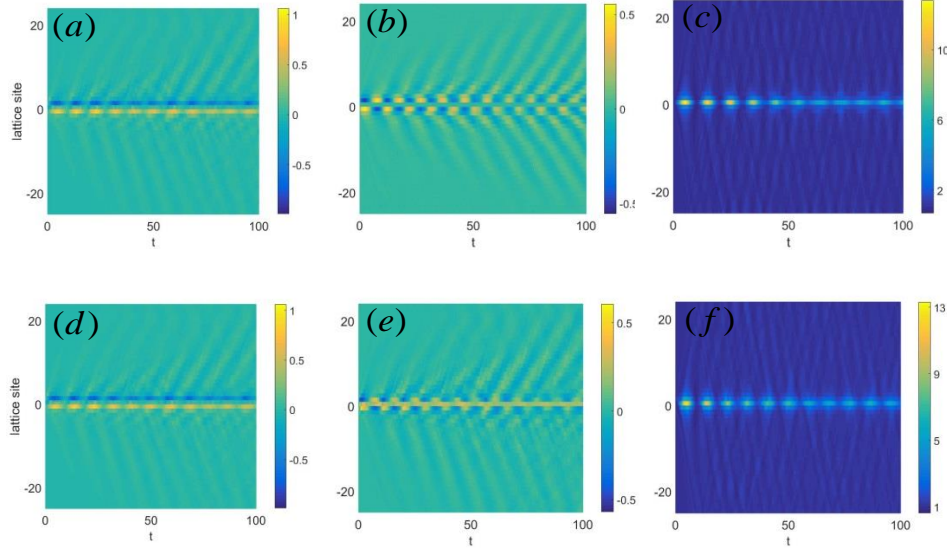


FIG. 7: The time evolution of average values  $\tilde{\Delta}_R$  and diagonal elements  $\langle \delta x_i^2 \rangle$  of  $\tilde{\Gamma}_b$  for the SSH model, where  $\omega_0 = 0.5$ ,  $g = 1$ , and  $t_0$  is taken as the unit. (a)-(c) The average values  $\langle x_i \rangle$ ,  $\langle p_i \rangle$ , and  $\langle \delta x_i^2 \rangle$  for  $k = 0$ ; (d)-(f) The average values  $\langle x_i \rangle$ ,  $\langle p_i \rangle$ , and  $\langle \delta x_i^2 \rangle$  for  $k = 0.88$ .

equations describing the real time evolution of  $\Delta_R$  and  $\Gamma_b$ . The result is shown in Eq. (31) [or equivalently Eq. (E29) with  $h_\Delta^t = h_\Delta$  and  $h_b^t = h_b$ ].

One of the challenges in computing  $G_R(t)$  is that it is defined as an overlap of the two wavefunctions:  $\langle 0 | \Psi_{GS}(t) \rangle$ . Therefore to obtain  $G_R(t)$  we need to compute the time dependent overall phase  $\theta_0(t)$  in  $|\Psi_{GS}(t)\rangle$ . In principle, this calculation can be done using equation

(71). It is more instructive however to use a different representation of the Gaussian transformation  $U_{GS}(t)$ , which allows to keep track of the explicit time evolution of the variational wavefunction. We use Wei-Norman algebra [52] to write the transformation in the form

$$U_{GS}(t) = e^{i\theta_0(t)} e^{i\frac{1}{2}R^T \sigma \Delta_R} e^{b^\dagger \Lambda_1 b^\dagger} e^{b^\dagger \Lambda_2 b} e^{b \Lambda_3 b}, \quad (72)$$

where  $b = (b_{q_1}, \dots, b_{q_N})^T$  should be understood as a vec-



tor. In Appendix G, we use the projected Schrödinger Eq. (70) to obtain the following equations for the real-time evolution

$$\begin{aligned}\partial_t \theta_0 &= -\delta E_k - \frac{1}{2} \text{tr} \omega_b - \text{tr}(\varpi^\dagger \Lambda_1), \\ i\partial_t \Lambda_1 &= \frac{1}{2} \varpi + \omega_b \Lambda_1 + \Lambda_1 \omega_b^T + 2\Lambda_1 \varpi^\dagger \Lambda_1\end{aligned}\quad (73)$$

of the global phase  $\theta_0$  and the symmetric matrix  $\Lambda_1$ . In Eq. (73) we used  $\delta E_k = E_k - \text{tr}(h_b \Gamma_b)/4 - \Delta_R^T h_\Delta/4$ , and matrices  $\omega_b$  and  $\varpi$  are defined using the single-particle Hamiltonian

$$\begin{pmatrix} \omega_b & \varpi \\ \varpi^\dagger & \omega_b^T \end{pmatrix} = \frac{1}{2} W_b^\dagger h_b W_b \quad (74)$$

in the bosonic Nambu representation  $(b, b^\dagger)^T$ . Equation (73) determines the evolution of the global phase.

In terms of  $\theta_0$  and  $\Lambda_1$ , the retarded Green's function is

$$G_R(t) = -ie^{i\theta_0(t)} e^{-\frac{1}{2} \Delta_b^\dagger \Delta_b} e^{\Delta_b^\dagger \Lambda_1 \Delta_b^*} \theta(t), \quad (75)$$

where the column vector  $\Delta_b = \langle b \rangle_{\text{GS}}$ . The Fourier transform of Eq. (75) gives the spectral function (66). In Figs. 5a-b, we show the spectral functions for the 1D Holstein and SSH models respectively. The solid blue and dashed red curves in Fig. 5a display spectral functions of the polaron at  $k = 0$  for coupling constants  $g = 0.5$  and  $g = 1$ . The solid blue and dashed red curves in Fig. 5b display the spectral functions of the polaron with  $k = 0$  for  $g = 0.5$  and  $k = 0.88$  for  $g = 1$ . Note that  $k = 0.88$  corresponds to the ground state of the SSH polaron for  $g = 1$ . An important feature of the spectral function is the presence of several shake-off peaks in the spectrum. The maximum value of the spectral function does not necessarily correspond to the lowest energy peak (different peaks are sometimes referred to as different polarons bands).

The time dependent non-Gaussian state

$$\begin{aligned}|\Psi_{\text{NGS}}\rangle &= U_{\text{LLP}} c_k^\dagger |0\rangle |\Psi_{\text{GS}}(t)\rangle \\ &= \sum_{j_0} e^{ikj_0} c_{j_0}^\dagger |0\rangle e^{-iQ_b j_0} |\Psi_{\text{GS}}(t)\rangle\end{aligned}\quad (76)$$

can be used to analyze the time evolution of all physical observables. We compute the phonon quadratures and correlation functions using equations (63) and (65). Note that the phonon parameters described by the state (76) only depend on the distance between the phonon site  $j$  and the electron coordinate  $j_0$ . Thus, it is sufficient to consider a single term in (76) with one specific  $j_0$ , which we will set to be at the origin,  $j_0 = 0$ . In Fig. 6, we show the time evolution of the phonon quadratures  $\tilde{\Delta}_R$  and the diagonal elements  $\langle \delta x_i^2 \rangle$  of the matrix  $\tilde{\Gamma}_b$  for the Holstein model with  $\omega_0/t_0 = 0.5$  and  $g/t_0 = 1$ . We consider the cases with polaron momenta  $k = 0$  (the first row) and  $k = \pi/2$  (the second row). In Fig. 7, we show the time evolution of the phonon quadratures  $\tilde{\Delta}_R$  and the diagonal

part of the phonon correlations  $\langle \delta x_i^2 \rangle$  for the SSH model with  $\omega_0/t_0 = 0.5$  and  $g/t_0 = 1$ . We again set the electron to be at  $j_0 = 0$  and choose polaron momenta  $k = 0$  (the first row) and  $k = 0.88$  (the second row).

### C. Summary of Section III

We used the non-Gaussian state approach to study the ground state properties and real time dynamics of polarons. We computed their dispersion, quasiparticle weight, and obtained full spectral functions. We discussed the quantum phase transition for SSH polarons, which corresponds to the lowest energy state of the polaron changing from  $k = 0$  to finite momentum. What makes the single polaron problems special is that the LLP transformation does not involve any variational parameters. Thus we could directly apply the Gaussian state variational approach to  $\tilde{H}_k$ , which describes a polaron in the co-moving frame. Excellent agreement between our results and those from earlier studies suggest that a combination of the LLP transformation and the Gaussian state approach is a powerful theoretical tool for describing polaronic systems. We point out that similar approach has also been successfully applied to describe polarons in cold atoms BECs [53] earlier. In the next two examples we consider more challenging systems in which we need to consider canonical transformations with time dependent variational parameters in the analysis of both the ground state and non-equilibrium dynamics.

## IV. NONEQUILIBRIUM DYNAMICS IN SPIN-BOSON AND KONDO MODELS

In this section we investigate the ground state properties and real-time dynamics of the spin-boson problem using variational non-Gaussian approach. The spin-boson problem describes a two level system, i.e. a spin, coupled to a reservoir of bosonic modes:

$$H_{\text{SB}} = \frac{\Delta}{2} \sigma_x + \sum_k \varepsilon_k b_k^\dagger b_k - \frac{1}{2} \sigma_z \sum_k g_k (b_k + b_k^\dagger). \quad (77)$$

Here,  $\varepsilon_k$  is the dispersion of the boson modes,  $g_k$  is their coupling to the spin, and we will use  $N_b$  to denote the total number of modes. This section is organized as follows. In the subsection IV A we review the relation between the spin-boson model and the fermionic Kondo model [54]. This connection relies on bosonizing the 1D Fermi gas, which can then be mapped onto a spin-boson model with Ohmic dissipation, which will be the focus of our discussion. The ferromagnetic/antiferromagnetic phase transition in the Kondo model corresponds to the localization/delocalization transition in the spin boson model [54]. When presenting the results of our analysis we will usually do it in the language of the Kondo model since we expect this system to be more familiar to the



readers. In subsections IV B-D we introduce two types of non-Gaussian transformations for analyzing the spin-boson model. While the two transformations appear to be very different, we show that they describe the same class of variational wavefunctions. We derive the equations of motion for the variational parameters for both imaginary and real time evolution. In the subsection IV E we present numerical results first for the ground state and then for the relaxation dynamics. One of the surprising findings of our analysis is how well the real time dynamics follows the RG flow of the equilibrium system. For example, we find that a system that has ferrimagnetic couplings but in the course of RG flow parameters flow to the AF regime, exhibits the same ferro to antiferro crossover in its dynamics.

### A. Relation to Kondo physics

The spin-boson Hamiltonian (77) is closely related to the Kondo model

$$H_K = \sum_{k\sigma} k c_{k\sigma}^\dagger c_{k\sigma} + \frac{J_\perp}{2} [\sigma_+ \psi_\downarrow^\dagger(0) \psi_\uparrow(0) + \text{H.c.}] + \frac{J_\parallel}{4} \sigma_z [\psi_\uparrow^\dagger(0) \psi_\uparrow(0) - \psi_\downarrow^\dagger(0) \psi_\downarrow(0)], \quad (78)$$

where the impurity spin couples anisotropically to the fermionic bath with strengths  $J_\perp$  and  $J_\parallel$ . In Eq. (78) we use fermionic operators at point  $x = 0$  defined as  $\psi_\sigma(x) = \sum_k c_{k\sigma} e^{ikx}/\sqrt{L}$ , where  $c_{k\sigma}$  are annihilation operators for fermions with momentum  $k$  and spin  $\sigma$ , and  $L$  is the system size. The connection between the two models (77) and (78) is established by the bosonization dictionary [55]

$$\begin{aligned} \psi_\sigma(x) &= \frac{1}{\sqrt{L}} F_\sigma e^{i\frac{2\pi N_\sigma}{L} x} \exp i\phi_\sigma(x); \\ \rho_\sigma(x) &= \psi_\sigma^\dagger(x) \psi_\sigma(x) = \frac{1}{2\pi} \partial_x \phi_\sigma(x), \end{aligned} \quad (79)$$

where the field

$$\phi_\sigma(x) = \sum_{q>0} \frac{e^{-ql_c/2}}{\sqrt{n_q}} (b_{q\sigma} e^{iqx} + b_{q\sigma}^\dagger e^{-iqx}) \quad (80)$$

is defined by the bosonic annihilation and creation operators  $b_{q\sigma}$  and  $b_{q\sigma}^\dagger$ , the integer  $n_q = qL/(2\pi)$ , and the short-distance cut-off is  $l_c$ . The Klein factor  $F_\sigma$  obeys the relations  $F_\sigma |N_\sigma\rangle = |N_\sigma - 1\rangle$ ,  $F_\sigma^\dagger F_\sigma = F_\sigma F_\sigma^\dagger = 1$ , and  $\{F_\sigma, F_{\sigma'}^\dagger\} = 2\delta_{\sigma\sigma'}$ , where  $|N_\sigma\rangle$  denotes the eigenstate of the number operator  $N_\sigma = \sum_k :c_{k\sigma}^\dagger c_{k\sigma}:$ .

The Kondo Hamiltonian can be expressed using the bosonic operators  $H_K = H_{\text{charge}} + H_{\text{spin}}$ , where we separated the charge part  $H_{\text{charge}} = \sum_k k b_{k\sigma}^\dagger b_{k\sigma}$  and the spin

part

$$H_{\text{spin}} = \sum_k k b_{k\sigma}^\dagger b_{k\sigma} + \frac{J_\parallel}{4\sqrt{2}\pi} \sigma_z \partial_x \phi_s(0) + \frac{J_\perp}{4\pi l_c} [\sigma_+ e^{i\sqrt{2}\phi_s(0)} + \text{H.c.}] \quad (81)$$

Here,  $\sigma_+$  is redefined as  $\sigma_+ F_\downarrow^\dagger F_\uparrow \rightarrow \sigma_+$ , and the charge and spin fields  $\phi_{c(s)} = (\phi_\uparrow \pm \phi_\downarrow)/\sqrt{2}$ :

$$\phi_{c(s)} = \sum_{q>0} \frac{e^{-ql_c/2}}{\sqrt{n_q}} (b_{q,c(s)} e^{iqx} + b_{q,c(s)}^\dagger e^{-iqx}) \quad (82)$$

are determined by  $b_{k,c(s)} = (b_{k\uparrow} \pm b_{k\downarrow})/\sqrt{2}$ . In the Hamiltonian  $H_K$ , the charge part  $H_{\text{charge}}$  is decoupled from the spin Hamiltonian  $H_{\text{spin}}$ , and the impurity spin only couples to the spin density excitation in the bath. In the following, we focus on the spin dynamics governed by the interacting Hamiltonian  $H_{\text{spin}}$ .

Under the unitary transformation  $U_\gamma = e^{i\sqrt{2}\gamma\sigma_z\phi_s(0)/2}$ , the Hamiltonian  $\bar{H}_\gamma = U_\gamma^\dagger H_{\text{spin}} U_\gamma$  in the new basis becomes

$$\begin{aligned} \bar{H}_\gamma &= \sum_k k b_{k\sigma}^\dagger b_{k\sigma} - i\frac{1}{2} \sigma_z \sum_{k>0} g_k^\gamma (b_{k\sigma} - b_{k\sigma}^\dagger) \\ &+ \frac{J_\perp}{4\pi l_c} [\sigma_+ e^{i\sqrt{2}(1-\gamma)\phi_s(0)} + \text{H.c.}] + E_0, \end{aligned} \quad (83)$$

where the energy  $E_0 = (\pi\gamma - J_\parallel/2)\gamma \sum_k e^{-kl_c}/L$ , and the coupling constant

$$g_k^\gamma = (2\pi\gamma - \frac{J_\parallel}{2}) \sqrt{\frac{k}{\pi L}} e^{-kl_c/2}. \quad (84)$$

For the choice  $\gamma = 1$ , the Hamiltonian (83) is exactly the spin-boson model (77) with the interaction  $g_k = g_k^\gamma$ , where  $b_k = ib_{k\sigma}$  and  $\Delta = J_\perp/(2\pi l_c)$ . At the Toulouse point  $J_\parallel = 4\pi\gamma$  and  $\gamma = 1 - 1/\sqrt{2}$ , the Hamiltonian is exactly solvable by the refermionization technique [55, 56]. The equivalence of the two models established via  $U_{\gamma=1}$  allows us to related states in the Kondo and spin-boson models as  $|\Psi_{\text{NGS}}^K\rangle = U_{\gamma=1} |\Psi_{\text{NGS}}^{\text{SB}}\rangle$ .

### B. Two non-Gaussian transformations

In this subsection, we introduce two types of non-Gaussian transformations for constructing variational states  $|\Psi_{\text{NGS}}\rangle$  which can be used to describe the spin-boson model (77).

*Unitary transformation based on parity conservation.* We observe that the the Hamiltonian (77) conserves the parity  $P_{\text{ex}} = e^{i\pi N_{\text{ex}}}$ , where the excitation number  $N_{\text{ex}}$  is defined as

$$N_{\text{ex}} = \frac{1}{2}(\sigma_x + 1) + \sum_k b_k^\dagger b_k. \quad (85)$$

We define the unitary transformation  $U_{\text{parity}} = e^{S_{\text{parity}}}$  with

$$S_{\text{parity}} = i\frac{\pi}{2}(\sigma_z - 1) \sum_k b_k^\dagger b_k. \quad (86)$$

Note that this transformation, which we will call parity transformation, belongs to the class  $U_5$  and has no variational parameters.

Under the parity transformation, the Hamiltonian  $\bar{H}_{\text{parity}} = U_{\text{parity}}^\dagger H_{\text{SB}} U_{\text{parity}}$  becomes

$$\begin{aligned} \bar{H}_{\text{parity}} &= \frac{\Delta}{2} \sigma_x e^{i\pi \sum_k b_k^\dagger b_k} + \sum_k \varepsilon_k b_k^\dagger b_k \\ &\quad - \frac{1}{2} \sum_k g_k (b_k + b_k^\dagger). \end{aligned} \quad (87)$$

Similarly to the LLP transformation the impurity spin degree of freedom has been effectively eliminated using the parity integral of motion. Indeed, while Eq. (87) still contains the spin operator  $\sigma_x$ , this operator now commutes with the Hamiltonian and is therefore conserved. It is easy to see that  $\sigma_x$  in the last equation corresponds to the parity operator in the original Hamiltonian  $U_{\text{parity}}^\dagger P_{\text{ex}} U_{\text{parity}} = -\sigma_x$ .

For the sake of comparison to the Selbey-type transformation discussed below, we present variational wavefunctions that obey parity conservation without performing  $U_{\text{parity}}$  explicitly. We define  $|\pm\rangle = (|\uparrow\rangle \pm |\downarrow\rangle)/\sqrt{2}$  as spin eigenstates of  $\sigma_x$  with eigenvalues  $\pm 1$  and observe that in the even subspace ( $P_{\text{ex}} = 1$ ), any state can be written as

$$\begin{aligned} |\Psi_{\text{NGS}}\rangle &= |-\rangle |\text{even}\rangle + |+\rangle |\text{odd}\rangle \\ &= \frac{1}{\sqrt{2}} (|\uparrow\rangle |\Psi^+\rangle - |\downarrow\rangle |\Psi^-\rangle), \end{aligned} \quad (88)$$

where and  $|\Psi^\pm\rangle = |\text{even}\rangle \pm |\text{odd}\rangle$ . Similarly, in the odd subspace ( $P_{\text{ex}} = -1$ ) all states have the form

$$\begin{aligned} |\Psi_{\text{NGS}}\rangle &= |-\rangle |\text{odd}\rangle + |+\rangle |\text{even}\rangle \\ &= \frac{1}{\sqrt{2}} (|\uparrow\rangle |\Psi^+\rangle + |\downarrow\rangle |\Psi^-\rangle). \end{aligned} \quad (89)$$

We employ the Gaussian ansatz for  $|\Psi^+\rangle = |\Psi_{\text{GS}}^{\text{parity}}\rangle_b$ , which leads to  $|\Psi^-\rangle = \exp(i\pi \sum_k b_k^\dagger b_k) |\Psi^+\rangle$ . Then we have the Gaussian states

$$|\Psi^\pm\rangle = e^{i\theta_0} e^{\pm i\frac{1}{2} R^T \sigma \Delta_R} e^{-i\frac{1}{4} R^T \xi_b R} |0\rangle. \quad (90)$$

We observe that the two Eqs. (88) and (89) can be combined into a single non-Gaussian ansatz

$$|\Psi_{\text{NGS}}\rangle = U_{\text{parity}} |\mp\rangle |\Psi_{\text{GS}}^{\text{parity}}\rangle_b, \quad (91)$$

From the Hamiltonian (87), we notice that in the even (odd) subspace, i.e.,  $\sigma_x = -1$  (1),  $\langle e^{i\pi \sum_k b_k^\dagger b_k} \rangle$  tends

to be positive (negative) to minimize the ground state energy. However, as we show in Eq. (C20) in Appendix C, the expectation value

$$\langle e^{i\pi \sum_k b_k^\dagger b_k} \rangle_{\text{GS}} = e^{-\frac{1}{2} \Delta_R^T \Gamma_b^{-1} \Delta_R} \quad (92)$$

is always positive for a Gaussian state. Thus we expect state (91) to be a good variational wavefunction only in the even subspace ( $P_{\text{ex}} = 1$ ). To study the ground state and real-time dynamics in the odd subspace ( $P_{\text{ex}} = -1$ ), we could use the non-Gaussian state

$$|\Psi_{\text{NGS}}\rangle = U_{\text{parity}} |+\rangle U_3 |\Psi_{\text{GS}}^{\text{parity}}\rangle_b, \quad (93)$$

where  $U_3$  is applied to tune the weights of the excitations with even and odd numbers in the Gaussian state  $|\Psi_{\text{GS}}^{\text{parity}}\rangle_b$  such that for  $|\tilde{\Psi}\rangle = U_3 |\Psi_{\text{GS}}^{\text{parity}}\rangle_b$

$$\langle \tilde{\Psi} | e^{i\pi \sum_k b_k^\dagger b_k} | \tilde{\Psi} \rangle = \langle U_3^\dagger e^{i\pi \sum_k b_k^\dagger b_k} U_3 \rangle_{\text{GS}} \quad (94)$$

can be negative. In this paper we only discuss the ground state and spin dynamics in the even subspace ( $P_{\text{ex}} = 1$ ) and relegate analysis of the odd sector to future publications.

*Approach based on partial polaron transformation.*

Another approach to constructing variational non-Gaussian states for the spin-boson model is motivated by Silbey's partial polaron transformation [24]. We consider the ansatz

$$|\Psi_{\text{NGS}}\rangle = U_{\text{polaron}} |\Psi_{\text{GS}}^{\text{polaron}}\rangle_s |\Psi_{\text{GS}}^{\text{polaron}}\rangle_b, \quad (95)$$

where the polaron transformation  $U_{\text{polaron}} = e^{S_{\text{polaron}}}$  belongs to the class  $U_4$  with

$$S_{\text{polaron}} = iR^T \lambda \sigma_z. \quad (96)$$

This transformation contains  $2N_b$  variational parameters in the vector  $\lambda = (\lambda_{x,k}, \lambda_{p,k})^T$ . Since  $U_{\text{polaron}}$  preserves the parity  $P_{\text{ex}}$ , the Gaussian state  $|\Psi_{\text{GS}}^{\text{polaron}}\rangle_b = e^{i\theta_0} e^{-i\frac{1}{4} R^T \xi_b R} |0\rangle$  is a squeezed state with an even number of bosonic excitations in the bath, and the spin state  $|\Psi_{\text{GS}}^{\text{polaron}}\rangle_s = |\pm\rangle$  determines the parity  $P_{\text{ex}} = \mp 1$ .

We focus on the even subspace ( $P_{\text{ex}} = 1$ ), where the non-Gaussian ansatz

$$\begin{aligned} |\Psi_{\text{NGS}}\rangle &= U_{\text{polaron}} |-\rangle |\Psi_{\text{GS}}^{\text{polaron}}\rangle_b \\ &= \frac{1}{\sqrt{2}} (|\uparrow\rangle |\Psi^+\rangle - |\downarrow\rangle |\Psi^-\rangle) \end{aligned} \quad (97)$$

is determined by  $|\Psi^\pm\rangle = e^{\pm iR^T \lambda} |\Psi_{\text{GS}}^{\text{polaron}}\rangle_b$ . Comparing the states (91) and (97), we notice that these two transformations lead to the same variational state, where  $\lambda = \sigma \Delta_R / 2$ .

Following the polaron transformation, the Hamiltonian  $\bar{H}_{\text{polaron}} = U_{\text{polaron}}^\dagger H_{\text{SB}} U_{\text{polaron}}$  becomes

$$\begin{aligned} \bar{H}_{\text{polaron}} = & \frac{\Delta}{2}(\sigma_+ e^{-2iR^T \lambda} + \text{H.c.}) + \frac{1}{4} R^T \varepsilon R \\ & - \frac{1}{2} \sigma_z R^T G + C_0, \end{aligned} \quad (98)$$

where the matrix  $\varepsilon = \mathbb{1}_2 \otimes \text{diag}(\varepsilon_k)$ , the vector  $G = (g_k + 2\varepsilon_k \lambda_{p,k}, -2\varepsilon_k \lambda_{x,k})^T$ , and  $C_0 = \lambda^T \varepsilon \lambda + g^T \lambda_p - \sum_k \varepsilon_k/2$  is defined by the vector  $g^T = (g_1, \dots, g_k, \dots)$ .

We remark that the Hamiltonian  $\bar{H}_{\text{polaron}}$  differs from the previously considered setting of Bose/Fermi systems because it contains spin operators. We can however proceed with our usual framework using a fermionic representation of spin operators. We define  $\sigma_+ = c_\uparrow^\dagger c_\downarrow$  and  $\sigma_z = c_\uparrow^\dagger c_\uparrow - c_\downarrow^\dagger c_\downarrow$ . The covariance matrix of the two-mode fermions is  $\Gamma_f = \langle CC^\dagger \rangle$ , where  $C = (c_\uparrow, c_\downarrow, c_\uparrow^\dagger, c_\downarrow^\dagger)^T$ . To describe the spin in the two-dimensional Hilbert space, the four-dimensional fermionic space must be restricted to the single occupation subspace. Then the pairing terms  $\langle c_\downarrow c_\uparrow \rangle$  and  $\langle c_\uparrow c_\downarrow \rangle$  are not allowed and  $\Gamma_f$  is block-diagonal.

In the next three subsections we present results for the ground state properties and real-time dynamics in the even subspace using only one of the transformations, since results for the other one should be identical.

### C. Parity transformation

In this subsection, we derive the equations of motion for  $\Delta_R$  and  $\Gamma_b$  in the non-Gaussian state (91) given by the parity transformation. Following the procedure in Appendix E, we obtain Eqs. (30) and (31) for the imaginary- and real-time evolutions, which are equivalent to Eqs. (E28) and (E29) with  $O_\Delta = 0$  and  $O_b = 0$ .

As shown in Eq. (E11), the vector  $h_\Delta = h_\Delta^t = 2\delta E_{\text{parity}}/\delta \Delta_R$  and the matrix  $h_b = h_b^t = 4\delta E_{\text{parity}}/\delta \Gamma_b$  are determined by the functional derivatives. The energy  $E_{\text{parity}} = \langle \bar{H}_{\text{parity}} \rangle_{\text{GS}}$  is

$$\begin{aligned} E_{\text{parity}} = & \frac{1}{4} \Delta_R^T \varepsilon \Delta_R + \frac{1}{4} \text{tr}(\varepsilon \Gamma_b) - \frac{1}{2} \sum_k \varepsilon_k \\ & - \frac{\Delta}{2} e^{-\frac{1}{2} \Delta_R^T \Gamma_b^{-1} \Delta_R} - \frac{1}{2} \sum_k g_k \langle x_k \rangle. \end{aligned} \quad (99)$$

It follows from Eqs. (99) and (E11) that

$$\begin{aligned} h_\Delta = & \varepsilon \Delta_R + \Delta e^{-\frac{1}{2} \Delta_R^T \Gamma_b^{-1} \Delta_R} \Gamma_b^{-1} \Delta_R - \begin{pmatrix} g \\ 0 \end{pmatrix}, \\ h_b = & \varepsilon - \Delta e^{-\frac{1}{2} \Delta_R^T \Gamma_b^{-1} \Delta_R} \Gamma_b^{-1} \Delta_R \Delta_R^T \Gamma_b^{-1}. \end{aligned} \quad (100)$$

Here,  $(g, 0)^T$  is a short hand notation for  $(g_1, g_2, \dots, g_k, 0, \dots, 0)^T$ . By solving Eqs. (30) and (31) with  $h_\Delta$  and  $h_b$  determined by Eq. (100), we obtain  $\Delta_R$  and  $\Gamma_b$  in the ground state and the real-time

dynamics. In the ground state, the solution of  $\Delta_R$  satisfies the nonlinear equation

$$\Delta_R = \frac{1}{\varepsilon + \Delta e^{-\frac{1}{2} \Delta_R^T \Gamma_b^{-1} \Delta_R} \Gamma_b^{-1}} \begin{pmatrix} g \\ 0 \end{pmatrix} \quad (101)$$

obtained from the fixed point condition  $h_\Delta = 0$ .

### D. Polaron transformation

In this subsection, we derive the equations of motion for  $\Delta_R$ ,  $\Gamma_{b,f}$ , and  $\lambda$  in the non-Gaussian state defined by the polaron transformation (95) and (96). We follow the general procedure discussed in Appendix E [see equations (E28) and (E29)] to determine time evolution of  $\lambda$ ,  $\Delta_R$ , and  $\Gamma_{b,f}$ . Expressions for the vectors  $O_\Delta$ ,  $h_\Delta$  and matrices  $O_{b,f}$ ,  $h_{b,f}$  can be obtained using functional derivatives as discussed in Eq. (E4), where the mean-values are

$$\langle O \rangle_{\text{GS}} = i\lambda^T \sigma \partial_\tau \lambda + i\Delta_R^T \partial_\tau \lambda \langle \sigma_z \rangle_{\text{GS}}, \quad (102)$$

and  $\langle \bar{H}_{\text{polaron}} \rangle_{\text{GS}} \equiv E_{\text{polaron}}$ :

$$\begin{aligned} E_{\text{polaron}} = & \Delta \text{Re} \langle \sigma_+ \rangle_{\text{GS}} \left\langle e^{-2iR^T \lambda} \right\rangle_{\text{GS}} + \frac{1}{4} \Delta_R^T \varepsilon \Delta_R \\ & + \frac{1}{4} \text{tr}(\varepsilon \Gamma_b) - \frac{1}{2} \langle \sigma_z \rangle_{\text{GS}} \Delta_R^T G + C_0. \end{aligned} \quad (103)$$

The expectation value  $\left\langle e^{-2iR^T \lambda} \right\rangle_{\text{GS}} = e^{-2i\Delta_R^T \lambda} e^{-2\lambda^T \Gamma_b \lambda}$  follows from Eq. (C3), and  $\langle \sigma_{z,\pm} \rangle_{\text{GS}}$  can be easily expressed as linear combinations of the matrix elements  $(\Gamma_f)_{ij}$ .

The functional derivatives of  $\langle O \rangle_{\text{GS}}$  and  $E_{\text{polaron}}$  result in

$$O_\Delta = 2i\partial_\tau \lambda \langle \sigma_z \rangle_{\text{GS}}, O_b = 0, O_f = \tau_z \otimes i\Delta_R^T \partial_\tau \lambda \tau_z, \quad (104)$$

and

$$\begin{aligned} h_\Delta = & \varepsilon \Delta_R + 4\Delta \text{Im} \langle \sigma_+ \rangle_{\text{GS}} \left\langle e^{-2iR^T \lambda} \right\rangle_{\text{GS}} \lambda - \langle \sigma_z \rangle_{\text{GS}} G, \\ h_b = & \varepsilon - 8\Delta \text{Re} \langle \sigma_+ \rangle_{\text{GS}} \left\langle e^{-2iR^T \lambda} \right\rangle_{\text{GS}} \lambda \lambda^T, \\ h_f = & \tau_z \otimes \frac{1}{2} [\Delta (\left\langle e^{-2iR^T \lambda} \right\rangle_{\text{GS}} \tau_+ + \text{H.c.}) - \Delta_R^T G \tau_z], \end{aligned} \quad (105)$$

where  $\tau_{z,\pm}$  are Pauli matrices defined in the basis  $C = (c_\uparrow, c_\downarrow, c_\uparrow^\dagger, c_\downarrow^\dagger)^T$ . The coefficients (104) and (105) in the normal ordering expansion lead to Eqs. (E28) and (E29) for  $\Delta_R$  and  $\Gamma_b$ .

The equations of motion for  $\lambda$  can be obtained using the projection on the tangent vector  $U_{\text{polaron}} U_{\text{GS}} |D_k\rangle$  that is equivalent to the projection of states (E6) and (E12) on the state  $|D_k\rangle = b_k^\dagger U_{\text{GS}}^\dagger \sigma_z U_{\text{GS}} |0\rangle$ , as shown in Appendix E. The projection leads to

$$\begin{aligned} \langle D_k | \delta O | 0 \rangle &= -\langle D_k | \delta \bar{H}_{\text{polaron}} | 0 \rangle, \\ \langle D_k | \delta O | 0 \rangle &= -i \langle D_k | \delta \bar{H}_{\text{polaron}} | 0 \rangle, \end{aligned} \quad (106)$$

for the imaginary- and real- time evolutions, respectively, where the operator  $\delta O = iR^T S_b^T \partial_\tau \lambda \tilde{\sigma}_z$  and the cubic operator

$$-\frac{1}{2}R^T S_b^T G \tilde{\sigma}_z - i\Delta \left\langle e^{-2iR^T \lambda} \right\rangle_{\text{GS}} R^T S_b^T \lambda \tilde{\sigma}_+ + \text{H.c.} \quad (107)$$

$$\begin{aligned} (1 - \langle \sigma_z \rangle_{\text{GS}}^2) \sigma \partial_\tau \lambda &= 2\Delta \text{Re}(\langle \sigma_+ \rangle_{\text{GS}} \left\langle e^{-2iR^T \lambda} \right\rangle_{\text{GS}}) \sigma \lambda - 2\Delta \langle \sigma_z \rangle_{\text{GS}} \text{Im}(\langle \sigma_+ \rangle_{\text{GS}} \left\langle e^{-2iR^T \lambda} \right\rangle_{\text{GS}}) \Gamma_b \lambda - \frac{1}{2}(1 - \langle \sigma_z \rangle_{\text{GS}}^2) \Gamma_b G, \\ (1 - \langle \sigma_z \rangle_{\text{GS}}^2) \partial_t \lambda &= -2\Delta \text{Re}(\langle \sigma_+ \rangle_{\text{GS}} \left\langle e^{-2iR^T \lambda} \right\rangle_{\text{GS}}) \sigma \Gamma_b \lambda + 2\Delta \langle \sigma_z \rangle_{\text{GS}} \text{Im}(\langle \sigma_+ \rangle_{\text{GS}} \left\langle e^{-2iR^T \lambda} \right\rangle_{\text{GS}}) \lambda + \frac{1}{2}(1 - \langle \sigma_z \rangle_{\text{GS}}^2) G. \end{aligned} \quad (108)$$

The solution of Eqs. (E28), (E29), and (108) in the even subspace has the following properties: (a)  $\Delta_R = 0$  and (b)

$$\langle \sigma_+ \rangle_{\text{GS}} = \langle \sigma_- \rangle_{\text{GS}} = -\frac{1}{2}, \langle \sigma_z \rangle_{\text{GS}} = 0, \quad (109)$$

which imply that in Eq. (95) the Gaussian state  $|\Psi_{\text{GS}}^{\text{polaron}}\rangle_s$  of the impurity is  $|-\rangle$  and the Gaussian state  $|\Psi_{\text{GS}}^{\text{polaron}}\rangle_b$  of the bath is a squeezed state, as we discussed in Sec. IV B. The squeezing part of the bosonic wavefunction around the impurity is described by  $\Gamma_b$  and  $\lambda$ , which obey equations of motion

$$\begin{aligned} \partial_\tau \Gamma_b &= \sigma^T h_b \sigma - \Gamma_b h_b \Gamma_b, \\ \partial_\tau \lambda &= -\Delta e^{-2\lambda^T \Gamma_b \lambda} \lambda + \frac{1}{2} \sigma \Gamma_b G, \end{aligned} \quad (110)$$

and

$$\begin{aligned} \partial_t \Gamma_b &= \sigma h_b \Gamma_b - \Gamma_b h_b \sigma, \\ \partial_t \lambda &= \Delta e^{-2\lambda^T \Gamma_b \lambda} \sigma \Gamma_b \lambda + \frac{1}{2} G, \end{aligned} \quad (111)$$

for the imaginary- and real- time evolution respectively.

In the ground state, the fixed point condition  $\partial_\tau \lambda = 0$  results in

$$\sigma \lambda = -\frac{1}{2} \frac{1}{\Delta e^{-2\lambda^T \Gamma_b \lambda} \Gamma_b^{-1} + \varepsilon} \begin{pmatrix} g \\ 0 \end{pmatrix}. \quad (112)$$

It immediately follows from Eqs. (101) and (112) that  $\lambda = \sigma \Delta_R / 2$  is in agreement with the result of Sec. IV B.

### E. Numerical results

In this subsection, we study the ground state and non-equilibrium dynamics of the anisotropic Kondo model in different parameter regimes. We use the transformation between the Kondo and spin-boson Hamiltonians

in  $\delta \bar{H}_{\text{polaron}}$  are determined by the normal ordered operators  $\tilde{\sigma}_{z,\pm} = U_{\text{GS}}^\dagger \sigma_{z,\pm} U_{\text{GS}}$ . Relation (106) then leads to the motion equations

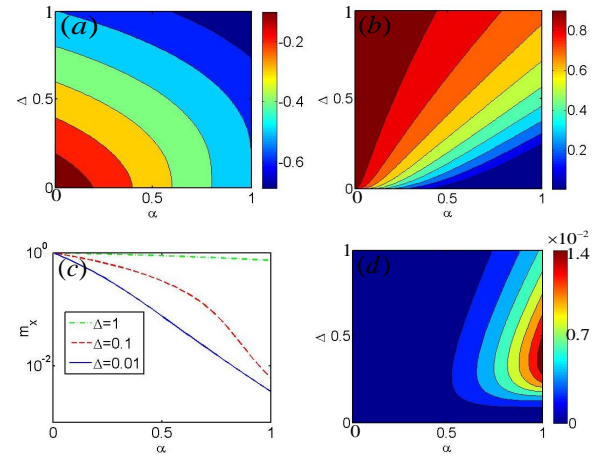


FIG. 8: The ground state energy, the magnetization, and the square norm  $\mathcal{N}_\perp$  in the  $\alpha$ - $\Delta$  plane for the spin-boson model with the Ohmic spectrum, where the frequency cut-off  $\omega_c$  is taken as the unit, and the system size is  $N_b = 200$ . (a) The ground state energy  $E_{\text{GS}}$ ; (b) The magnetization  $m_x$  along  $x$ -direction; (c) The magnetization along the cuts  $\Delta = 0.01, 0.1$ , and  $1$ ; (d) The small norm  $\mathcal{N}_\perp$ .

$|\Psi_{\text{NGS}}^{\text{K}}\rangle = U_{\gamma=1} |\Psi_{\text{NGS}}^{\text{SB}}\rangle$  (see discussion above) to translate the problems into the spin-boson model and analyze the latter. We remind the readers that Kondo Hamiltonian is mapped to the spin-boson models with Ohmic dissipation, i.e.,  $\varepsilon_k \equiv k$  and  $g_k = \sqrt{2\alpha\omega_c k/N_b} \theta(\omega_c - k)$ . The relation between the interaction parameters in the two models is  $\alpha = [1 - J_\parallel/(4\pi)]^2$  ( $\alpha = 1/2$  is the Toulouse point). To analyze the spin-boson model we solve equations (E28), (E29), and (108) numerically, using the cut-off frequency  $\omega_c$  as the unit of energy. We used mode discretization as  $k = \omega_c n_k / N_b$  where  $n_k = 1, 2, \dots, N$  and  $N_b$ . Since the parity and polaron transformations lead to equivalent variational states, numerical results obtained using Eqs. (100), (110), and (111) give identical results. In the numerical calculation we use the same energy level spacing  $\omega_c/N_b = 2\pi/L$  for the bath field in the spin-boson and Kondo models, and the short-distance cut-off

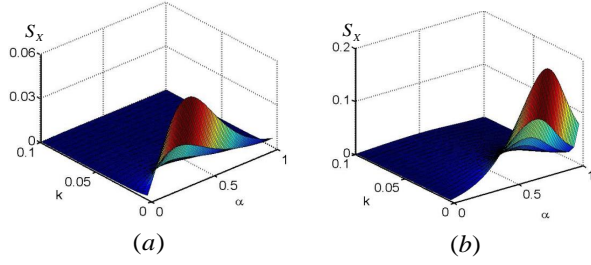


FIG. 9: The squeezing parameters  $S_X$  for  $\Delta = 0.01$  (a) and  $\Delta = 0.1$  (b). Here, system size  $N_b = 200$ .

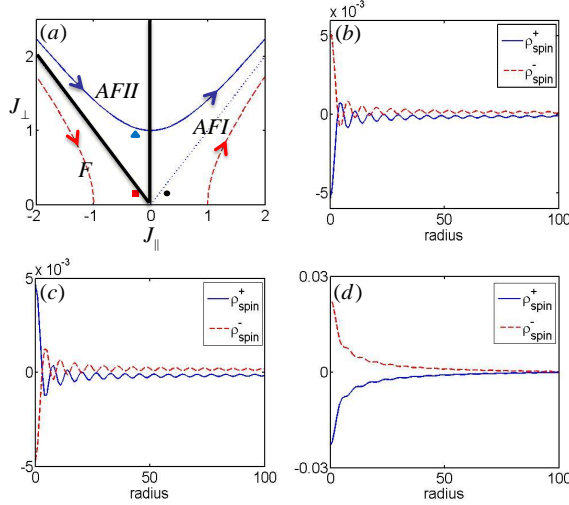


FIG. 10: (a) Phase diagram and RG flows of Kondo model. (b)-(d) The spin density fluctuations display the transition between the antiferromagnetic and ferromagnetic phases, where  $N_b = 200$ : (b)  $J_\perp = 0.1$  and  $J_\parallel = 0.2$ ; (c)  $J_\perp = 0.1$  and  $J_\parallel = -0.2$ ; (d)  $J_\perp = 1$  and  $J_\parallel = -0.2$ .

$l_c$  in equation (80) and the sharp frequency cut-off  $\omega_c$  in equation (77) are related via

$$\psi(N_b + 1) + \gamma_0 = -\ln(1 - e^{-\frac{\omega_c}{N_b} l_c}), \quad (113)$$

Here  $\psi(z)$  is the digamma function and  $\gamma_0$  is Euler constant.

In Fig. 8a-b, we show the ground state energy  $E_{GS} = E_{\text{parity}} = E_{\text{polaron}}$  and the magnetization

$$m_x = -\langle \sigma_x \rangle = e^{-2\lambda^T \Gamma_b \lambda} \quad (114)$$

in the  $\alpha$ - $\Delta$  parameter plane. In Fig. 8c, the magnetization  $m_x$  is shown along the horizontal cuts  $\Delta = 0.01, 0.1$ , and  $1$ . Compared with the Silbey transformation [24], results for the magnetization  $m_x$  are considerably improved and are in excellent agreement with the NRG calculation [25]. To check the validity of the variational approach we can check the energy variance  $\mathcal{N}_\perp = \|\Psi_\perp\|^2$ , i.e., the square norm

$$\mathcal{N}_\perp = \frac{\Delta^2}{8} (2 - e^{-4y}) - 2\Delta^2 e^{-4y} (y + \frac{1}{4})^2 \quad (115)$$

of the state  $|\Psi_\perp\rangle$  orthogonal to the tangent space in the limit  $\tau \rightarrow \infty$ , where  $y = \lambda^T \Gamma_b \lambda$ . In Fig. 8d, the small energy variance  $\mathcal{N}_\perp < 1.5 \times 10^{-2}$  in the  $\alpha$ - $\Delta$  plane justifies the validity of the non-Gaussian variational state in the even excitation subspace.

The magnetization  $m_x$  in Figs. 8b-c shows that for fixed  $\Delta$ , increasing the coupling constant  $\alpha$  reduces the magnetization. For a small coupling constant  $\alpha \ll 1$ , the state (91) in the even subspace can be approximated as  $|- \rangle |0\rangle$ . As  $\alpha$  increases, the spin is entangled with the bath degree of freedom. When the weights  $|\text{even}\rangle^2 \sim |\text{odd}\rangle^2$ , the spin magnetization  $m_x \sim 0$  due to the strong entanglement.

The main difference between the variational ansatz (97) and the variational state  $e^{S_{\text{polaron}}} |- \rangle |0\rangle_b$  used by Silbey and collaborators (see e.g. Ref. [24]) is the vacuum state of the bath degrees of freedom. The imaginary time evolution allows us to minimize the energy with respect to the covariance matrix with  $\sim 3N_b^2$  variational parameters. Figure 9 shows the  $k$ -mode squeezing parameter  $(S_X)_k = \langle x_k^2 \rangle - 1$ , where  $\Delta = 0.01$  and  $\Delta = 0.1$  in Figs. 9a and 9b, respectively. The low frequency modes are squeezed along the  $p$ -direction in phase space, and the high frequency modes are in the vacuum state. As  $\Delta$  increases, the peak position of  $S_X$  shifts towards a larger  $\alpha$ , and the peak value increases.

The ground state

$$|\Psi_{\text{NGS}}^K\rangle = \frac{1}{\sqrt{2}} (|\uparrow\rangle |\Psi_{\text{sdw}}^+\rangle - |\downarrow\rangle |\Psi_{\text{sdw}}^-\rangle) \quad (116)$$

of the Kondo model describes the spin density configuration in the fermionic bath by  $|\Psi_{\text{sdw}}^\pm\rangle = e^{\pm i\sqrt{2}\phi_s(0)/2} |\Psi^\pm\rangle$ . The spin density fluctuation around the impurity is characterized by

$$\begin{aligned} \rho_{\text{spin}}^\pm &= \frac{1}{\sqrt{2}\pi} \langle \Psi_{\text{sdw}}^\pm | \partial_x \phi_s(x) | \Psi_{\text{sdw}}^\pm \rangle \\ &= \mp \frac{\omega_c}{\pi N_b} \sum_{q>0} [\sqrt{2n_q} \lambda_{x,q} \sin qx + \\ &\quad (1 + \sqrt{2n_q} \lambda_{p,q}) \cos qx]. \end{aligned} \quad (117)$$

It is well-known that the anisotropic Kondo model exhibits a quantum phase transition between the ferromagnetic and antiferromagnetic phases [54]. In Fig. 10a we show the phase diagram in the  $J_\perp$ - $J_\parallel$  parameter plane. We label the antiferromagnetic phase ( $J_\parallel > 0$ ) “AFI”, the upper-left triangular antiferromagnetic phase ( $J_\perp > -J_\parallel > 0$ ) “AFII”, and the lower-left triangular ferromagnetic phase ( $-J_\parallel > J_\perp > 0$ ) “F”. The renormalization flows in different regions are shown by the arrows.

In Figs. 10b-c, the spin density distributions of the ground states are shown for the “AFI” phase (the black dot in Fig. 10a) and the “F” phase (the red square in Fig. 10a), which display the singlet and triplet pairs of the impurity spin and the surrounding electrons. In Fig. 10d, the spin density distributions for the “AFII” phase

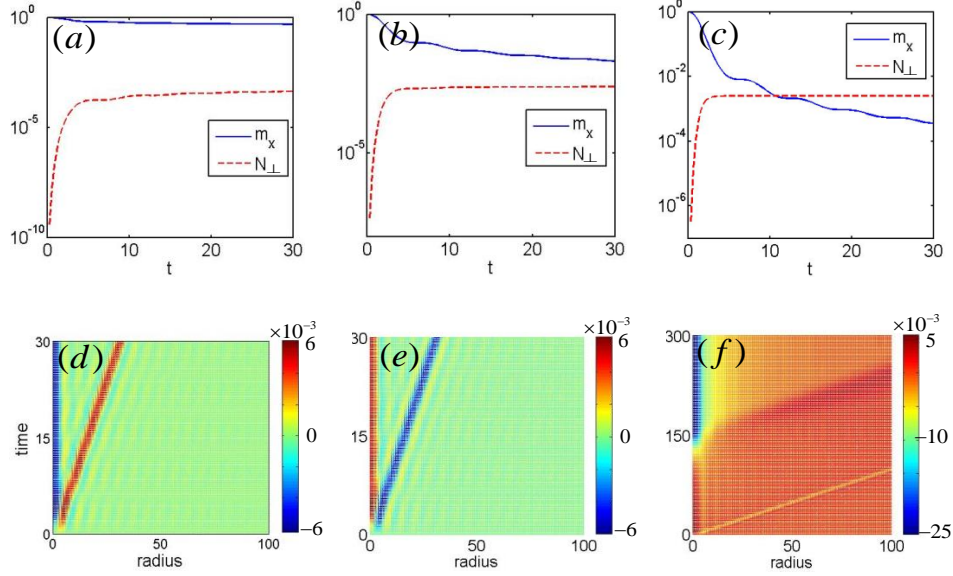


FIG. 11: (a)-(c) Time evolution of the magnetization  $m_x$  and the square norm  $N_\perp$  for  $\Delta = 0.01$  and the initial state  $|- \rangle |0\rangle_b$ , where  $\alpha = 0.1, 0.5$ , and  $1.2$  in (a), (b), and (c), respectively; system size  $N_b = 200$ . (d)-(f) Time evolutions of spin density fluctuations for the initial state  $|- \rangle |\text{FS}\rangle$  in antiferromagnetic and ferromagnetic phases of Kondo model, where  $J_\perp = 0.1$  and  $J_\parallel = 0.2$  (d),  $J_\perp = 0.1$  and  $J_\parallel = -0.2$  (e), and  $J_\perp = 1$  and  $J_\parallel = -0.2$  (f).

(the blue triangle) exhibit an antiferromagnetic ground state.

In Figs. 11a-c, for the system initially prepared in the state  $|- \rangle |0\rangle_b$ , we show time evolutions of the magnetization  $m_x(t)$  for different coupling strength  $\alpha = 0.1$  (a),  $0.5$  (b), and  $1$  (c), with  $\Delta = 0.01$ . The small square norm  $N_\perp < 2 \times 10^{-3}$  justifies the validity of the variational state. The larger the coupling constant  $\alpha$ , the faster the magnetization  $m_x(t)$  relaxes to zero, which agrees with our intuition regarding the entanglement between the spin and the bosonic bath described by the states (91) and (97).

Time evolution of the spin density configuration  $\rho_{\text{spin}}^+ = -\rho_{\text{spin}}^-$  for  $J_\perp = 0.1$  and  $J_\parallel = 0.2$  (Fig. 11d),  $J_\perp = 0.1$  and  $J_\parallel = -0.2$  (Fig. 11e), and  $J_\perp = 1$  and  $J_\parallel = -0.2$  (Fig. 11f) are shown in Figs. 11d-f. The initial state  $|- \rangle |\text{FS}\rangle$  describes the impurity spin in the state  $|- \rangle$  and the unperturbed Fermi sea. Note that  $b_{qs} |\text{FS}\rangle = 0$  indicates that there are no spin density fluctuations in the initial state.

Figure 11d shows that in the AFI regime, following the quench bath electrons quickly screen the impurity spin. This is consistent with our intuition of the spin singlet ground state in the AF Kondo model. Formation of the screening cloud is accompanied by the spin wavepacket propagating away from the impurity. Figure 11e shows the spin dynamics in the opposite regime of the ferromagnetic phase F. In this case, bath electrons become co-aligned with the impurity spin, which is what we expect based on the triplet ground state of the system. Notice again a single wavepacket propagating away from the im-

purity. The AFII phase shows the most surprising case of the dynamics. At short times, the electron bath develops a polarization which is co-aligned with the impurity spin. However, at longer times, the polarization cloud changes sign and we find the impurity spin screened by the surrounding electrons. This polarization cloud dynamics is accompanied by two wavepackets propagating away from the impurity. The first one appears when the electrons develop a transient ferromagnetic cloud around the impurity, and the second one when the final antiferromagnetic cloud is formed. This two-stage spin dynamics is easily understood if we consider the RG flow diagram in Fig. 10a. Short time dynamics corresponds to the high energy Hamiltonian characterized by the ferromagnetic  $J_\parallel$  interactions. At longer times we observe low energy degrees of freedom, which correspond to the antiferromagnetic  $J_\parallel$  arising from the RG flow in Fig. 10a.

## F. Summary of Section IV

We now summarize the main results obtained in this section. We introduced variational approach for describing the ground state and non-equilibrium dynamics of the spin-boson model. This model is known to be equivalent to the Kondo Hamiltonian, hence our results have direct implications for the non-equilibrium dynamics in Kondo-related systems, such as transport through a quantum dot [57]. We showed that variational approaches can be introduced either utilizing the conserved parity operator or using a Silbey-type polaron transformation. Sur-

prisingly both approaches result in the same variational family of wavefunctions. We used this class of wavefunctions to analyze the ground state of the Kondo problem and found excellent agreement with the results of earlier studies. Our variational approach improves over earlier variational states introduced by Silbey and collaborators by including squeezing between the bosonic bath modes, which becomes significant for larger values of dissipation strength  $\alpha$ . We applied our variational wavefunctions to study the non-equilibrium dynamics of the Kondo model with a focus on the dynamical formation of electron spin polarization following a rapid introduction of the impurity spin. In the regime of anti-ferromagnetic interaction in  $J_{\parallel}$  we found the formation of the screening cloud with faster relaxation for larger  $J_{\parallel}$ . In the regime of ferromagnetic easy axis in  $J_{\parallel}$  we observed the dynamics of surrounding electrons getting co-aligned with the impurity spin. Our most surprising results were obtained in the regime of ferromagnetic  $J_{\parallel}$  with easy plane anisotropy. We observed a transient ferromagnetic cloud formation, which was followed by the ultimate formation of the screening cloud. These dynamics are in agreement with the equilibrium RG flow diagram. We are not aware of earlier work on dynamics of the Kondo in the latter regime. Its special challenge is the requirement of analyzing both the low temperature and long time dynamics, which is crucial for capturing the dynamical crossover. In all cases we examined the validity of the non-Gaussian approximation by evaluating  $\mathcal{N}_{\perp}$  [see Eq (115)].

## V. SUPERCONDUCTING AND CDW PHASES IN HOLSTEIN MODELS

In this section, we investigate the quantum phase transition between the SC and CDW phases in the Holstein model. In contrast to our discussion in Section III, here we consider systems with a finite electron density. An important feature of the Holstein model that will play a prominent role in our analysis is that phonons interact with electrons locally, i.e., phonon operators couple to the on-site energy of electrons. The system Hamiltonian reads

$$H = \sum_{nm} (\omega_b)_{nm} b_n^{\dagger} b_m + \sum_{nm,\sigma} t_{nm} c_{n\sigma}^{\dagger} c_{m\sigma} - \mu \sum_{n,\sigma} c_{n\sigma}^{\dagger} c_{n\sigma} + g \sum_{n,\sigma} c_{n\sigma}^{\dagger} c_{n\sigma} (b_n + b_n^{\dagger}). \quad (118)$$

For the Einstein phonon  $(\omega_b)_{nm} = \omega_0 \delta_{nm}$ , the Holstein model has been studied extensively using the Lang-Firsov type polaron transformation  $U = e^S$  characterized by a single variational parameter

$$S = i\lambda \sum_n p_n c_{n\sigma}^{\dagger} c_{n\sigma}. \quad (119)$$

After this transformation, the effective electron-phonon interaction in the Hamiltonian  $\bar{H} = e^{-S} H e^S$  is reduced, the effective hopping strength is suppressed, reflecting the so-called polaronic dressing, and there is explicit attractive interaction between electrons. The ground state of  $\bar{H}$  is then approximated using a vacuum state of phonons and a Slater determinant state for electrons. Our goal is to introduce a broader class of variational states, which can provide a better description of the Holstein model (see also [58]). Firstly we point out that the procedure outlined above is equivalent to analyzing a non-Gaussian state

$$|\Psi_{\text{NGS}}\rangle = e^S |\Psi_{\text{GS}}\rangle_f |0\rangle_b, \quad (120)$$

where  $|\Psi_{\text{GS}}\rangle_f$  is the Gaussian state of electrons and  $|0\rangle_b$  is the vacuum state of phonons. The parameter  $\lambda$  can be obtained by the minimization of the ground state energy  $E = \langle \Psi_{\text{NGS}} | H | \Psi_{\text{NGS}} \rangle$ .

We notice that the non-Gaussian state (120) with the generating function (119) belongs to the family

$$|\Psi_{\text{NGS}}\rangle = e^S |\Psi_{\text{GS}}\rangle_f |\Psi_{\text{GS}}\rangle_b \quad (121)$$

with the general generating function

$$S = i \sum_{n,m\sigma} (x_n \lambda_{n,m\sigma}^x + p_n \lambda_{n,m\sigma}^p) c_{m\sigma}^{\dagger} c_{m\sigma}. \quad (122)$$

Since the state (121) contains many variational parameters  $\lambda_{n,m\sigma}^{x,p}$ ,  $\Delta_R$ , and  $\Gamma_{b,f}$ , the brute force minimization of  $E$  may seem difficult and inefficient. However, a variational approach utilizing wavefunction evolution in imaginary time strongly reduces the difficulty of the problem. As we discuss below it is possible to analyze the ground state of the Holstein model using the full set of variational parameters in Eq. (122).

To find the ground state of the Holstein model with local electron-phonon interaction, it suffices to limit the generating function to the form

$$S = i \sum_{n,m\sigma} p_n \lambda_{n,m\sigma} c_{m\sigma}^{\dagger} c_{m\sigma}. \quad (123)$$

Notice that the last equation is a special case of Eq. (122) with  $\lambda_{n,m\sigma}^x = 0$  and  $\lambda_{n,m\sigma}^p \equiv \lambda_{n,m\sigma}$  (see discussion below for justification of setting  $\lambda^x = 0$ ). In the next subsections, we derive the equations of motion for  $\lambda_{n,m\sigma}$ ,  $\Delta_R$ , and  $\Gamma_{b,f}$  in the imaginary time evolution, which we use to find the non-Gaussian state (121) with the minimal energy.

### A. Equations of motion for the variational parameters

For the imaginary time evolution, the vectors  $O_{\Delta}$ ,  $h_{\Delta}$  and the matrices  $O_{b,f}$ ,  $h_{b,f}$  in the flow Eqs. (E28) and



(E30) are determined by the functional derivatives of the average values

$$\begin{aligned}\langle O \rangle_{\text{GS}} &= \langle e^{-S} \partial_\tau e^S \rangle_{\text{GS}} \\ &= i \sum_{l, n\sigma} \langle p_l \rangle_{\text{GS}} \partial_\tau \lambda_{l, n\sigma} \langle c_{n\sigma}^\dagger c_{n\sigma} \rangle_{\text{GS}}\end{aligned}\quad (124)$$

and  $E = \langle \bar{H} \rangle_{\text{GS}}$ .

The energy

$$\begin{aligned}E &= \sum_{nm, \sigma} t_{nm} \left\langle e^{-i \sum_l R_l w_{l, nm\sigma}} \right\rangle_{\text{GS}} \langle c_{n\sigma}^\dagger c_{m\sigma} \rangle_{\text{GS}} - \sum_{n, \sigma} \mu_{n, \sigma} \langle c_{n\sigma}^\dagger c_{n\sigma} \rangle_{\text{GS}} + \frac{1}{2} \sum_{n\sigma, ms} V_{n\sigma, ms}^e \langle c_{n\sigma}^\dagger c_{ms}^\dagger \rangle_{\text{GS}} \langle c_{ms} c_{n\sigma} \rangle_{\text{GS}} \\ &+ \frac{1}{2} \sum_{n\sigma, ms} V_{n\sigma, ms}^e \langle c_{n\sigma}^\dagger c_{n\sigma} \rangle_{\text{GS}} \langle c_{ms}^\dagger c_{ms} \rangle_{\text{GS}} - \frac{1}{2} \sum_{n\sigma, ms} V_{n\sigma, ms}^e \langle c_{n\sigma}^\dagger c_{ms} \rangle_{\text{GS}} \langle c_{ms}^\dagger c_{n\sigma} \rangle_{\text{GS}} \\ &+ \frac{1}{4} \text{tr}(\omega \Gamma_b) + \frac{1}{4} \Delta_R^T \omega \Delta_R + \sum_{l, n\sigma} \delta g_{l, n\sigma} \langle x_l \rangle_{\text{GS}} \langle c_{n\sigma}^\dagger c_{n\sigma} \rangle_{\text{GS}} - \frac{1}{2} \sum_n \omega_{nn}\end{aligned}\quad (125)$$

is obtained by means of the Wick theorem, where the matrix  $w_{l, nm\sigma} = (0_{N \times 2N^2}, \lambda_{ln, \sigma} - \lambda_{lm, \sigma})^T$  contains the  $N \times 2N^2$ -dimensional zero matrix  $0_{N \times 2N^2}$ , the site-dependent chemical potential  $\mu_{n, \sigma} = \mu - V_{n\sigma, n\sigma}^e/2$ , the effective electron-electron interaction

$$V_{n\sigma, ms}^e = 2(\lambda^T \omega_b \lambda)_{n\sigma, ms} - 2g\lambda_{n, ms} - 2g\lambda_{m, n\sigma}, \quad (126)$$

$\omega = \mathbb{1}_2 \otimes \omega_b$ , and the renormalized electron-phonon interaction  $\delta g_{l, n\sigma} = g\delta_{ln} - (\omega_b \lambda)_{l, n\sigma}$ . The average values like  $\langle c_\alpha^\dagger c_\beta \rangle$  and  $\langle c_\alpha^\dagger c_\beta^\dagger \rangle$  are elements of the covariance matrix  $\Gamma_f$ , and the phonon-dressed hopping strength

$$\begin{aligned}\tilde{t}_{nm\sigma} &\equiv t_{nm} \left\langle e^{-i \sum_l R_l w_{l, nm\sigma}} \right\rangle_{\text{GS}} \\ &= t_{nm} e^{-i(\Delta_R^T w)_{nm\sigma}} e^{-\frac{1}{2}(w^T \Gamma_b w)_{nm\sigma, nm\sigma}}\end{aligned}\quad (127)$$

is obtained through Eq. (C3).

It follows from Eqs. (E4) and (E11) that the vectors

$$O_\Delta = 2i \sum_{n\sigma} \langle c_{n\sigma}^\dagger c_{n\sigma} \rangle_{\text{GS}} \begin{pmatrix} 0 \\ \partial_\tau \lambda_{l, n\sigma} \end{pmatrix}, \quad (128)$$

and

$$\begin{aligned}h_\Delta &= \omega \langle R \rangle + 2 \sum_{n\sigma} \langle c_{n\sigma}^\dagger c_{n\sigma} \rangle_{\text{GS}} \begin{pmatrix} \delta g_{l, n\sigma} \\ 0_N \end{pmatrix} \\ &- 2i \sum_{nm, \sigma} \tilde{t}_{nm\sigma} \langle c_{n\sigma}^\dagger c_{m\sigma} \rangle_{\text{GS}} w_{l, nm\sigma}\end{aligned}\quad (129)$$

are obtained by the functional derivatives of  $\langle O \rangle_{\text{GS}}$  and  $E$  with respect to  $\Delta_R$ . By the functional derivatives of  $E$  to  $\Gamma_b$ , we obtain the matrix  $O_b = 0$  and

$$(h_b)_{ll'} = \omega_{ll'} - 2 \sum_{nm, \sigma} \tilde{t}_{nm\sigma} \langle c_{n\sigma}^\dagger c_{m\sigma} \rangle_{\text{GS}} w_{l, nm\sigma} w_{nm\sigma, l'}^T. \quad (130)$$

The functional derivative of  $\langle O \rangle_{\text{GS}}$  with respect to  $\Gamma_f$  determines the matrix  $O_f = \tau_z \otimes o_f$ , where  $\tau_z$  is the Pauli

matrix, and the diagonal matrix  $o_f$  has nonzero elements  $(o_f)_{n\sigma, n\sigma} = i \sum_l \langle p_l \rangle_{\text{GS}} \partial_\tau \lambda_{l, n\sigma}$ . The mean-field single particle Hamiltonian

$$h_f = \begin{pmatrix} \mathcal{E} & \Delta \\ \Delta^\dagger & \mathcal{E}^T \end{pmatrix} \quad (131)$$

is determined by the functional derivative of  $E$  with respect to  $\Gamma_f$ , where the diagonal term

$$\mathcal{E}_{n\sigma, ms} = \tilde{t}_{nm\sigma} \delta_{\sigma s} - \tilde{\mu}_{n, \sigma} \delta_{nm} \delta_{\sigma s} - V_{n\sigma, ms}^e \langle c_{ms}^\dagger c_{n\sigma} \rangle_{\text{GS}} \quad (132)$$

contains the effective chemical potential

$$\tilde{\mu}_{n, \sigma} = \mu_{n, \sigma} - \sum_l \delta g_{l, n\sigma} \langle x_l \rangle_{\text{GS}} - \sum_{ms} V_{n\sigma, ms}^e \langle c_{ms}^\dagger c_{ms} \rangle_{\text{GS}}, \quad (133)$$

and the off-diagonal term is the order parameter  $\Delta_{n\sigma, ms} = V_{n\sigma, ms}^e \langle c_{ms} c_{n\sigma} \rangle_{\text{GS}}$ . To obtain flow equations for the Gaussian part of the wavefunction we use Eq. (E28) together with expressions (128)-(131).

Equations of motion for  $\lambda$  can be obtained by taking the projection of states (E6) and (E12) onto the states  $|D_{ln}\rangle = b_l^\dagger : U_{\text{GS}}^{-1} c_{n\sigma}^\dagger c_{n\sigma} U_{\text{GS}} : |0\rangle$ , i.e.,

$$\langle D_{ln} | \delta O | 0 \rangle = - \langle D_{ln} | \delta \bar{H} | 0 \rangle. \quad (134)$$

The state

$$\delta O | 0 \rangle = i \sum_{l, m\sigma} (R^T S_b^T)_l \partial_\tau \lambda_{l, m\sigma} : U_{\text{GS}}^{-1} c_{m\sigma}^\dagger c_{m\sigma} U_{\text{GS}} : | 0 \rangle \quad (135)$$

on the left hand side of Eq. (134) contains only the cubic operator acting on the vacuum state, and the cubic terms in the state  $\delta \bar{H} | 0 \rangle$  on the right hand side of Eq. (134) is

$$\begin{aligned}&[i \sum_{nm, \sigma} \tilde{t}_{nm\sigma} : U_{\text{GS}}^{-1} c_{n\sigma}^\dagger c_{m\sigma} U_{\text{GS}} : (R^T S_b^T w)_{nm\sigma} \\ &- \sum_{l, n\sigma} (R^T S_b^T)_l \delta \tilde{g}_{l, n\sigma} : U_{\text{GS}}^{-1} c_{n\sigma}^\dagger c_{n\sigma} U_{\text{GS}} :] | 0 \rangle, \quad (136)\end{aligned}$$



where the electron-phonon coupling matrix  $\delta\tilde{g} = (\delta g, 0_{N \times 2N})^T$ .

The projection (134) leads to the equation

$$\begin{aligned} \sum_{ms} \partial_\tau \lambda_{l,ms} \langle c_{ms}^\dagger c_{ms} c_{n\sigma}^\dagger c_{n\sigma} \rangle_c &= -i \frac{1}{2} \sum_{l'n's} (\Gamma_b)_{ll'} w_{l',n's} \tilde{t}_{n's} \langle \{c_{n\sigma}^\dagger c_{n\sigma}, c_{n's}^\dagger c_{ms}\} \rangle_c \\ &+ \sum_{l'ms} (\Gamma_b)_{ll'} \delta\tilde{g}_{l',ms} \langle c_{ms}^\dagger c_{ms} c_{n\sigma}^\dagger c_{n\sigma} \rangle_c + \sum_{l'm} \sigma_{ll'} w_{l',nm\sigma} \text{Re}(\tilde{t}_{nm\sigma} \langle c_{n\sigma}^\dagger c_{m\sigma} \rangle_{\text{GS}}), \end{aligned} \quad (137)$$

and the constraint

$$0 = \sum_{l'ms} (\Gamma_b)_{l_1 l'} \delta\tilde{g}_{l',ms} \langle c_{ms}^\dagger c_{ms} c_{n\sigma}^\dagger c_{n\sigma} \rangle_c - i \frac{1}{2} \sum_{l'n's} (\Gamma_b)_{l_1 l'} w_{l',n's} \tilde{t}_{n's} \langle \{c_{n\sigma}^\dagger c_{n\sigma}, c_{n's}^\dagger c_{ms}\} \rangle_c \quad (138)$$

In the equations above the connected correlation function is defined as  $\langle A_1 A_2 \rangle_c = \langle A_1 A_2 \rangle_{\text{GS}} - \langle A_1 \rangle_{\text{GS}} \langle A_2 \rangle_{\text{GS}}$ , and the indices  $1 \leq l \leq N$ ,  $1 + N \leq l_1 \leq 2N$ . Note that Eq. (138) has the form of a constraint only because we set  $\lambda_x = 0$  in Eq. (123). Otherwise, the left hand side of equation (138) would contain the  $\partial_\tau \lambda^x$  term.

The equation (137) determines the imaginary time flow of  $\lambda_{n,m}$ . In the next subsection, we show that the constraint (138) is automatically satisfied for the ground state in the SC and CDW phase of the Holstein model. We emphasize that  $\lambda_{n,m\sigma}^x = 0$  is only a special case of a more general class of transformations, which turns out to be sufficient for analyzing the ground state of the Holstein model. A special feature of the Holstein model which makes this simplification possible is the local character of the electron-phonon interaction. In cases of more general electron-phonon interacting systems, including the SSH model, the ansatz (121) with the full generating function (122) should be applied. Then, the term containing the time derivative  $\partial_\tau \lambda^x$  appears on the left-hand side of Eq. (138), which determines the variational state with the minimal ground state energy.

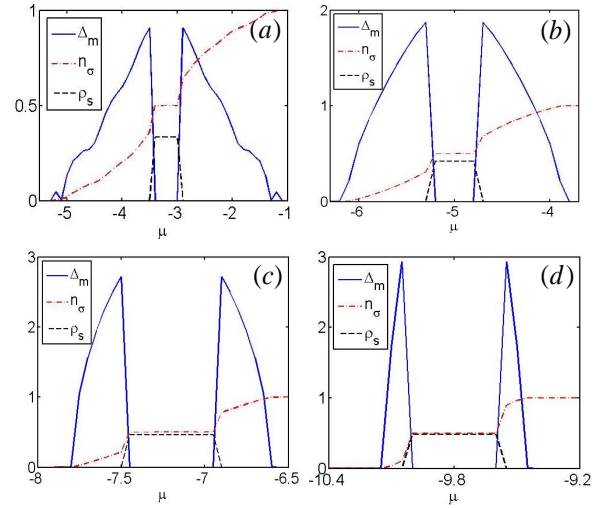


FIG. 12: The superconducting gap  $\Delta$ , the electron density  $n_\sigma$ , and the staggered component  $\rho_s$  for the  $10 \times 10$  lattice with the phonon frequency  $\omega_0 = 10t_0$ , where the hopping constant  $t_0$  is taken as the unit. (a)  $g = 0.4\omega_0$ ; (b)  $g = 0.5\omega_0$ ; (c)  $g = 0.6\omega_0$ ; (d)  $g = 0.7\omega_0$ .

duce

$$\lambda_{nm,\sigma} = \frac{1}{N} \sum_q \lambda_q e^{iq(n-m)}. \quad (139)$$

Note that the translational symmetry of  $\lambda_{n,m}$  does not rule out finite expectation values of  $\lambda_q$  for  $q \neq 0$ . On the other hand, the phonon displacements  $R$  can only have finite expectation value at  $q = 0$  in states which do not break translational invariance.

Results of our analysis are presented in Figs. 12 and 13. We find that away from half-filling, i.e., when the electron density  $n_\sigma = \sum_n \langle c_{n\sigma}^\dagger c_{n\sigma} \rangle / N \neq 0.5$ , the system is in the superconducting phase, which preserves translational symmetry. There is a uniform displacement of all local phonons given by  $d_j = \langle \Psi_{\text{NGS}} | x_j | \Psi_{\text{NGS}} \rangle =$

## B. Transitions between superconducting and CDW phases

We now analyze the phase diagram of the 2D Holstein model by numerically solving flow Eqs. (E29) and (137). We consider Hamiltonian (118) with the nearest neighbor hopping  $t_{nm} = -t_0 \delta_{mn+e_\alpha}$ , where  $m = n + e_\alpha$  correspond to nearest neighboring sites in the  $\alpha = x, y$  directions. We assume an Einstein model of dispersionless phonons with  $\omega_{b,nm} = \omega_0 \delta_{nm}$ .

The variational parameter  $\lambda_{n,m}$  that do not break translational symmetry only depends on the difference between sites  $n$  and  $m$ , hence it is convenient to intro-

$-4gn_\sigma/\omega_0$ . To describe electronic correlations it is convenient to use electron operators in momentum space  $c_{p\sigma} = \sum_n c_{n\sigma} e^{-ipn}/\sqrt{N}$ . The self-consistency equation for the anomalous expectation value is

$$\Delta_k = \frac{2}{N} \sum_p \lambda_{k-p} (\omega_0 \lambda_{k-p} - 2g) \langle c_{-p\downarrow} c_{p\uparrow} \rangle_{\text{GS}}. \quad (140)$$

Note that  $\Delta_k$  determines the quasiparticle gap for electrons.

When the system is half-filled, i.e.,  $n_\sigma = 0.5$ , CDW phase emerges. While the CDW state breaks translational invariance we find that the optimized values of  $\lambda_{nm,\sigma}$  still only depend on the difference between  $n$  and  $m$  and representation (139) applies. The electron density

$$\rho_j = \langle c_{j\sigma}^\dagger c_{j\sigma} \rangle_{\text{GS}} = \frac{1}{2} + e^{iQ_\pi j} \rho_s \quad (141)$$

has a finite Fourier component at momentum  $Q_\pi = (\pi, \pi)$ . The staggered part of the density  $\rho_s = \sum_k \langle c_{k-\pi\sigma}^\dagger c_{k\sigma} \rangle_{\text{GS}}/N$  is determined by the elements  $\langle c_{k\sigma} c_{k-\pi\sigma}^\dagger \rangle_{\text{GS}}$  of the covariance matrix. The phonon displacement

$$d_j = -2 \frac{g}{\omega_0} + e^{iQ_\pi j} d_s \quad (142)$$

shows that the phonon quadrature  $\Delta_R$  has non-zero expectation values not only at  $q = 0$ , but also at  $Q_\pi$ . We define  $\langle x_{Q_\pi} \rangle_{\text{GS}} = \sum_j e^{iQ_\pi n} \langle x_j \rangle_{\text{GS}}/\sqrt{N}$  then the staggered part  $d_s = \langle x_{Q_\pi} \rangle_{\text{GS}}/\sqrt{N} - 4\lambda_{Q_\pi} \rho_s$  of  $d_j$ . Surprisingly we find that in the CDW phase the phonon covariance matrix  $\Gamma_{b,nm}$  still depends on  $n - m$  only, which we would generally expect only for translationally invariant systems. Thus, in both the SC and CDW phases all information about phonon covariance can be represented using

$$\Gamma_{b,nm} = \frac{1}{N} \sum_q e^{iq(n-m)} \Gamma_{b,q}, \quad (143)$$

namely, it has the translational symmetry.

The figure 12 shows the transition between the SC and CDW phases for  $\omega_0 = 10t_0$  and  $g/\omega_0 = 0.4, 0.5, 0.6$ , and  $0.7$ , where the hopping constant  $t_0$  is taken as the unit of energy. The local order parameter  $\Delta = \sum_k \Delta_k/N$ , the density  $n_\sigma$ , and the staggered components  $\rho_s$  show that the transition from the SC to the CDW phase takes place at half-filling.

For  $\omega_0 = 10t_0$  and  $g = 0.5\omega_0$ , the order parameter  $\Delta_k$  in the SC phase ( $\mu = -5.3$ ) and the displacement  $d_j$  in the CDW phase ( $\mu = -5$ ) are shown in Figs. 13a and 13b respectively. In Figs. 13c and 13d, we show the squeezing  $(\Gamma_{b,q})_{xx}$  of phonons as a function of momentum  $q$  in the SC and CDW phases respectively.

In both phases, the constraint (138) is satisfied because  $\langle p_l \rangle_{\text{GS}} = 0$  and  $(\Gamma_{b,nm})_{xp} = \langle \{\delta x_n, \delta p_m\} \rangle_{\text{GS}}/2 = 0$ . In

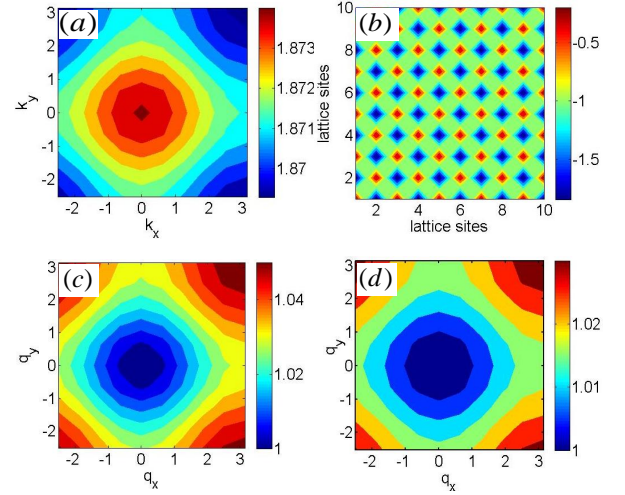


FIG. 13: The order parameter, the displacement and the covariant matrices of phonons, where the system size is  $10 \times 10$ , the phonon frequency is  $\omega_0 = 10t_0$ , the coupling  $g = 0.5\omega_0$ , and the hopping constant  $t_0$  is taken as the unit. (a) The superconducting order parameter in the momentum space for  $\mu = -5.3$ ; (b) The displacement of phonons in the CDW phase with  $\mu = -5$ ; (c)-(d) The covariant matrix of phonons in the momentum space for the superconducting ( $\mu = -5.3$ ) and CDW ( $\mu = -5$ ) phases.

Eq. (138), the first term vanishes due to  $(\Gamma_{b,nm})_{xp} = 0$ , and the second term vanishes due to  $\langle p_l \rangle_{\text{GS}} = 0$ . As a result, Eq. (138) is automatically satisfied by the optimal variational parameters in the ground state.

### C. Summary of Section V

In this section we introduced a class of non-Gaussian states constructed using a generalization of the Lang-Firsov polaron transformation. They provide a useful variational family of states for analyzing many-body electron-phonon systems. We studied the ground state of the Holstein model using the imaginary time flow approach and found that the CDW phase exists only at half-filling, and away from half-filling the system is always in the superconducting state. We presented results for the SC and CDW order parameters, phonon quadratures and covariance matrix, and the optimal values of the polaron transformation parameters  $\lambda_{n,m\sigma}$ .

## VI. SUMMARY, DISCUSSION, AND OUTLOOK

In this section we review the main results of the paper and suggest several promising directions for future studies.

We introduced a new family of variational wavefunctions to describe both the ground state and non-

equilibrium dynamics of interacting many-body systems. The essence of our approach is combining generalized canonical transformations with the Gaussian ansatz for bosons and fermions. These wavefunctions retain the simplicity of Gaussian wavefunctions yet they are characterized by non-factorizable correlations due to the canonical transformations which introduce entanglement between the fields. By allowing time-dependence of both the canonical transformation parameters and of the Gaussian wavefunctions our method goes beyond approaches based on standard canonical transformations, such as Lang-Firsov for electron-phonon systems or Silbey's partial polaron transformation for the spin bath problem [24]. We obtained explicit equations for the time evolution of the variational parameters by analyzing the differential structure of the variational wavefunctions manifold. Ground state can be found by solving the imaginary time equations of motion until the system reaches a fixed point. This fixed point can then be used to find collective modes in the system by solving the linearized real time equations of motion. The full real time dynamics can be used to calculate spectral functions of operators, or to analyze out of equilibrium phenomena.

While the focus of our paper was on non-Gaussian states we devote one of the subsections to reviewing interesting questions that can be studied using time-dependent Gaussian states.

### A. Overview of results

*Single polaron in a lattice.* We considered lattice polaron problems in the cases of Holstein and Su-Schrieffer-Heeger models. We used the LLP transformation to eliminate the impurity degree of freedom and reduce the problem to interacting bosons. We then considered a Gaussian state of phonons as an ansatz for the polaron wavefunction. This provides an extension of earlier studies which were limited to coherent variational states for phonons [59]. In the analysis of the ground state we found a phase transition for the SSH polaron. We also calculated polaron spectral functions using the real time dynamics. We showed the importance of the non-classical Gaussian part of the phonon wavefunctions in both the ground state and non-equilibrium calculations. Our results are in excellent agreement with the numerical approaches using exact diagonalization, Diagrammatic Monte Carlo, and the Bold Diagrammatic Monte Carlo.

*Anisotropic Kondo problem and Ohmic bosonic bath model.* We analyzed both the ground state and dynamics of the Ohmic bosonic bath model, which is equivalent to the anisotropic Kondo model. We showed that the problem can be studied using two seemingly different types of canonical transformations, which however lead to the same class of wavefunctions. The first one uses the parity conservation and the second one is a generalization of the partial polaron transformation introduced by Silbey and co-authors [24] (see also [25, 26] and references

therein for more recent work). Our work differs from the earlier papers utilizing partial polaron transformation in that we allow the parameters of the transformation to be time dependent and consider a general Gaussian state of bosons. When applied to the analysis of the ground state of the anisotropic Kondo problem we find that we correctly reproduce the phase diagram known from RG calculations. What is more exciting is that we can study real time dynamics in the regimes and at times which are not accessible for any other technique. In particular, we considered the relaxation of the impurity spin in the ferromagnetic easy plane case. The real time dynamics in this case is particularly difficult to analyze since the RG flow has several distinct regimes. At first, Kondo interactions flow to smaller values, while staying ferromagnetic. Then, at lower energy scales, the z-component of the interaction changes sign and starts flowing to larger values. Tantalizingly, we observed that these crossovers appear in the real time dynamics. At short times, the impurity spin gets dressed by the co-aligned polarization of the surrounding fermions (ferromagnetic screening) but then at longer times the polarization cloud switches into an anti-aligned configuration (antiferromagnetic screening). To our knowledge, this is the first analysis of the Kondo model dynamics in this regime.

*Competition of superconductivity and charge density wave orders in the Holstein model.* We analyzed the phase diagram of the Holstein model in the case when the phonon frequency is relatively high: ten times the electron hopping. We found a direct transition between the CDW phase at half filling and the SC phase away from half-filling. This is consistent with the expectation that for large phonon frequency the Holstein model should be similar to the negative-U Hubbard model, in which there is a degeneracy between the CDW to the SC phases at half-filling (the so-called C.N. Yang's SU(2) symmetry), while the superconducting phase is favored at other electron concentrations. In agreement with earlier studies we find that finite phonon frequency breaks the degeneracy of the two phases at half-filling in favor of the CDW phase.

### B. Interesting questions for time-dependent Gaussian states

The equations of motion (30) and (31) in the imaginary- and real- time provide a systematic way to study the ground state properties and real-time dynamics in the subspace of variational Gaussian states. For many-body systems that only contain fermions they agree with the generalized Hartree-Fock-BCS mean field theory [40]. In the usual implementation of the Hartree-Fock-BCS approximation one needs to solve a challenging multi-parameter minimization problem. The formalism of imaginary time flow presented in this paper makes the search for the optimal mean-field states more efficient.

1. *Competing phases.*— The analysis of the supercon-

ducting state is easy in fermionic systems with equal densities of the two spins components and attraction in the  $s$ -wave channel only. BCS mean-field theory assumes that the variational Gaussian state is determined by the single order parameter  $\Delta_0 \sim \sum_k \langle c_{-k\downarrow} c_{k\uparrow} \rangle$  [3]. Due to the simple structure of the order parameter, one can analyze properties of conventional weakly coupled BCS regime as well as the BCS-BEC crossovers by solving self-consistent equations for the gap and the chemical potential [60]. For systems with more complicated interactions, e.g., dipolar Fermi gases [61–64], the mixture of order parameters  $\Delta_l \sim \sum_k w_l(k) \langle c_{-k\downarrow} c_{k\uparrow} \rangle$  with different spatial and spin symmetries may co-exist in the ground state [61]. Here the orthonormal functions  $w_l(k)$  describe the structure of electron pairing in momentum space. In this case, the common approach is to guess which order parameters  $\Delta_l$  will be present in the ground state, and solve the nonlinear gap and Fermi occupation numbers equations self-consistently. This is often a demanding task since nonlinear equations may have multiple non-trivial self-consistent solutions [63]. Another competing instability in dipolar fermions that has been previously discussed is the Pomeranchuk type instabilities in the particle-hole channel [65, 66]. To find the actual ground state one needs to compare different saddle points and determine which of them provides a global minimum of the energy (or free energy at finite temperature). The equations of motion in imaginary time (30) provide a powerful alternative technique for identifying the lowest energy mean-field state.

*Inhomogeneous states.* Many interesting systems are characterized by spatially inhomogeneous order parameters. One important example is the Fulde-Ferrel-Larkin-Ovchinnikov superconducting phase [67, 68], which may appear when there is spin imbalance in the system. In the FFLO phase, the condensed fermion pairs have non-zero center of mass momenta  $Q$ , i.e., the system develops non-vanishing pairing amplitudes  $\Delta_{Q,l} \sim \sum_k w_l(k) \langle c_{Q/2-k\downarrow} c_{Q/2+k\uparrow} \rangle$  with  $Q \neq 0$ . Additional order parameters  $\Delta_{Q,l}$  make the numerical solution of the nonlinear gap equations particularly challenging. The difficulty of analyzing such states comes from the near degeneracy of many configurations. At the quadratic level, states with the same magnitude of the ordering wavevector are degenerate regardless of the wavevector direction. One needs to consider effects of the coupling between different components of the order parameter at different wavevectors [69], including higher harmonics, to determine the lowest energy state. Other important cases of inhomogeneous phases include stripe phases and frustrated phase separation in electron systems [70]; vortex lattice states in superconductors, in which the pairing amplitude is suppressed near vortex cores; systems with disorder, in which the order parameter may be suppressed in the vicinity of impurities. Generalized Gaussian states include all possible two-point correlation functions and provide a powerful toolbox for finding optimal configurations.

*2. Fluctuations.*— When discussing mean-field Gaussian states one usually separates two types of excitations: single-particle Bogoliubov excitations described by Eq. (32a) and collective excitations described by Eqs. (32b) and (33). For instance, in the SC phase single-particle Bogoliubov excitations describe fermionic quasiparticles which result from breaking up Cooper pairs. And the simplest example of a collective excitation is a gapless mode describing the phase fluctuation of the superconducting order parameter, which corresponds to the Goldstone mode originating from the spontaneous breaking of the  $U(1)$  symmetry. The spectrum of Bogoliubov excitations can be directly obtained by diagonalizing the mean field Hamiltonians  $h_f$ .

To describe collective excitations, one usually introduces a Hubbard-Strantanovich (HS) field to represent the collective pairing field, and integrates out the fermionic fields in order to obtain an effective theory for the HS field [71]. The low-energy effective theory of the HS field then describes the linear Goldstone modes. In superconductors, the Meissner effect arises from the external electromagnetic field coupling to the low-energy HS field and acquiring a “mass”. When the system contains multiple order parameters  $\Delta_l$ , many HS fields corresponding to order parameters with different symmetries should be introduced. This makes the analysis of the effective action of the coupled HS fields rather cumbersome. The Gaussian state approach provides an efficient way to study the properties of collective excitations by solving the linearized equations of motion (14). The low energy spectrum of these collective modes is determined by the eigenvalues of the matrix  $\mathbf{L}$ . In systems with spontaneous breaking of a continuous symmetry these equations are guaranteed to give a gapless Goldstone mode.

*3. Real time dynamics.*— In non-equilibrium superconductors and superfluidities, one is often interested in analyzing the coherent evolution of order parameters (such as the superconducting gaps) after sudden changes in system parameters [72] or following an electromagnetic pulse [73]. This dynamics is captured by Eq. (31).

*4. Open systems.*— The Gaussian state ansatz can be generalized to study dynamics and steady state behavior in open systems [74], such as optical parametric oscillators [75]. The real-time evolution of the reduced density matrix  $\rho_s$  for the system coupled to the bath is governed by the master equation  $\partial_t \rho_s = \mathcal{L} \rho_s$  in the Markovian limit [42]. The reduced density matrix can be approximated by the Gaussian mixed state, and equations of motion of  $\Delta_R$  and  $\Gamma_{b,m}$  are determined by

$$\begin{aligned} \partial_t \Delta_R &= \text{tr}(\mathcal{L} \rho_s R), \\ \partial_t \Gamma_b &= \frac{1}{2} \text{tr}(\mathcal{L} \rho_s \{\delta R, \delta R^T\}), \\ \partial_t \Gamma_m &= \frac{i}{2} \text{tr}(\mathcal{L} \rho_s [A, A^T]). \end{aligned} \quad (144)$$

We expect that interesting new insight into phase transitions and far-from-equilibrium dynamics of open systems can be obtained using time-dependent variational

Gaussian state approach.

### C. Possible extensions of the non-Gaussian state analysis

Before concluding this paper we would like to outline several promising directions in which our work can be extended.

*Fractional Quantum Hall Effect and Topological Phases.* In Sec. II C1 we discussed the canonical transformation equivalent to the flux attachment procedure. We pointed out that one can consider a broader class of transformations, e.g., when one first makes Wannier type orbitals as a linear superposition of the original single particle states and then performs flux attachment for such Wannier orbitals. One interesting question to consider is the nature of the excitations described by our variational wavefunctions. We expect that neutral excitations of composite fermions and bosons correspond to fluctuations in the Gaussian state part, while fluctuations in  $\omega_{ij}^{b,f}$  have a more subtle topological nature [7, 76]. This class of wavefunctions should be useful for studying FQHE states in lattices, including out of equilibrium situations relevant to systems realized with cold atoms and photons.

*Analysis of Fermionic Bogoliubov Quasiparticles.* In the current paper we focused on bosonic degrees of freedom. For example, collective excitations which we discussed in Sec. II A3 correspond to the Goldstone and amplitude (Higgs) modes of the ordered phases, or the incoherent particle hole excitations of Fermi systems. Fermionic quasiparticles should also be readily available from our analysis using time dependent effective quadratic Hamiltonian [see e.g., Eq. (E10)]. They can be used for analyzing time-resolved photoemission spectroscopy in pump and probe experiments [77, 78].

*Non-equilibrium Dynamics of Electron Phonon Systems.* Recent experiments demonstrated several intriguing phenomena in non-equilibrium electron-phonon systems. This includes photo-induced superconductivity [79–83], the observation of the amplitude Higgs model excited with light, pump and probe spectroscopy of CDW states. A special feature of our formalism is that it allows to treat on equal footing electron and phonon degrees of freedom. Hence it goes beyond the usual approach of solving the time dependent BCS model [84]. This will be particularly important for analyzing systems in which the non-equilibrium state of phonons plays an important role [79, 80].

*Systems with Competing and Intertwined Orders.* A ubiquitous feature of many-body systems is the interplay of competing [85] or intertwined [86] orders. In this paper we discussed the competition between superconductivity and CDW order, which is a common feature in electron-phonon systems. Another general feature of strongly correlated Fermi systems is the competition of superconducting phases with different symmetries of the

order parameter. A canonical example is the competition between the  $A$  and  $B$  phases in superfluid  $^3\text{He}$ . The analysis of Gaussian states is not sufficient to understand this transition since it is important to consider the feedback from the quasiparticle spectrum on the magnetic fluctuations mediating attraction between quasiparticles [87]. Similar questions about the interplay of several types of fluctuations and the analysis beyond Gaussian states are common in electron systems. One important problem is identifying the best “hidden” order parameter for explaining the pseudogap phase in high Tc cuprates [88–90]. Candidates include simple spin and charge density wave phases, as well as a more exotic d-density wave and Amperian pairing states. In iron based superconductors it is important to understand the competition between d-wave and extended s-wave [91] pairing symmetries, which strongly depends on the nature of the magnetic fluctuations in these materials. The variational approach that we discussed in this paper should be a useful tool for analyzing the interplay of several order parameters. When variational wavefunctions evolve in the imaginary time they find local energy minima. It is possible, however, that the system has several local minima. In this case one needs to compare energies of several locally stable states.

Our formalism can be a powerful tool for analyzing competing orders in nonequilibrium systems, such as when system parameters are changing in time. Examples include the competition between fermion pairing and ferromagnetism near a Feshbach resonance in ultracold atoms [92], or pump and probe experiments in solids [93].

*Magnetic Polarons.* The problem of magnetic polarons in the fermionic Hubbard t-J models plays an important role in the physics of strongly correlated electron systems (see e.g., [94, 95]). Here the goal is to understand the dynamics of a single charge carrier, e.g., a hole, in the background of an antiferromagnetically ordered Mott insulator. This system is reminiscent of the phonon-polaron problem, but with a hole exciting the magnons rather than phonons. In the magnetic polaron system, the hole hopping causes frustration in the antiferromagnetic background and leads to more dramatic polaronic effects. The LLP transformation presented earlier and generalized squeezed states can be used to study the spectral functions of polarons [95] which can be measured in solid state systems using ARPES [96, 97].

*Electrons interacting with nearly critical fields.* An important class of models in strongly correlated electron systems comes from considering electrons coupled to fluctuating bosonic fields in the vicinity of a Quantum Critical Point (QCP). Physically relevant cases include anti- and ferromagnetic spin fluctuations, CDW and orbital nematic fluctuations [98]. For example, in the case of antiferromagnetic fluctuations an effective model can be written as  $\mathcal{H} = \mathcal{H}_e + \mathcal{H}_{\text{AF}} + \mathcal{H}_{\text{int}}$ : (a) The electron hop-

ping term  $\mathcal{H}_e = \sum_{nm\sigma} t_{nm} c_{n\sigma}^\dagger c_{m\sigma}$ ; (b) The Hamiltonian

$$\begin{aligned} \mathcal{H}_{\text{AF}} = & \sum_{q_i < \Lambda} \left[ \frac{1}{2} \vec{\pi}_q \vec{\pi}_{-q} + \frac{(r+q^2)}{2} \vec{\phi}_q \vec{\phi}_{-q} \right. \\ & \left. + u(\vec{\phi}_{q1} \vec{\phi}_{q2})(\vec{\phi}_{q3} \vec{\phi}_{q2}) \delta_{\sum q_i} \right] \end{aligned} \quad (145)$$

describes the antiferromagnetic fluctuations by the vector field  $\vec{\phi}_q$  and its conjugate momentum  $\vec{\pi}_q$ ; (c) The interaction term  $\mathcal{H}_{\text{int}} = g \sum_{kq} c_{k+Q_\pi+q,\alpha}^\dagger \vec{\sigma}_{\alpha\beta} c_{k,\beta} \vec{\phi}_q$ . Here,  $\Lambda$  sets a UV energy cut-off for magnetic fluctuations and  $r$  controls the distance to QCP. It is easy to see a considerable resemblance between this model and the Holstein model (118) that we considered before. We expect that the generalized polaron transformation of the type defined in Eq. (122), together with the Gaussian state for electrons and bosons can provide a good variational ansatz for studying the ground state and response functions of the system. The latter includes electron spectral functions, optical conductivities, and spin response functions. An important advantage of this method is that it allows to work directly with real time and frequencies as we demonstrated in this paper.

*Gauge fields.* We expect that variational non-Gaussian states can also be applied in the study of QCD and lattice gauge theories [99, 100]. The simplest possible system to consider would be a one dimensional Schwinger model in which Dirac fermions interacts with photons. We can find not only the ground state but also analyze “emergent” elementary particles by solving the linearized equations of motion around the steady state.

*Open Systems.* Another interesting direction for extending our work on non-Gaussian states is to consider open systems. Considering the density matrix describing the system as a vector in super-space  $|\rho_s\rangle$  (see e.g., [74]), we can write the master equation as

$$\partial_t |\rho_s\rangle = \mathcal{L} |\rho_s\rangle, \quad (146)$$

where  $\mathcal{L}$  is the Lindblad super-operator that contains both the Hamiltonian evolution and decoherence due to coupling to the bath. We expect that the method of generalized Gaussian transformations can be extended to the superspace thus allowing to explore a broader class of dynamical phenomena [101, 102].

### Acknowledgments

This project has been supported by the EU project SIQS. The authors acknowledge Max-Planck-Harvard Research Center for Quantum Optics. The authors thank the useful discussions with Fabian Grusdt, Richard Schmidt, Yulia E. Shchadilova, Valentin Kasper, Marton Kanasz-Nagy, Erez Zohar, Alejandro Gonzalez Tudela, Yue Chang, Yinghai Wu, Chengyi Luo, XiaoLiang Qi, Pablo Sala, Jan von Delft, Peter Zoller, and Su Yi. ED acknowledges support from Harvard-MIT CUA, NSF Grant No. DMR-1308435, AFOSR Quantum Simulation MURI, AFOSR grant number FA9550-16-1-0323, the Humboldt Foundation, and the Max Planck Institute for Quantum Optics.

### Appendix A: Imaginary and real time evolutions from the geometric point of view

In this Appendix, from the differential geometry perspective [28], we derive the general equations of motion (6) for variational parameters and the constraint (11) in the imaginary- and real- time evolutions. We focus on the imaginary time evolution first, and equations of motion in the real time evolution can be obtained following a similar procedure.

The time derivative on the left hand side of Eq. (5) is

$$\partial_\tau |\Psi(\xi)\rangle = \sum_j d_\tau \xi_j |\Psi_j\rangle, \quad (A1)$$

where the states  $|\Psi_j\rangle = \partial_{\xi_j} |\Psi(\xi)\rangle$  span the tangent space of the variational manifold  $|\Psi(\xi)\rangle$  and  $\partial_\tau |\Psi(\xi)\rangle$  is a tangent vector, as denoted by the dashed (red) arrow in Fig. 14. Note that  $|\Psi_j\rangle$  might not be linearly independent. If the rank  $r_{\mathbf{G}}$  of the Gram matrix  $\mathbf{G}_{ij} = \langle \Psi_i | \Psi_j \rangle$  is smaller than the number of variational parameters, namely, some redundant parameters in  $\xi$  have been introduced, one can always fix the value of some of the parameters until the Gram matrix becomes invertible. Thus, in general, the tangent vector  $\partial_\tau |\Psi(\xi)\rangle$  is a superposition of  $r_{\mathbf{G}}$  linear independent vectors  $|\Psi_{j=1,\dots,r_{\mathbf{G}}}\rangle$ .

The right hand side  $|\mathbf{R}_\Psi\rangle = -(H - E) |\Psi(\xi)\rangle$  in Eq. (5) can be decomposed into the vectors  $|\Psi_\parallel\rangle = \mathbf{P}_\xi |\mathbf{R}_\Psi\rangle$  and  $|\Psi_\perp\rangle = (\mathbf{1} - \mathbf{P}_\xi) |\mathbf{R}_\Psi\rangle$  in and orthogonal to the tangent space, as denoted by the solid (black) arrows in Fig. 14, where  $E = \langle \Psi(\xi) | H | \Psi(\xi) \rangle$  is the average energy, and  $\mathbf{P}_\xi$  is the projector onto the tangent space.

By projecting the motion Eq. (5) onto the tangent space, we obtain

$$\sum_{j=1}^{r_{\mathbf{G}}} d_\tau \xi_j |\Psi_j\rangle = |\Psi_\parallel\rangle, \quad (A2)$$

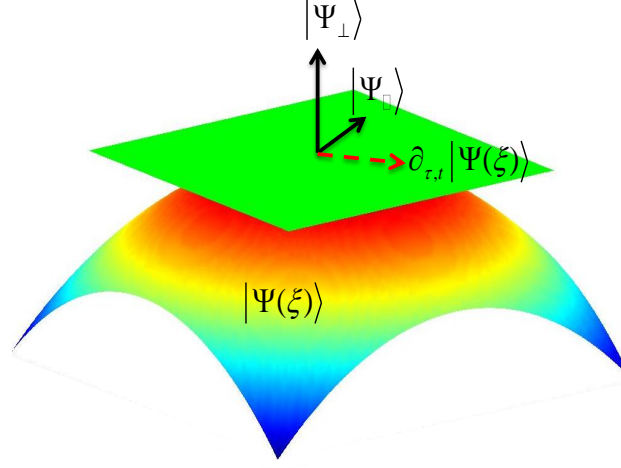


FIG. 14: The schematic of the non-Gaussian state manifold in the Hilbert space, where the green plane denotes the tangent space. The Hamiltonian generates the vector  $|\Psi_{\parallel}\rangle + |\Psi_{\perp}\rangle$ .

which leads to the motion Eq. (6), i.e.,

$$d_{\tau}\xi_i = \sum_{j=1}^{r_G} \mathbf{G}_{ij}^{-1} \langle \Psi_j | \Psi_{\parallel} \rangle. \quad (\text{A3})$$

We remark that the motion Eq. (6) minimizes the distance  $\mathbf{d}_0 = |\partial_{\tau} |\Psi(\xi)\rangle - |\mathbf{R}_{\Psi}\rangle| = ||\Psi_{\perp}\rangle|$  at each instant  $\tau$ .

It follows from Eq. (A2) that the energy  $E$  evolves as

$$\begin{aligned} d_{\tau}E &= 2\text{Re} \langle \Psi(\xi) | H \partial_{\tau} |\Psi(\xi)\rangle = 2\text{Re} \langle \Psi(\xi) | H | \Psi_{\parallel} \rangle \\ &= -2 \langle \mathbf{R}_{\Psi} | \mathbf{P}_{\xi} | \mathbf{R}_{\Psi} \rangle + 2E \text{Re} \langle \Psi(\xi) | \mathbf{P}_{\xi} | \mathbf{R}_{\Psi} \rangle. \end{aligned} \quad (\text{A4})$$

Since the state  $|\Psi(\xi)\rangle$  is normalized, the condition

$$\partial_{\tau} \langle \Psi(\xi) | \Psi(\xi) \rangle = 2\text{Re} \langle \Psi(\xi) | \Psi_{\parallel} \rangle = 0 \quad (\text{A5})$$

is always satisfied, which results in the monotonic decreasing behavior

$$d_{\tau}E = -2 \langle \mathbf{R}_{\Psi} | \mathbf{P}_{\xi} | \mathbf{R}_{\Psi} \rangle \leq 0. \quad (\text{A6})$$

For the variational ground state in the limit  $\tau \rightarrow \infty$ ,  $|\Psi_{\parallel}\rangle = 0$  and the energy  $E$  stops flowing, i.e.,  $d_{\tau}E = 0$ . The square norm  $||\Psi_{\perp}\rangle|^2 = \langle \mathbf{R}_{\Psi} | \mathbf{R}_{\Psi} \rangle$  of the vector orthogonal to the tangent space is the variance of the energy, which should be very small if the state we reach in the limit  $\tau \rightarrow \infty$  is close to the real ground state.

In the real time evolution, we project the Schrödinger equation on the tangent space as

$$\partial_t |\Psi(\xi)\rangle = \mathbf{P}_{\xi} |\mathbf{R}_{\Psi}\rangle, \quad (\text{A7})$$

where  $|\mathbf{R}_{\Psi}\rangle = -iH |\Psi(\xi)\rangle$ . The projected Schrödinger Eq. (A7) results in Eq. (6), where the derivative is taken with respect to the real time  $t$ . It follows from the motion Eq. (6) that the total energy obeys

$$d_t E = \langle d_t H \rangle + 2\text{Re} \langle \Psi_{\parallel} | H | \Psi(\{\xi\}) \rangle. \quad (\text{A8})$$

The second term

$$2\text{Re} \langle \Psi_{\parallel} | H | \Psi(\{\xi\}) \rangle = 2\text{Re} i ||\Psi_{\parallel}\rangle|^2 = 0 \quad (\text{A9})$$

in Eq. (A8) always vanishes, thus the condition (11) is satisfied.

The ground state  $|\Psi_G\rangle$  obtained from the imaginary time evolution satisfies the relation

$$|\Psi_\parallel\rangle = \mathbf{P}_\xi(H - E_G)|\Psi_G\rangle = 0. \quad (\text{A10})$$

It follows from Eq. (A10) that the real time evolution  $|\Psi_G(t)\rangle = e^{-iE_G t}|\Psi_G\rangle$  of the variational ground state obeys the projected Schrödinger equation

$$\partial_t |\Psi_G(t)\rangle = -iE_G \mathbf{P}_\xi |\Psi_G(t)\rangle = -i\mathbf{P}_\xi H |\Psi_G(t)\rangle. \quad (\text{A11})$$

We consider the fluctuation  $\xi = \xi_G + \epsilon$  around the ground state solution  $\xi_G$  of Eq. (6) in the limit  $\tau \rightarrow \infty$ , we expand the state

$$|\Psi(\xi)\rangle = |\Psi_G\rangle e^{-iE_G t} + \sum_j \epsilon_j |\Psi_j\rangle \quad (\text{A12})$$

to the linear order of  $\epsilon$ , where the vectors  $|\Psi_j\rangle = \delta|\Psi(\xi)\rangle/\delta\xi|_{\xi=\xi_G}$  span the tangent space at  $\xi_G$ . The projected Schrodinger Eq. (A7) results in

$$-iE_G \mathbf{P}_\xi |\Psi_G(t)\rangle + \sum_j d_t \epsilon_j |\Psi_j\rangle = -i\mathbf{P}_\xi H |\Psi_G(t)\rangle - i \sum_j \epsilon_j \mathbf{P}_\xi H |\Psi_j\rangle, \quad (\text{A13})$$

where the first terms on the right- and left- hand sides of Eq. (A13) cancel each other due to the relation (A11). Finally, we obtain Eq. (13) by projecting Eq. (A13) on the tangent vector  $|\Psi_i\rangle$ .

### Appendix B: Tangent vector $\partial_{\tau,i}|\Psi_{\text{NGS}}\rangle$ and $H|\Psi_{\text{NGS}}\rangle$

In this Appendix, we prove that  $H|\Psi_{\text{NGS}}\rangle$  and the tangent vector  $\partial_\tau|\Psi_{\text{NGS}}\rangle$  are composed of states with the form (41). The non-Gaussian states  $|\Psi_{\text{NGS}}\rangle = U_S|\Psi_{\text{GS}}\rangle$  are determined by the transformations  $U_S = U_{3,4,5}$ .

By moving the transformation  $U_S$  to the most left side, we rewrite the tangent vector as  $\partial_\tau|\Psi_{\text{NGS}}\rangle = U_S(u_L + O)|\Psi_{\text{GS}}\rangle$ , where  $u_L = (\partial_\tau U_{\text{GS}})U_{\text{GS}}^{-1}$  and  $O = U_S^{-1}\partial_\tau U_S$ . The operator  $u_L$  can be obtained by the time derivatives  $\partial_\tau e^{i\frac{1}{2}R^T\sigma\Delta_R}$ ,  $\partial_\tau e^{-i\frac{1}{4}R^T\xi_b R}$ , and  $\partial_\tau e^{i\frac{1}{4}A^T\xi_m A}$ . The derivative of the displacement operator is

$$\begin{aligned} \partial_\tau e^{i\frac{1}{2}R^T\sigma\Delta_R} &= \partial_\tau (e^{-\frac{1}{4}i\Delta_x^T\Delta_p} e^{\frac{1}{2}ix^T\Delta_p} e^{-\frac{1}{2}ip^T\Delta_x}) \\ &= [\frac{1}{2}i\Delta_p^T\partial_\tau\Delta_x - \frac{1}{4}i\partial_\tau(\Delta_x^T\Delta_p) + i\frac{1}{2}R^T\sigma\partial_\tau\Delta_R] e^{i\frac{1}{2}R^T\sigma\Delta_R} \\ &= (\phi_0 + i\frac{1}{2}R^T\sigma\partial_\tau\Delta_R) e^{i\frac{1}{2}R^T\sigma\Delta_R}, \end{aligned} \quad (\text{B1})$$

where  $\Delta_R = (\Delta_x, \Delta_p)^T$  and  $\phi_0 = -\frac{1}{4}i\Delta_R^T\sigma\partial_\tau\Delta_R$ . In the first row of Eq. (B1), we used the canonical commutation relation  $[x, p] = 2i$  and the Baker-Campbell-Hausdorff (BCH) formula  $e^{O_1+O_2} = e^{-[O_1, O_2]/2}e^{O_1}e^{O_2}$  for operators  $O_1 = ix^T\Delta_p/2$  and  $O_2 = -ip^T\Delta_x/2$ . In the second row, the displacement operator is moved to the most right side of other operators by the relation  $e^{ix\Delta_p/2}pe^{-ix\Delta_p/2} = p - \Delta_p$ . The derivative of the bosonic squeezing operator is

$$\begin{aligned} \partial_\tau e^{-i\frac{1}{4}R^T\xi_b R} &= -i\frac{1}{4}\int_0^1 du e^{-iu\frac{1}{4}R^T\xi_b R} R^T(\partial_\tau\xi_b) R e^{iu\frac{1}{4}R^T\xi_b R} e^{-i\frac{1}{4}R^T\xi_b R} \\ &= -i\frac{1}{4}\int_0^1 du R^T e^{u\xi_b\sigma}(\partial_\tau\xi_b) e^{-u\sigma\xi_b} R e^{-i\frac{1}{4}R^T\xi_b R} \\ &= i\frac{1}{4}R^T\sigma(\partial_\tau S_b)S_b^{-1} R e^{-i\frac{1}{4}R^T\xi_b R}, \end{aligned} \quad (\text{B2})$$

where in the first row of Eq. (B2) we used the formula

$$\partial_\tau e^{J(\tau)} = \int_0^1 du e^{uJ(\tau)}(\partial_\tau J) e^{(1-u)J(\tau)} = \int_0^1 du e^{(1-u)J(\tau)}(\partial_\tau J) e^{uJ(\tau)} \quad (\text{B3})$$

for any exponential operator  $e^{J(\tau)}$ , in the second row we used the transformation

$$e^{-iu\frac{1}{4}R^T\xi_b R} R e^{iu\frac{1}{4}R^T\xi_b R} = e^{-u\sigma\xi_b} R, \quad (\text{B4})$$



and in the third row we calculated the integral

$$\int_0^1 du e^{u\xi_b\sigma}(\partial_\tau\xi_b)e^{-u\sigma\xi_b} = -\sigma(\partial_\tau e^{\sigma\xi_b})e^{-\sigma\xi_b} = -\sigma(\partial_\tau S_b)S_b^{-1} \quad (\text{B5})$$

using Eq. (B3) and the property  $e^{u\xi_b\sigma}e^{-u\sigma\xi_b} = \sigma$  of the symplectic matrix  $e^{-u\sigma\xi_b}$ .

The derivative of the fermionic squeezing operator is

$$\begin{aligned} \partial_\tau e^{i\frac{1}{4}A^T\xi_m A} &= i\frac{1}{4}\int_0^1 du e^{iu\frac{1}{4}A^T\xi_m A} A^T(\partial_\tau\xi_m) A e^{-iu\frac{1}{4}A^T\xi_m A} e^{i\frac{1}{4}A^T\xi_m A} \\ &= i\frac{1}{4}A^T\int_0^1 du e^{iu\xi_m}(\partial_\tau\xi_m)e^{-iu\xi_m} A e^{i\frac{1}{4}A^T\xi_m A} \\ &= \frac{1}{4}A^T(\partial_\tau U_m)U_m^T A e^{i\frac{1}{4}A^T\xi_m A}, \end{aligned} \quad (\text{B6})$$

where Eq. (B3) is applied in the first and the third rows of Eq. (B6), and in the second row we use the transformation

$$e^{iu\frac{1}{4}A^T\xi_m A} A e^{-iu\frac{1}{4}A^T\xi_m A} = e^{-iu\xi_m} A \quad (\text{B7})$$

for fermions. The results (B1), (B2), and (B6) show that  $u_L$  only contains the constant, linear, and quadratic terms of  $R$  and  $A$ .

In the next step, we analyze the structure of the operator  $O$ . For the transformation  $U_3$ , the operator  $O = U_3^{-1}\partial_\tau U_3$  is

$$O = (\partial_\tau\lambda)P - \frac{1}{2\mathcal{N}}\partial_\tau\mathcal{N}. \quad (\text{B8})$$

For the transformation  $U_4$ , the operator  $O = U_4^{-1}\partial_\tau U_4$  is

$$\begin{aligned} O &= U_4^{-1}[(\partial_\tau e^{i\frac{1}{2}C^\dagger\bar{\xi}_f C})e^{i\frac{1}{2}\sum_{ij}\omega_{ij}^f:n_i^f n_j^f}:e^{i\sum_{ij}\bar{\omega}_{ij}R_i n_j^f} \\ &\quad + e^{i\frac{1}{2}C^\dagger\bar{\xi}_f C}(\partial_\tau e^{i\frac{1}{2}\sum_{ij}\omega_{ij}^f:n_i^f n_j^f}:e^{i\sum_{ij}\bar{\omega}_{ij}R_i n_j^f} \\ &\quad + e^{i\frac{1}{2}C^\dagger\bar{\xi}_f C}e^{i\frac{1}{2}\sum_{ij}\omega_{ij}^f:n_i^f n_j^f}:(\partial_\tau e^{i\sum_{ij}\bar{\omega}_{ij}R_i n_j^f})]. \end{aligned} \quad (\text{B9})$$

The derivative

$$\partial_\tau e^{i\frac{1}{2}C^\dagger\bar{\xi}_f C} = e^{i\frac{1}{2}C^\dagger\bar{\xi}_f C}\frac{1}{2}C^\dagger\bar{U}_f^\dagger(\partial_\tau\bar{U}_f)C \quad (\text{B10})$$

in the first term can be obtained by the same procedure in Eq. (B6), where  $\bar{U}_f = e^{i\bar{\xi}_f}$  is the unitary transformation and the Gaussian transformation  $e^{i\frac{1}{2}C^\dagger\bar{\xi}_f C}$  is moved to the most left side of other operators. The derivative

$$\partial_\tau e^{i\frac{1}{2}\sum_{ij}\omega_{ij}^f:n_i^f n_j^f}: = e^{i\frac{1}{2}\sum_{ij}\omega_{ij}^f:n_i^f n_j^f}:i\frac{1}{2}\sum_{ij}(\partial_\tau\omega_{ij}^f):n_i^f n_j^f: \quad (\text{B11})$$

in the second term is obtained by the commutation relation

$$[e^{i\frac{1}{2}\sum_{ij}\omega_{ij}^f:n_i^f n_j^f}: , i\frac{1}{2}\sum_{ij}(\partial_\tau\omega_{ij}^f):n_i^f n_j^f:] = 0. \quad (\text{B12})$$

The derivative

$$\partial_\tau e^{i\sum_{ij}\bar{\omega}_{ij}R_i n_j^f} = e^{i\sum_{ij}\bar{\omega}_{ij}R_i n_j^f}[i\sum_{ij}n_i^f(\bar{\omega}^T\sigma\partial_\tau\bar{\omega})_{ij}n_j^f + i\sum_{ij}(\partial_\tau\bar{\omega}_{ij})R_i n_j^f] \quad (\text{B13})$$

in the third term is obtained by the same procedure in Eq. (B1), where the exponential operator is moved to the most left side. Eventually, the operator  $O$  becomes

$$\begin{aligned} O &= \frac{1}{2}\bar{C}^\dagger\bar{U}_f^\dagger(\partial_\tau\bar{U}_f)\bar{C} + i\sum_i(\bar{\omega}^T\sigma\partial_\tau\bar{\omega})_{ii}n_i^f \\ &\quad + i\sum_{ij}(\partial_\tau\bar{\omega}_{ij})R_i n_j^f + i\sum_{ij}(\frac{1}{2}\partial_\tau\omega_{ij}^f + \bar{\omega}^T\sigma\partial_\tau\bar{\omega})_{ij}:n_i^f n_j^f:, \end{aligned} \quad (\text{B14})$$

where the operator  $\bar{C} = (\bar{c}, \bar{c}^\dagger)^T$  is determined by the transformation

$$\bar{c}_i = e^{-i \sum_j \bar{\omega}_{ij} R_j n_j^f} e^{-i \frac{1}{2} \sum_{ij} \omega_{ij}^f : n_i^f n_j^f :} c_i e^{i \frac{1}{2} \sum_{ij} \omega_{ij}^f : n_i^f n_j^f :} e^{i \sum_{ij} \bar{\omega}_{ij} R_j n_j^f} = e^{i \sum_j [(\omega^f - \bar{\omega}^T \sigma \bar{\omega})_{ij} n_j^f + R_j \bar{\omega}_{ji}]} c_i. \quad (\text{B15})$$

For the transformation  $U_5$ , the operator  $O = U_5^{-1} \partial_\tau U_5$  is

$$O = U_5^{-1} \partial_\tau (e^{i \frac{1}{2} C^\dagger \bar{\xi}_f C} e^{i \frac{1}{2} R^T \sigma \bar{\Delta}_R} e^{-i \frac{1}{4} R^T \bar{\xi}_b R}) e^{J_0} + \partial_\tau J_0, \quad (\text{B16})$$

where we used the commutation relation  $[\partial_\tau J_0, e^{J_0}] = 0$  for the operator

$$J_0 = i \sum_{ij} \left( \frac{1}{2} \omega_{ij}^f : n_i^f n_j^f : + \frac{1}{2} \omega_{ij}^b : n_i^b n_j^b : + \omega_{ij}^{bf} n_i^b n_j^f \right). \quad (\text{B17})$$

By the same procedure in Eqs. (B1), (B2), and (B6), the time derivative to the Gaussian transformation part is obtained, which leads to

$$\begin{aligned} O = & -\phi_0 + i \frac{1}{2} \bar{R}^T \bar{S}_b^T \sigma \partial_\tau \Delta_R + \frac{1}{2} \bar{C}^\dagger \bar{U}_f^\dagger (\partial_\tau \bar{U}_f) \bar{C} \\ & + i \frac{1}{4} \bar{R}^T \bar{S}_b^T \sigma (\partial_\tau \bar{S}_b) \bar{R} + \partial_\tau J_0. \end{aligned} \quad (\text{B18})$$

Here,  $\bar{S}_b = e^{\sigma \bar{\xi}_b}$ , and the operators  $\bar{C} = (\bar{c}, \bar{c}^\dagger)^T$  and  $\bar{R} = (\bar{b}^\dagger + \bar{b}, i(\bar{b}^\dagger - \bar{b}))^T$  are determined by the transformations

$$\begin{aligned} \bar{c}_i &= e^{i \sum_j (w_{ij}^f n_j^f + w_{ij}^{bf} n_j^b)} c_i, \\ \bar{b}_i &= e^{i \sum_j (w_{ij}^b n_j^b + w_{ij}^{bf} n_j^f)} b_i. \end{aligned} \quad (\text{B19})$$

The equations (B8), (B14), and (B18) show that the operator  $O$  has the form (43). As a result, the tangent vector  $\partial_{\xi_j} |\Psi_{\text{NGS}}\rangle$  is composed of terms like those in Eq. (41).

In the end of this section, we investigate the structure of the vector  $|\mathbf{R}_\Psi\rangle$  determined by  $H(R, C) |\Psi_{\text{NGS}}\rangle$ . For the transformation  $U_3$ ,

$$H(R) |\Psi_{\text{NGS}}\rangle = \frac{1}{\sqrt{\mathcal{N}}} [H(R) \cosh \lambda + PH(-R) \sinh \lambda] |\Psi_{\text{GS}}\rangle. \quad (\text{B20})$$

For the transformations  $U_S = U_{4,5}$ , we move  $U_S$  on the most left side as

$$H(R, C) |\Psi_{\text{NGS}}\rangle = U_S \bar{H}(R, C) |\Psi_{\text{GS}}\rangle \quad (\text{B21})$$

where  $\bar{H}(R, C) = U_S^\dagger H(R, C) U_S$  is the Hamiltonian in the rotating frame. The transformations  $U_{S=4,5}$  act on the arguments of  $H(R, C)$  as  $\bar{H}(R, C) = H(R_S, C_S)$ , where  $R_S = U_S^\dagger R U_S$  and  $C_S = U_S^\dagger C U_S$ . For  $U_S = U_4$ , the operators are

$$\begin{aligned} R_S &= U_4^\dagger R U_4 = R - 2\sigma \bar{\omega} n^f, \\ C_S &= U_4^\dagger C U_4 = \bar{U}_f \bar{C}, \end{aligned} \quad (\text{B22})$$

where  $\bar{C}$  is determined by Eq. (B15). For  $U_S = U_5$ , the operators are

$$\begin{aligned} R_S &= U_5^\dagger R U_5 = \bar{S}_b \bar{R} + \bar{\Delta}_R, \\ C_S &= U_5^\dagger C U_5 = \bar{U}_f \bar{C}, \end{aligned} \quad (\text{B23})$$

where  $\bar{R}$  and  $\bar{C}$  are determined by Eq. (B19).

For the Hamiltonian  $H$  composed of the polynomials of  $R$  and  $C$ , Eqs. (B20), (B22), and (B23) show that the state  $H(R, C) |\Psi_{\text{NGS}}\rangle$  contains terms with the form (41).

### Appendix C: Mean values on bosonic Gaussian states

In this Appendix, we show how to evaluate the mean values

$$\left\langle e^{i \sum_j \gamma_j R_j} \text{poly}(R) \right\rangle_{\text{GS}} \quad (\text{C1})$$

and

$$\left\langle e^{i \sum_j \beta_j n_j^b} \text{poly}(R) \right\rangle_{\text{GS}} \quad (\text{C2})$$

on the bosonic Gaussian state, which appear in Eq. (45) for  $U_S = U_{4,5}$ .

We can use the normal ordering expansion

$$\begin{aligned} U_{\text{GS}}^\dagger e^{iR^T \gamma} U_{\text{GS}} &= e^{i\Delta_R^T \gamma} e^{iR^T S_b^T \gamma} \\ &= e^{i\Delta_R^T \gamma} e^{-\frac{1}{2} \gamma^T \Gamma_b \gamma} e^{iR^T S_b^T \gamma}, \end{aligned} \quad (\text{C3})$$

to obtain  $\left\langle e^{iR^T \gamma} \right\rangle_{\text{GS}} = e^{i\Delta_R^T \gamma} e^{-\frac{1}{2} \gamma^T \Gamma_b \gamma}$ , where  $\gamma$  is the vector with the element  $\gamma_j$ . In the first row of Eq. (C3), the quadrature is displaced and squeezed by the Gaussian transformation  $U_{\text{GS}}$ , and in the second row the BCH formula is used, where the normal ordering is defined with respect to the vacuum state.

The mean value (C2) contains the quadratic operators in the exponential term. To evaluate this mean value, we introduce the Weyl representation [42, 43]

$$\rho_{\text{GS}} = \int \frac{d^{2N_b} r}{(4\pi)^{N_b}} \chi(r) e^{-\frac{i}{2} \sum_j (\delta \hat{x}_j p_j - \delta \hat{p}_j x_j)}, \quad (\text{C4})$$

where the c-number vector  $r = (x_j, p_j)$ , and  $\delta \hat{x} = \hat{x} - \Delta_x$  ( $\delta \hat{p} = \hat{p} - \Delta_p$ ) describes the position (momentum) fluctuation. For the bosonic Gaussian state, the characteristic function is

$$\chi(r) = \text{tr}[\rho_{\text{GS}} e^{\frac{i}{2} \sum_j (\delta \hat{x}_j p_j - \delta \hat{p}_j x_j)}] = e^{-\frac{1}{8} r^T \sigma^T \Gamma_b \sigma r}. \quad (\text{C5})$$

As an example, we calculate the mean value

$$A_b = \left\langle e^{i \sum_i \beta_i b_i^\dagger b_i} b_{j_1}^\dagger \dots b_{j_a}^\dagger b_{k_1} \dots b_{k_b} \right\rangle_{\text{GS}}. \quad (\text{C6})$$

In terms of the density matrix (C4), the mean value becomes

$$\begin{aligned} A_b &= \int \frac{d^{2N_b} r}{(4\pi)^{N_b}} \chi(r) \text{tr}[e^{i \sum_i \beta_i b_i^\dagger b_i} b_{j_1}^\dagger \dots b_{j_a}^\dagger b_{k_1} \dots b_{k_b} e^{-\frac{i}{2} \sum_j (\delta \hat{x}_j p_j - \delta \hat{p}_j x_j)}] \\ &= \mathcal{F}_J \int \frac{d^{2N_b} r}{(4\pi)^{N_b}} \chi(r) \text{tr}[e^{i \sum_i \beta_i b_i^\dagger b_i} e^{\sum_k J_k b_k^\dagger} e^{\sum_k J_k^* b_k} e^{-\frac{i}{2} \sum_j (\delta \hat{x}_j p_j - \delta \hat{p}_j x_j)}], \end{aligned} \quad (\text{C7})$$

where

$$\mathcal{F}_J = \lim_{J \rightarrow 0} \frac{\delta}{\delta J_{j_1}} \dots \frac{\delta}{\delta J_{j_a}} \frac{\delta}{\delta J_{k_1}^*} \dots \frac{\delta}{\delta J_{k_b}^*} \quad (\text{C8})$$

denotes the functional derivative. By inserting the identity operator  $I = \int d^2 \mu |\mu\rangle \langle \mu| / 2\pi i$ , we obtain

$$\begin{aligned} A_b &= \mathcal{F}_J \int \frac{d^{2N_b} r}{(4\pi)^{N_b}} \chi(r) e^{-i \frac{1}{2} r^T \sigma \Delta_R} \int \frac{d^{2N_b} \mu}{(2\pi i)^{N_b}} \times \\ &\quad \langle \{\mu_j\} | e^{\sum_k J_k b_k^\dagger} e^{i \sum_i \beta_i b_i^\dagger b_i} e^{\sum_k J_k^* b_k} e^{-\frac{i}{2} \sum_j (\hat{x}_j p_j - \hat{p}_j x_j)} | \{\mu_j\} \rangle, \end{aligned} \quad (\text{C9})$$

where the coherent state  $|\mu\rangle = e^{-|\mu|^2/2} e^{\mu b^\dagger} |0\rangle$ . Using  $b_j |\mu_j\rangle = \mu_j |\mu_j\rangle$  and the relation

$$e^{-\frac{i}{2} \sum_j (\hat{x}_j p_j - \hat{p}_j x_j)} | \{\mu_j\} \rangle = e^{\frac{1}{2} \sum_j (\nu_j^* \mu_j - \mu_j^* \nu_j)} e^{\sum_j [(\mu_j - \nu_j) b_j^\dagger - (\mu_j^* - \nu_j^*) b_j]} |0\rangle, \quad (\text{C10})$$

we obtain

$$\begin{aligned} A_b &= \mathcal{F}_J \int \frac{d^{2N_b} r}{(4\pi)^{N_b}} \chi(r) e^{-i \frac{1}{2} r^T \sigma \Delta_R} e^{-\sum_j J_j^* \nu_j - \frac{1}{2} \sum_j \nu_j^* \nu_j} \\ &\quad \int \frac{d^{2N_b} \mu}{(2\pi i)^{N_b}} \prod_j e^{-(1 - e^{i\beta_j}) \mu_j^* \mu_j + (J_j^* + \nu_j^*) \mu_j + \mu_j^* (J_j - \nu_j) e^{i\beta_j}}, \end{aligned} \quad (\text{C11})$$

where  $\nu_j = (x_j + ip_j)/2$ .

In Eq. (C11), the integrals over  $r$  and  $\mu$  are Gaussian integrals, which can be evaluated analytically. The Gaussian integral over  $\mu$  leads to

$$A_b = \prod_j (1 - e^{i\beta_j})^{-1} \mathcal{F}_J e^{\sum_j J_j^* \frac{e^{i\beta_j}}{1 - e^{i\beta_j}} J_j} \int \frac{d^{2N_b} r}{(4\pi)^{N_b}} e^{-\frac{1}{8} r^T \sigma^T (\Gamma_b + \frac{1 + e^{i\beta}}{1 - e^{i\beta}}) \sigma r + \frac{1}{2} r^T (\Sigma \mathbf{J} - i \sigma \Delta_R)}, \quad (C12)$$

where the vector  $\mathbf{J} = (J_{j=1, \dots, N_b}, J_{j=1, \dots, N_b}^*)^T$ , the diagonal matrix  $\beta = \mathbb{1}_2 \otimes \text{diag}(\beta_j)$ , and the matrix

$$\Sigma = \begin{pmatrix} \frac{e_\beta}{1 - e_\beta} & -\frac{1}{1 - e_\beta} \\ -i \frac{e_\beta}{1 - e_\beta} & -i \frac{1}{1 - e_\beta} \end{pmatrix} \quad (C13)$$

is define by  $e_\beta = \exp[i \text{diag}(\beta_j)]$  and the diagonal matrix  $\text{diag}(\beta_j)$  with elements  $\beta_j$ .

Redefining the variables  $r = \sqrt{1 - e^{i\beta}} \tilde{r}$ , we rewrite

$$\begin{aligned} A_b &= \mathcal{F}_J e^{\sum_j J_j^* \frac{e^{i\beta_j}}{1 - e^{i\beta_j}} J_j} \int \frac{d^{2N_b} \tilde{r}}{(4\pi)^{N_b}} e^{-\frac{1}{8} \tilde{r}^T \sigma^T \Gamma_B \sigma \tilde{r} + \frac{1}{2} \tilde{r}^T \sqrt{1 - e^{i\beta}} (\Sigma \mathbf{J} - i \sigma \Delta_R)} \\ &= I_G e^{-\frac{1}{2} \Delta_R^T \sqrt{1 - e^{i\beta}} \Gamma_B^{-1} \sqrt{1 - e^{i\beta}} \Delta_R} \times \\ &\quad \mathcal{F}_J e^{\sum_j J_j^* \frac{e^{i\beta_j}}{1 - e^{i\beta_j}} J_j} e^{\frac{1}{2} \mathbf{J}^\dagger \Sigma^\dagger \sigma^T \sqrt{1 - e^{i\beta}} \Gamma_B^{-1} \sqrt{1 - e^{i\beta}} \sigma \Sigma \mathbf{J} + i \Delta_R^T \sqrt{1 - e^{i\beta}} \Gamma_B^{-1} \sqrt{1 - e^{i\beta}} \sigma \Sigma \mathbf{J}}, \end{aligned} \quad (C14)$$

in terms of the Gaussian integral

$$I_G = \int \frac{d^{2N_b} \tilde{r}}{(4\pi)^{N_b}} e^{-\frac{1}{8} \tilde{r}^T \sigma^T \Gamma_B \sigma \tilde{r}}, \quad (C15)$$

where the symmetric matrix

$$\Gamma_B = \sqrt{1 - e^{i\beta}} \Gamma_b \sqrt{1 - e^{i\beta}} + 1 + e^{i\beta} = U_\Gamma^T d_\Gamma U_\Gamma \quad (C16)$$

can be diagonalized by the positive-definite diagonal matrix  $d_\Gamma$  and the unitary transformation  $U_\Gamma$  [47].

Performing the Gaussian integral, we obtain

$$\begin{aligned} I_G &= \int \frac{d^{2N_b} \tilde{r}}{(4\pi)^{N_b}} e^{-\frac{1}{8} \tilde{r}^T U_\Gamma^T d_\Gamma U_\Gamma \tilde{r}} = J(U_\Gamma^\dagger) \int \frac{d^{2N_b} r'}{(4\pi)^{N_b}} e^{-\frac{1}{8} r'^T d_\Gamma r'} \\ &= J(U_\Gamma^\dagger) \frac{1}{\sqrt{\det \frac{d_\Gamma}{2}}} = \frac{p_0}{\sqrt{\det \frac{\Gamma_B}{2}}} \text{sign}(\text{Re det } U_\Gamma), \end{aligned} \quad (C17)$$

where  $J(U_\Gamma^\dagger)$  is the Jacobian for the change of integral variables  $r' = U_\Gamma \tilde{r}$ , and the sign  $p_0 = J(U_\Gamma^\dagger) / \det U_\Gamma^\dagger$ . Finally, the mean value

$$\begin{aligned} A_b &= \frac{s_0}{\sqrt{\det \frac{\Gamma_B}{2}}} e^{-\frac{1}{2} \Delta_R^T \sqrt{1 - e^{i\beta}} \Gamma_B^{-1} \sqrt{1 - e^{i\beta}} \Delta_R} \times \\ &\quad \mathcal{F}_J e^{\sum_j J_j^* \frac{e^{i\beta_j}}{1 - e^{i\beta_j}} J_j} e^{\frac{1}{2} \mathbf{J}^\dagger \Sigma^\dagger \sigma^T \sqrt{1 - e^{i\beta}} \Gamma_B^{-1} \sqrt{1 - e^{i\beta}} \sigma \Sigma \mathbf{J} + i \Delta_R^T \sqrt{1 - e^{i\beta}} \Gamma_B^{-1} \sqrt{1 - e^{i\beta}} \sigma \Sigma \mathbf{J}} \end{aligned} \quad (C18)$$

is obtained analytically, where

$$s_0 = p_0 \text{sign}(\text{Re det } U_\Gamma^\dagger). \quad (C19)$$

Here, we list the results several mean values

$$\left\langle e^{i \sum_i \beta_i b_i^\dagger b_i} \right\rangle_{\text{GS}} = \frac{s_0}{\sqrt{\det \frac{\Gamma_B}{2}}} e^{-\frac{1}{2} \Delta_R^T \sqrt{1 - e^{i\beta}} \Gamma_B^{-1} \sqrt{1 - e^{i\beta}} \Delta_R}, \quad (C20)$$

$$\begin{aligned}
\left\langle e^{i \sum_i \beta_i b_i^\dagger b_i} b_k \right\rangle_{\text{GS}} &= \left\langle e^{i \sum_i \beta_i b_i^\dagger b_i} \right\rangle_{\text{GS}} \frac{\delta}{\delta J_k^*} i \Delta_R^T \sqrt{1 - e^{i\beta}} \Gamma_B^{-1} \sqrt{1 - e^{i\beta}} \sigma \Sigma \mathbf{J} \\
&= \left\langle e^{i \sum_i \beta_i b_i^\dagger b_i} \right\rangle_{\text{GS}} \Delta_R^T \tilde{\Gamma}_B^{-1} \begin{pmatrix} \mathbf{1}_k \\ \mathbf{i}_k \end{pmatrix},
\end{aligned} \tag{C21}$$

and

$$\begin{aligned}
\left\langle e^{i \sum_i \beta_i b_i^\dagger b_i} b_j^\dagger b_k \right\rangle_{\text{GS}} &= e^{i\beta_j} \left\langle e^{i \sum_i \beta_i b_i^\dagger b_i} \right\rangle_{\text{GS}} \left\{ \frac{1}{1 - e^{i\beta_j}} [\delta_{jk} - (\mathbf{1}_j, -\mathbf{i}_j) \tilde{\Gamma}_B^{-1} \begin{pmatrix} \mathbf{1}_k \\ \mathbf{i}_k \end{pmatrix}] \right. \\
&\quad \left. + (\mathbf{1}_j, -\mathbf{i}_j) (\tilde{\Gamma}_B^{-1})^T \Delta_R \Delta_R^T \tilde{\Gamma}_B^{-1} \begin{pmatrix} \mathbf{1}_k \\ \mathbf{i}_k \end{pmatrix} \right\},
\end{aligned} \tag{C22}$$

where  $\tilde{\Gamma}_B = (1 - e^{i\beta})\Gamma_b + (1 + e^{i\beta})$ , and vectors  $\mathbf{1}_k = (0, \dots, 1_k, \dots, 0)^T$ ,  $\mathbf{i}_k = (0, \dots, i_k, \dots, 0)^T$ .

#### Appendix D: Mean values on fermionic Gaussian states

In this Appendix, we calculate the mean value

$$\left\langle e^{i \sum_j \alpha_j n_j^f} \text{poly}(C) \right\rangle_{\text{GS}} \tag{D1}$$

on the fermionic Gaussian state. We introduce the fermionic Gaussian state in the coherent representation as [44]

$$\rho_{\text{GS}} = \int d^{2N} \eta \chi_N(\eta) e^{\frac{1}{2} \eta^* \eta} \int d^{2N} f e^{f \eta^* - \eta f^*} |f\rangle \langle -f|, \tag{D2}$$

by Grassmann numbers  $\eta$  and  $f$ , where the characteristic function

$$\chi_N(\eta) = \text{tr}[\rho_{\text{GS}} e^{\eta c^\dagger - c \eta^*}] = \exp\left[i \frac{1}{8} (\eta_1, \eta_2) \Gamma_m \begin{pmatrix} \eta_1 \\ \eta_2 \end{pmatrix}\right] \tag{D3}$$

is determined by the covariance matrix  $\Gamma_m$  and the real Grassmann numbers  $\eta_1 = \eta^* + \eta$  and  $\eta_2 = i(\eta^* - \eta)$ .

We consider the mean value

$$A_f = \left\langle e^{i \sum_i \alpha_i n_i^f} c_{j_1}^\dagger \dots c_{j_a}^\dagger c_{k_1} \dots c_{k_b} \right\rangle_{\text{GS}}. \tag{D4}$$

In terms of the density matrix (D3),  $A_f$  becomes

$$A_f = \mathcal{F}_J \int d^{2N} \eta \chi_N(\eta) e^{\frac{1}{2} \eta^* \eta} \int d^{2N} f \prod_k e^{-(1 - e^{i\alpha_k}) f_k^* f_k + (J_k^* - \eta_k^*) f_k + (J_k e^{i\alpha_k} - \eta_k) f_k^*}. \tag{D5}$$

In Eq. (D5), the integrals over Grassmann numbers  $\xi$  and  $f$  are Gaussian integrals, which can be calculated analytically.

The Gaussian integral over  $f$  leads to

$$\begin{aligned}
A_f &= \prod_j (1 - e^{i\alpha_j}) \mathcal{F}_J e^{-\sum_k \frac{e^{i\alpha_k} J_k^* J_k}{1 - e^{i\alpha_k}}} \times \\
&\quad \int d^{2N} \eta \exp\left[i \frac{1}{8} (\eta_1, \eta_2) \left(\Gamma_m - \frac{1 + e^{i\alpha}}{1 - e^{i\alpha}} \sigma\right) \begin{pmatrix} \eta_1 \\ \eta_2 \end{pmatrix} + \frac{1}{2} (\eta_1, \eta_2) \Sigma_F \mathbf{J}\right],
\end{aligned} \tag{D6}$$

where  $\alpha = \mathbf{1}_2 \otimes \text{diag}(\alpha_j)$ , and

$$\Sigma_F = \begin{pmatrix} \frac{e_\alpha}{1 - e_\alpha} & -\frac{1}{1 - e_\alpha} \\ -i \frac{e_\alpha}{1 - e_\alpha} & -i \frac{1}{1 - e_\alpha} \end{pmatrix} \tag{D7}$$

is defined by  $e_\alpha = \exp[i \text{diag}(\alpha_j)]$  and the diagonal matrix  $\text{diag}(\alpha_j)$  with elements  $\alpha_j$ . Defining the new Grassmann variable  $\eta = \sqrt{1 - e_\alpha} \tilde{\eta}$ , we obtain

$$A_f = \left(-\frac{1}{2}\right)^N s_f \text{Pf}(\Gamma_F) \mathcal{F}_J e^{\sum_k \frac{J_k^* J_k}{1 - e^{-i\alpha_k}} - \frac{1}{2} i \mathbf{J}^\dagger \Sigma_F^\dagger \sqrt{1 - e^{i\alpha}} \Gamma_F^{-1} \sqrt{1 - e^{i\alpha}} \Sigma_F \mathbf{J}}, \tag{D8}$$

where  $\text{Pf}(\Gamma_F)$  denotes the Pfaffian of the anti-symmetric matrix

$$\Gamma_F = \sqrt{1 - e^{i\alpha}} \Gamma_m \sqrt{1 - e^{i\alpha}} - (1 + e^{i\alpha}) \sigma. \quad (\text{D9})$$

The sign  $s_f$  is  $(-1)^{N/2}$  for the even  $N$  and  $(-1)^{(N-1)/2}$  for the odd  $N$ .

By taking the derivatives to  $J$  and  $J^*$ , we obtain the average values, e.g.,

$$\left\langle e^{i \sum_i \alpha_i n_i^f} \right\rangle_{\text{GS}} = (-\frac{1}{2})^N s_f \text{Pf}(\Gamma_F), \quad (\text{D10})$$

and

$$\left\langle e^{i \sum_i \alpha_i n_i^f} c_j^\dagger c_k \right\rangle_{\text{GS}} = \frac{1}{4} i e^{i\alpha_j} \left\langle e^{i \sum_i \alpha_i n_i^f} \right\rangle_{\text{GS}} (\mathbf{1}_k, \mathbf{i}_k) (\Gamma_m + \sigma) \frac{1}{1 + \frac{1}{2}(1 - e^{i\alpha})(\sigma \Gamma_m - 1)} \begin{pmatrix} \mathbf{1}_j \\ -\mathbf{i}_j \end{pmatrix}. \quad (\text{D11})$$

### Appendix E: Equations of motion of $\Delta_R$ and $\Gamma_{b,m}$

In this Appendix, we explicitly derive the equations of motion for  $\Delta_R$  and  $\Gamma_{b,m}$  in the non-Gaussian state determined by the unitary transformation  $U_S = U_{4,5}$ . We focus on the case  $\xi_{f,b} = \bar{\Delta}_R = 0$ . In the Gaussian limit  $U_S = I$ , these equations reproduce the results (30) and (31) in Sec. II B.

For  $U_S = U_{4,5}$  with  $\xi_{f,b} = \bar{\Delta}_R = 0$ , the tangent vector  $\partial_\tau |\Psi_{\text{NGS}}\rangle$  has the form  $U_S \text{poly}(R, C) |\Psi_{\text{GS}}\rangle$ . We shall construct the orthogonal tangent vectors explicitly, such that the Gram matrix becomes diagonal. To orthogonalize the tangent vectors, we move the unitary operators  $U_S$  and  $U_{\text{GS}}$  to the most left side in the tangent vector  $\partial_\tau |\Psi_{\text{NGS}}\rangle = U_S U_{\text{GS}} U_L |0\rangle$ . The relations (B1), (B2), and (B6) obtained in Appendix B give rise to

$$\begin{aligned} U_L = & \tilde{\phi} + i \frac{1}{2} R^T S_b^T \sigma \partial_\tau \Delta_R + i \frac{1}{4} : R^T S_b^T \sigma (\partial_\tau S_b) R : \\ & + \frac{1}{4} : A^T U_m^T (\partial_\tau U_m) A : + U_{\text{GS}}^\dagger O U_{\text{GS}} - \langle O \rangle_{\text{GS}}, \end{aligned} \quad (\text{E1})$$

where the imaginary number

$$\tilde{\phi} = -\phi_0 + i \frac{1}{4} \text{tr}[S_b^T \sigma (\partial_\tau S_b) \Gamma_b] + i \frac{1}{4} \text{tr}[U_m^T (\partial_\tau U_m) \Gamma_m] + \langle O \rangle_{\text{GS}}, \quad (\text{E2})$$

the term  $O = U_S^{-1} \partial_\tau U_S$  higher than the quadratic order, and all operators in  $U_L$  is normal ordered with respect to the vacuum state.

To express the higher order term  $U_{\text{GS}}^\dagger O U_{\text{GS}}$  in the normal ordering form, we employ the following theorem for the arbitrary operator  $\Xi$ : the normal ordering expansion

$$\begin{aligned} U_{\text{GS}}^\dagger \Xi U_{\text{GS}} = & \langle \Xi \rangle_{\text{GS}} + \frac{1}{2} R^T S_b^T \Xi_\Delta + \frac{1}{4} : R^T S_b^T \Xi_b S_b R : \\ & + i \frac{1}{4} : A^T U_m^T \Xi_m U_m A : + \delta \Xi \end{aligned} \quad (\text{E3})$$

of the operator  $U_{\text{GS}}^\dagger \Xi U_{\text{GS}}$  is determined by the Wick theorem, where  $\langle \Xi \rangle_{\text{GS}}$  is the average value of  $\Xi$  on the Gaussian state  $U_{\text{GS}} |0\rangle$ , and the operator  $\delta \Xi$  contains the finite higher order normal ordered terms, e.g., the cubic and quartic terms. The expansion coefficients

$$\Xi_\Delta = 2 \frac{\delta \langle \Xi \rangle_{\text{GS}}}{\delta \Delta_R}, \Xi_b = 4 \frac{\delta \langle \Xi \rangle_{\text{GS}}}{\delta \Gamma_b}, \Xi_m = 4 \frac{\delta \langle \Xi \rangle_{\text{GS}}}{\delta \Gamma_m} \quad (\text{E4})$$

are the functional derivatives of the average value  $\langle \Xi \rangle_{\text{GS}}$  with respect to  $\Delta_R$  and  $\Gamma_{b,m}$ . Since the analytic result  $\langle \Xi \rangle_{\text{GS}}$  is obtained by the approach in Appendices C and D, the normal ordering expansion (E3) can be determined analytically by Eq. (E4).

By applying the result (E3) on the operator  $U_{\text{GS}}^\dagger O U_{\text{GS}}$ , we obtain the normal ordering expansion

$$\begin{aligned} U_{\text{GS}}^\dagger O U_{\text{GS}} = & \langle O \rangle_{\text{GS}} + \frac{1}{2} R^T S_b^T O_\Delta + \frac{1}{4} : R^T S_b^T O_b S_b R : \\ & + i \frac{1}{4} : A^T U_m^T O_m U_m A : + \delta O, \end{aligned} \quad (\text{E5})$$

where  $O_\Delta$ ,  $O_b$ , and  $O_m$  are obtained by replacing  $\Xi$  to  $O$  in Eq. (E4).

Applying  $U_L$  on the vacuum state, we obtain

$$U_L |0\rangle = \sum_{n=0}^2 |L_n\rangle + \delta O |0\rangle \quad (\text{E6})$$

by Eqs. (E1) and (E3), where  $|L_0\rangle = \tilde{\phi}|0\rangle$ , the linear term

$$|L_1\rangle = \frac{1}{2} R^T S_b^T (i\sigma \partial_\tau \Delta_R + O_\Delta) |0\rangle, \quad (\text{E7})$$

and the quadratic terms

$$\begin{aligned} |L_2\rangle = & \left[ \frac{1}{4} :R^T S_b^T (i\sigma \partial_\tau S_b + O_b S_b) R: \right. \\ & \left. + \frac{1}{4} :A^T U_m^T (\partial_\tau U_m + iO_m U_m) A: \right] |0\rangle. \end{aligned} \quad (\text{E8})$$

Since the operators in  $U_L$  are normal ordered, the states  $|L_n\rangle$  and  $\delta O |0\rangle$  in Eq. (E6) only contain the creation operators acting on the vacuum state. As a result, the states  $|L_{n=0,1,2}\rangle$  and  $\delta O |0\rangle$  form the orthogonal basis in the tangent space, which describe the different numbers  $n = 0, 1, 2, \dots$  of excitations on the vacuum state.

Moving the unitary operators  $U_S$  and  $U_{GS}$  to the most left side, we obtain the state  $|\mathbf{R}_\Psi\rangle = U_S U_{GS} |\Psi_R\rangle$ , where

$$|\Psi_R\rangle = \begin{cases} -(U_R - \langle \bar{H} \rangle_{GS}) |0\rangle, & \text{imaginary time evolution} \\ -iU_R |0\rangle, & \text{real time evolution} \end{cases}, \quad (\text{E9})$$

and  $U_R = U_{GS}^\dagger \bar{H} U_{GS}$  is determined by the Hamiltonian  $\bar{H} = U_S^\dagger H U_S$  in the rotating frame. The normal ordering expansion

$$\begin{aligned} U_R = & \langle \bar{H} \rangle_{GS} + \frac{1}{2} R^T S_b^T h_\Delta + \frac{1}{4} :R^T S_b^T h_b S_b R: \\ & + i \frac{1}{4} :A^T U_m^T h_m U_m A: + \delta \bar{H} \end{aligned} \quad (\text{E10})$$

of  $U_R$  are obtained by Eq. (E3), where the expansion coefficients

$$h_\Delta = 2 \frac{\delta \langle \bar{H} \rangle_{GS}}{\delta \Delta_R}, h_b = 4 \frac{\delta \langle \bar{H} \rangle_{GS}}{\delta \Gamma_b}, h_m = 4 \frac{\delta \langle \bar{H} \rangle_{GS}}{\delta \Gamma_m} \quad (\text{E11})$$

follow from Eq. (E4), and  $\delta \bar{H}$  contains the higher order normal ordered operators.

Applying  $U_R$  on the vacuum state, we obtain

$$U_R |0\rangle = \sum_{n=0}^2 |\tilde{L}_n\rangle + \delta \bar{H} |0\rangle, \quad (\text{E12})$$

where  $|\tilde{L}_0\rangle = \langle \bar{H} \rangle_{GS} |0\rangle$ , the linear term  $|\tilde{L}_1\rangle = R^T S_b^T h_\Delta |0\rangle / 2$ , the quadratic term

$$|\tilde{L}_2\rangle = \left( \frac{1}{4} :R^T S_b^T h_b S_b R: + i \frac{1}{4} :A^T U_m^T h_m U_m A: \right) |0\rangle, \quad (\text{E13})$$

and  $\delta \bar{H} |0\rangle$  are the orthogonal to each other.

The equations of motion for  $\Delta_R$  and  $\Gamma_{b,m}$  are obtained by the comparison of tangent vectors  $|L_{1,2}\rangle$  and  $|\tilde{L}_{1,2}\rangle$ . For the imaginary- and real- time evolutions, we have  $|L_{1,2}\rangle = -|\tilde{L}_{1,2}\rangle$  and  $|L_{1,2}\rangle = -i|\tilde{L}_{1,2}\rangle$ , respectively. For the imaginary time evolution, the relations  $|L_{1,2}\rangle = -|\tilde{L}_{1,2}\rangle$  give rise to

$$R^T S_b^T (i\sigma \partial_\tau \Delta_R + O_\Delta) |0\rangle = -R^T S_b^T h_\Delta |0\rangle, \quad (\text{E14})$$

$$:R^T S_b^T (i\sigma \partial_\tau S_b + O_b S_b) R: |0\rangle = -:R^T S_b^T h_b S_b R: |0\rangle, \quad (\text{E15})$$

and

$$:A^T U_m^T (\partial_\tau U_m + i O_m U_m) A: |0\rangle = -i :A^T U_m^T h_m U_m A: |0\rangle. \quad (\text{E16})$$

Here, since all terms are normal ordered, only the creation operators survive in Eqs. (E14)-(E16). The left and right hand sides of Eq. (E14) become

$$\begin{aligned} & R^T S_b^T (i\sigma \partial_\tau \Delta_R + O_\Delta) |0\rangle \\ &= (b^\dagger, ib^\dagger) S_b^T (i\sigma \partial_\tau \Delta_R + O_\Delta) |0\rangle \\ &= -(b^\dagger, ib^\dagger) \sigma S_b^{-1} \sigma (i\sigma \partial_\tau \Delta_R + O_\Delta) |0\rangle \\ &= i(b^\dagger, ib^\dagger) S_b^{-1} \sigma (i\sigma \partial_\tau \Delta_R + O_\Delta) |0\rangle, \end{aligned} \quad (\text{E17})$$

and

$$-R^T S_b^T h_\Delta |0\rangle = -(b^\dagger, ib^\dagger) S_b^T h_\Delta |0\rangle, \quad (\text{E18})$$

where  $b^\dagger = (b_1^\dagger, \dots, b_{N_b}^\dagger)$  and we used the relation  $S_b^T \sigma S_b = \sigma$ . By comparing the real and imaginary parts in Eqs. (E17) and (E18), we obtain the motion equation

$$\partial_\tau \Delta_R = -\Gamma_b h_\Delta - i\sigma O_\Delta. \quad (\text{E19})$$

The left and right hand sides of Eq. (E15) are

$$:R^T S_b^T (i\sigma \partial_\tau S_b + O_b S_b) R: |0\rangle = (b^\dagger, ib^\dagger) S_b^T (i\sigma \partial_\tau S_b + O_b S_b) \begin{pmatrix} b^\dagger \\ ib^\dagger \end{pmatrix} |0\rangle, \quad (\text{E20})$$

and

$$-:R^T S_b^T h_b S_b R: |0\rangle = \frac{1}{2} i(b^\dagger, ib^\dagger) (S_b^T h_b S_b \sigma - \sigma S_b^T h_b S_b) \begin{pmatrix} b^\dagger \\ ib^\dagger \end{pmatrix} |0\rangle. \quad (\text{E21})$$

Here, we notice that the motion equation of  $S_b$  can not be uniquely determined, since the variational parameters in Eq. (19) has some gauge degrees of freedoms, as discussed in Sec. II B. However, the motion equation of  $\Gamma_b$  for each equivalent class is uniquely determined, namely,  $\Gamma_b$  is gauge invariant. Thus, we can choose the motion equation for one  $S_b$  in the equivalent class, and derive the motion equation of  $\Gamma_b$ .

By comparing the right hand sides in Eqs. (E20) and (E21), we obtain

$$\partial_\tau S_b = -\frac{1}{2} \sigma h_b S_b \sigma - \frac{1}{2} \Gamma_b h_b S_b - i\sigma O_b S_b, \quad (\text{E22})$$

where  $\partial_\tau (S_b \sigma S_b^T) = 0$  maintains the symplecticity of  $S_b$ . The motion Eq. (E22) of  $S_b$  leads to

$$\partial_\tau \Gamma_b = -\sigma h_b \sigma - \Gamma_b h_b \Gamma_b + i\Gamma_b O_b \sigma - i\sigma O_b \Gamma_b. \quad (\text{E23})$$

The left and right hand sides of Eq. (E16) are

$$:A^T U_m^T (\partial_\tau U_m + i O_m U_m) A: |0\rangle = : (c^\dagger, ic^\dagger) U_m^T (\partial_\tau U_m + i O_m U_m) \begin{pmatrix} c^\dagger \\ ic^\dagger \end{pmatrix} : |0\rangle, \quad (\text{E24})$$

and

$$-i :A^T U_m^T h_m U_m A: |0\rangle = \frac{1}{2} : (c^\dagger, ic^\dagger) (\sigma U_m^T h_m U_m - U_m^T h_m U_m \sigma) \begin{pmatrix} c^\dagger \\ ic^\dagger \end{pmatrix} : |0\rangle, \quad (\text{E25})$$

where  $c^\dagger = (c_1^\dagger, \dots, c_{N_b}^\dagger)$ . Similar to the bosonic case, the motion equation of  $U_m$  is not unique, however, the motion equation of  $\Gamma_b$  can be determined uniquely in each equivalent case. By comparing the right hand sides in Eqs. (E24) and (E25), we obtain

$$\partial_\tau U_m = -\frac{1}{2} h_m U_m \sigma - \frac{1}{2} \Gamma_m h_m U_m - i O_m U_m, \quad (\text{E26})$$



which leads to

$$\partial_\tau \Gamma_m = -h_m - \Gamma_m h_m \Gamma_m + i[\Gamma_m, O_m]. \quad (\text{E27})$$

Here,  $\partial_\tau(U_m U_m^T) = 0$  justifies the orthogonality of  $U_m$ .

The imaginary-time evolution equations of motion are summerized as follows

$$\begin{aligned} \partial_\tau \Delta_R &= -\Gamma_b h_\Delta - i\sigma O_\Delta, \\ \partial_\tau \Gamma_b &= \sigma^T h_b \sigma - \Gamma_b h_b \Gamma_b + i\Gamma_b O_b \sigma - i\sigma O_b \Gamma_b, \\ \partial_\tau \Gamma_m &= -h_m - \Gamma_m h_m \Gamma_m + i[\Gamma_m, O_m]. \end{aligned} \quad (\text{E28})$$

By the samilar procedure, the real-time equations of motion are

$$\begin{aligned} \partial_t \Delta_R &= \sigma h_\Delta^t, \\ \partial_t \Gamma_b &= \sigma h_b^t \Gamma_b - \Gamma_b h_b^t \sigma, \\ \partial_t \Gamma_m &= [h_m^t, \Gamma_m], \end{aligned} \quad (\text{E29})$$

where  $h_\Delta^t = h_\Delta - iO_\Delta$ ,  $h_b^t = h_b - iO_b$ , and  $h_m^t = h_m - iO_m$ . In Appendix F, we provide another approach to derive Eqs. (E28) and (E29).

We notice that in the motion Eqs. (E28) and (E29),  $O_\Delta$ ,  $O_b$ , and  $O_m$  still contain the time derivatives of the variational parameters in  $U_S$ , e.g.,  $\partial_\tau \bar{\omega}$ ,  $\partial_\tau \omega^f$ ,  $\partial_\tau \omega^b$ , and  $\partial_\tau \omega^{bf}$ . The equations of motion of these rest variational parameters can be obtained by the procedure shown in Sec. II A (see Secs. IV and V as examples).

From the equations of motion, one can use the relation (29) to derive the equations of motion

$$\partial_\tau \Gamma_f = \{\Gamma_f, h_f\} - 2\Gamma_f h_f \Gamma_f + [\Gamma_f, O_f] \quad (\text{E30})$$

and

$$\partial_t \Gamma_f = i[\Gamma_f, h_f^t] \quad (\text{E31})$$

for the correlation matrix  $\Gamma_f$  in the imaginary- and real- time evolutions, respectively, where in the Dirac fermion basis the matrices  $h_f^t = h_f - iO_f$  and

$$h_f = i\frac{1}{2}W_m^\dagger h_m W_m, O_f = i\frac{1}{2}W_m^\dagger O_m W_m. \quad (\text{E32})$$

For Gaussian states, i.e.,  $U_S = I$ , the quantities  $O_\Delta = O_b = O_m = 0$  and the motion Eqs. (E28)-(E29) result in Eqs. (30) and (31) in Sec. II B.

In Appendix A, we show that the relation (11) is guaranteed for the general variational ansatz. Here, we show the condition (11) for Gaussian states by using the motion Eqs. (30) and (31) directly. Since the Gaussian state energy  $E(t, \Delta_R, \Gamma_{b,m})$  is the function of  $t$ ,  $\Delta_R$  and  $\Gamma_{b,m}$ , the time derivative of the energy has the form

$$\begin{aligned} \frac{dE}{dt} &= \left\langle \frac{\partial H}{\partial t} \right\rangle + \sum_j \frac{\delta E}{\delta \Delta_{R,j}} \partial_t \Delta_{R,j} \\ &\quad + \sum_{ij} \left( \frac{\delta E}{\delta \Gamma_{b,ij}} \partial_t \Gamma_{b,ij} + \frac{\delta E}{\delta \Gamma_{m,ij}} \partial_t \Gamma_{m,ij} \right). \end{aligned} \quad (\text{E33})$$

The motion Eqs. (30) and (31) lead to

$$\begin{aligned} \sum_j \frac{\delta E}{\delta \langle R_j \rangle} \partial_t \langle R_j \rangle &= \frac{1}{2} h_\Delta^T \sigma h_\Delta = 0, \\ \sum_{ij} \frac{\delta E}{\delta \Gamma_{b,ij}} \partial_t \Gamma_{b,ij} &= \frac{1}{4} \text{tr}[h_b \sigma h_b, \Gamma_b] = 0, \\ \sum_{ij} \frac{\delta E}{\delta \Gamma_{m,ij}} \partial_t \Gamma_{m,ij} &= -\frac{1}{4} \text{tr}(h_m [h_m, \Gamma_m]) = 0, \end{aligned} \quad (\text{E34})$$

which eventually give rise to the constraint (11), i.e.,

$$\frac{dE}{dt} = \left\langle \frac{\partial H}{\partial t} \right\rangle. \quad (\text{E35})$$

### Appendix F: Alternative derivation of motion Eqs. (E28) and (E29)

In this Appendix, we derive the motion Eqs. (E28) and (E29) from another point of view. For the imaginary time evolution,  $|L_{1,2}\rangle = -|\tilde{L}_{1,2}\rangle$  leads to  $\sum_{j=1,2}|L_j\rangle = -\sum_{j=1,2}|\tilde{L}_j\rangle$ , i.e.,

$$\begin{aligned} & [\frac{1}{2}R^T S_b^T (i\sigma\partial_\tau\Delta_R + O_\Delta) + \frac{1}{4}:R^T S_b^T (i\sigma\partial_\tau S_b + O_b S_b)R: + \frac{1}{4}:A^T U_m^T (\partial_\tau U_m + iO_m U_m)A:]|0\rangle \\ &= -[\frac{1}{2}R^T S_b^T h_\Delta + \frac{1}{4}:R^T S_b^T h_b S_b R: + i\frac{1}{4}:A^T U_m^T h_m U_m A:]|0\rangle. \end{aligned} \quad (F1)$$

The left hand side of Eq. (F1) can be written as

$$U_{\text{GS}}^{-1}\partial_\tau|\Psi_{\text{GS}}\rangle + [\frac{1}{2}R^T S_b^T O_\Delta + \frac{1}{4}:R^T S_b^T O_b S_b R: + i\frac{1}{4}:A^T U_m^T O_m U_m A:]|0\rangle. \quad (F2)$$

By multiplying  $U_{\text{GS}}^{-1}$  on both sides of Eq. (F1), we obtain the motion equation

$$\partial_\tau|\Psi_{\text{GS}}\rangle = -[\frac{1}{2}\delta R^T (h_\Delta + O_\Delta) + \frac{1}{4}\delta R^T (h_b + O_b)\delta R: + i\frac{1}{4}:A^T (h_m + O_m)A:]|\Psi_{\text{GS}}\rangle. \quad (F3)$$

The equation (F3) gives the motion equation

$$\begin{aligned} \partial_\tau\rho_{\text{GS}} &= -\{\frac{1}{2}\delta R^T h_\Delta + \frac{1}{4}\delta R^T h_b \delta R: + i\frac{1}{4}:A^T h_m A:, \rho_{\text{GS}}\} \\ &\quad -[\frac{1}{2}\delta R^T O_\Delta + \frac{1}{4}\delta R^T O_b \delta R: + i\frac{1}{4}:A^T O_m A:, \rho_{\text{GS}}] \end{aligned} \quad (F4)$$

of the density matrix  $\rho_{\text{GS}} = |\Psi_{\text{GS}}\rangle\langle\Psi_{\text{GS}}|$ .

By taking the trace of operators  $R$ ,  $\{\delta R, \delta R^T\}/2$ , and  $i[A, A^T]/2$  on both sides of Eq. (F4) as

$$\begin{aligned} \partial_\tau\Delta_R &= \text{tr}[R\partial_\tau\rho_{\text{GS}}], \\ \partial_\tau\Gamma_b &= \text{tr}[\frac{1}{2}\{\delta R, \delta R^T\}\partial_\tau\rho_{\text{GS}}], \\ \partial_\tau\Gamma_m &= \text{tr}[\frac{i}{2}[A, A^T]\partial_\tau\rho_{\text{GS}}], \end{aligned} \quad (F5)$$

we can reproduce Eq. (E28) by the Wick theorem. Following the samilar procedure, we can obtain the real-time motion Eqs. (E29) in the real time evolution.

### Appendix G: Equations of motion of $\theta_0$ and $\Lambda_1$

In this Appendix, we derive the motion Eq. (73) from the projected Schrödinger Eq. (70). The evolution of  $U_{\text{GS}}(t)$  obeys

$$i\partial_t U_{\text{GS}}(t) = \bar{H}_{\text{MF}} U_{\text{GS}}(t), \quad (G1)$$

where  $U_{\text{GS}}(t) = e^{iR^T\sigma\Delta_R/2}V_{\text{GS}}(t)$  is determined by

$$V_{\text{GS}}(t) = e^{i\theta_0(t)}e^{b^\dagger\Lambda_1 b^\dagger}e^{b^\dagger\Lambda_2 b}e^{b\Lambda_3 b}, \quad (G2)$$

and  $\Lambda_{1,3}$  are symmetric matrices.

It follows from Eq. (G1) that the motion equation of  $V_{\text{GS}}(t)$  is

$$i\partial_t V_{\text{GS}}(t) = (\frac{1}{4}R^T h_b R + \delta E_k)V_{\text{GS}}(t), \quad (G3)$$

where  $\delta E_k = E_k - \Delta_R^T h_\Delta/4 - \text{tr}(h_b \Gamma_b)/4$ , and the last term in  $\delta E_k$  originates from removing the normal ordering of the first quadratic term in Eq. (G3).

The left- hand side of Eq. (G3) is

$$\begin{aligned} i\partial_t V_{\text{GS}}(t) = & -\partial_t \theta_0(t) e^{i\theta_0(t)} e^{b^\dagger \Lambda_1 b^\dagger} e^{b^\dagger \Lambda_2 b} e^{b \Lambda_3 b} + b^\dagger i\partial_t \Lambda_1 b^\dagger e^{i\theta_0(t)} e^{b^\dagger \Lambda_1 b^\dagger} e^{b^\dagger \Lambda_2 b} e^{b \Lambda_3 b} \\ & + i e^{i\theta_0(t)} e^{b^\dagger \Lambda_1 b^\dagger} (\partial_t e^{b^\dagger \Lambda_2 b}) e^{b \Lambda_3 b} + i e^{i\theta_0(t)} e^{b^\dagger \Lambda_1 b^\dagger} e^{b^\dagger \Lambda_2 b} (b \partial_t \Lambda_3 b) e^{b \Lambda_3 b}. \end{aligned} \quad (\text{G4})$$

Using Eq. (B3) in Appendix B, we obtain the time derivative in the third term of Eq. (G4) as

$$\partial_t e^{b^\dagger \Lambda_2 b} = b^\dagger (\partial_t e^{\Lambda_2}) e^{-\Lambda_2} b e^{b^\dagger \Lambda_2 b}. \quad (\text{G5})$$

In Eq. (G4), all exponential operators can be moved to the most right side by the relations

$$\begin{aligned} e^{b^\dagger \Lambda_1 b^\dagger} b &= (b - 2\Lambda_1 b^\dagger) e^{b^\dagger \Lambda_1 b^\dagger}, \\ e^{b^\dagger \Lambda_2 b} b &= e^{-\Lambda_2} b e^{b^\dagger \Lambda_2 b}, \end{aligned} \quad (\text{G6})$$

which leads to

$$\begin{aligned} i\partial_t V_{\text{GS}}(t) = & \{-\partial_t \theta_0 - 2i \text{tr}[e^{-\Lambda_2^T} (\partial_t \Lambda_3) e^{-\Lambda_2} \Lambda_1] \\ & + i b^\dagger [(\partial_t e^{\Lambda_2}) e^{-\Lambda_2} - 4\Lambda_1 e^{-\Lambda_2^T} (\partial_t \Lambda_3) e^{-\Lambda_2}] b \\ & + i b^\dagger [\partial_t \Lambda_1 - 2(\partial_t e^{\Lambda_2}) e^{-\Lambda_2} \Lambda_1 + 4\Lambda_1 e^{-\Lambda_2^T} (\partial_t \Lambda_3) e^{-\Lambda_2} \Lambda_1] b^\dagger \\ & + i b e^{-\Lambda_2^T} (\partial_t \Lambda_3) e^{-\Lambda_2} b\} V_{\text{GS}}(t). \end{aligned} \quad (\text{G7})$$

The right-hand side of Eq. (G3) is

$$\left(\frac{1}{4} R^T h_b R + \delta E_k\right) V_{\text{GS}}(t) = (b^\dagger \omega_b b + \frac{1}{2} b^\dagger \varpi b^\dagger + \frac{1}{2} b \varpi^\dagger b + \frac{1}{2} \text{tr} \omega_b + \delta E_k) V_{\text{GS}}(t), \quad (\text{G8})$$

where the matrices  $\omega_b$  and  $\varpi$  are defined by

$$\begin{pmatrix} \omega_b & \varpi \\ \varpi^\dagger & \omega_b^T \end{pmatrix} = \frac{1}{2} W_b^\dagger h_b W_b. \quad (\text{G9})$$

Comparing Eqs. (G7) and (G8), we obtain the equations of motion

$$\begin{aligned} \partial_t \theta_0 &= -\delta E_k - \frac{1}{2} \text{tr} \omega_b - \text{tr}(\varpi^\dagger \Lambda_1), \\ i\partial_t \Lambda_1 &= \frac{1}{2} \varpi + \omega_b \Lambda_1 + \Lambda_1 \omega_b^T + 2\Lambda_1 \varpi^\dagger \Lambda_1, \\ i\partial_t e^{\Lambda_2} &= \omega_b e^{\Lambda_2} + 2\Lambda_1 \varpi^\dagger e^{\Lambda_2}, \\ i\partial_t \Lambda_3 &= \frac{1}{2} e^{\Lambda_2^T} \varpi^\dagger e^{\Lambda_2}. \end{aligned} \quad (\text{G10})$$

- 
- |   |  |
|---|--|
| <p>[1] E. P. Gross, <i>II Nuovo Cimento</i>. <b>20</b>, 454 (1961); L. P. Pitaevskii, <i>Sov. Phys. JETP</i>. <b>13</b>, 451 (1961).<br/> [2] F. Dalfovo, S. Giorgini, L. P. Pitaevskii, and S. Stringari, <i>Rev. Mod. Phys.</i> <b>71</b>, 463 (1999).<br/> [3] J. Bardeen, L. N. Cooper, and J. R. Schrieffer, <i>Phys. Rev.</i> <b>108</b>, 1175 (1957).<br/> [4] N. N. Bogoliubov, <i>J. Phys. (USSR)</i> <b>11</b>, 23 (1947).<br/> [5] K. v. Klitzing, G. Dorda, M. Pepper, <i>Phys. Rev. Lett.</i> <b>45</b>, 494 (1980).<br/> [6] H. L. Stormer and D. C. Tsui, <i>Science</i> <b>220</b>, 1241 (1983).<br/> [7] R. B. Laughlin, <i>Phys. Rev. Lett.</i> <b>50</b>, 1395 (1983).</p> | <p>[8] C. Weedbrook, S. Pirandola, R. García-Patrón, N. J. Cerf, T. C. Ralph, J. H. Shapiro, and S. Lloyd, <i>Rev. Mod. Phys.</i> <b>84</b>, 621 (2012).<br/> [9] G. C. Wick, <i>Phys. Rev.</i> <b>80</b>, 268 (1950).<br/> [10] C. J. Pethick and H. Smith, <i>Bose–Einstein Condensation in Dilute Gases</i>. (Cambridge: Cambridge University Press).<br/> [11] V. L. Ginzburg and L. D. Landau, <i>Zh. Eksp. Teor. Fiz.</i> <b>20</b>, 1064 (1950).<br/> [12] N. Kopnin, <i>Theory of Nonequilibrium Superconductivity</i> (Oxford University Press, 1st edition).</p> |
|---|--|

- [13] R. A. Barankov, L. S. Levitov, and B. Z. Spivak, Phys. Rev. Lett. **93**, 160401 (2004); R. A. Barankov and L. S. Levitov, Phys. Rev. Lett. **96**, 230403 (2006).
- [14] Emil A. Yuzbashyan, Oleksandr Tsypliyatyev, and Boris L. Altshuler, Phys. Rev. Lett. **96**, 097005 (2006).
- [15] T. Holstein and H. Primakoff, Phys. Rev. **58**, 1098 (1940).
- [16] S. Sachdev, *Quantum Phase Transitions* (Cambridge University Press, 2nd Edition).
- [17] S. K. Kim, J. Math. Phys. **28**, 2540 (1987).
- [18] P. Coleman, Phys. Rev. B **29**, 3035 (1984).
- [19] I. Affleck, arXiv:0809.3474.
- [20] M. Randeria and E. Taylor, Annual Review of Condensed Matter Physics **5**, 209 (2014).
- [21] S. Tan, Ann. Phys. (N.Y.) **323**, 2952 (2008).
- [22] S. Tan, Ann. Phys. (N.Y.) **323**, 2971 (2008).
- [23] S. Tan, Ann. Phys. (N.Y.) **323**, 2987 (2008).
- [24] R. Silbey and R. A. Harris, J. Chem. Phys. **80**, 2615 (1984); R. A. Harris and R. Silbey, *ibid.* **83**, 1069 (1985).
- [25] S. Bera, S. Florens, H. U. Baranger, N. Roch, A. Nazir, and A. W. Chin, Phys. Rev. B **89**, 121108(R) (2014).
- [26] D. P. S. McCutcheon, N. S. Dattani, E. M. Gauger, B. W. Lovett, and A. Nazir, Phys. Rev. B **84**, 081305(R) (2011).
- [27] R. Bulla, N.-H. Tong, and M. Vojta, Phys. Rev. Lett. **91**, 170601 (2003).
- [28] J. Haegeman, J. I. Cirac, T. J. Osborne, I. Pizorn, H. Verschelde, and F. Verstraete, Phys. Rev. Lett. **107**, 070601 (2011).
- [29] R. Rajaraman and S. L. Sondhi, Int. J. Mod. Phys. B, **10**, 793 (1996).
- [30] R. Shankar and G. Murthy, Phys. Rev. Lett. **79** 4437 (1997);
- [31] R. Shankar and G. Murthy, arXiv:cond-mat/9802244.
- [32] J. K. Jain, *Composite Fermions* (Cambridge University Press, 1st edition).
- [33] A. I. Streltsov, L. S. Cederbaum, and N. Moiseyev, Phys. Rev. A **70**, 053607 (2004).
- [34] L. S. Cederbaum and A. I. Streltsov, Phys. Rev. A **70**, 023610 (2004).
- [35] T. D. Lee, F. E. Low, and D. Pines, Phys. Rev. **90**, 297 (1953).
- [36] D. J. J. Marchand, G. De Filippis, V. Cataudella, M. Berciu, N. Nagaosa, N. V. Prokof'ev, A. S. Mishchenko, and P. C. E. Stamp, Phys. Rev. Lett. **105**, 266605 (2010).
- [37] T. Shi, Y. Chang, J. J. Garcia-Ripoll, arXiv:1701.04709.
- [38] Note that the minimum does not necessarily has to be global.
- [39] D. Pekker and C. M. Varma, Annu. Rev. Condens. Ma. P. **6**, 269 (2015).
- [40] C. V. Kraus and J. I. Cirac, New J. Phys. **12**, 113004 (2010).
- [41] D. Podolsky and E. Demler, New J. Phys. **7**, 59 (2005).
- [42] D. Walls and G. Milburn, *Quantum Optics* (Springer, Berlin 1994).
- [43] C. Navarrete-Benlloch, arXiv:1504.05270.
- [44] K. E. Cahill and R. J. Glauber, Phys. Rev. A **59** 1538 (1999).
- [45] M. Berciu, Phys. Rev. Lett. **97**, 036402 (2006).
- [46] F. Grusdt, A. Shashi, D. Abanin, and E. Demler, Phys. Rev. A **90**, 063610 (2014).
- [47] T. Takagi, Japan J. Math. **1**, 83 (1925).
- [48] A. S. Alexandrov and J. Ranninger, Phys. Rev. B **45**, 13109 (1992).
- [49] N.V. Prokof'ev and B.V. Svistunov, Phys. Rev. Lett. **81**, 2514 (1998).
- [50] Y. Toyozawa, Prog. Theor. Phys. **26**, 29 (1961).
- [51] V. M. Stojanović, T. Shi, C. Bruder, and J. I. Cirac, Phys. Rev. Lett. **109**, 250501 (2012).
- [52] J. Wei and E. Norman, J. Math. Phys. **4**, 575 (1963).
- [53] Y. E. Shchadilova, R. Schmidt, F. Grusdt, and E. Demler, Phys. Rev. Lett. **117**, 113002 (2016).
- [54] A. J. Leggett, S. Chakravarty, A. T. Dorsey, M. P. A. Fisher, A. Garg, and W. Zwerger, Rev. Mod. Phys. **59**, 1 (1987).
- [55] J. von Delft and H. Schoeller, Annalen Phys. **7**, 225 (1998).
- [56] G. Zarand and J. von Delft, Phys. Rev. B **61**, 6918 (2000).
- [57] R. Fazio *et al.* *New Directions in Mesoscopic Physics* (Erice, 2002).
- [58] M. Hohenadler, H. G. Evertz, and W. von der Linden, Phys. Rev. B **69**, 024301 (2004).
- [59] V. D. Lakhno, Physics-Uspekhi, **58**, 295 (2015).
- [60] A. J. Leggett, *Modern Trends in the Theory of Condensed Matter*, Springer, New York (1980).
- [61] T. Shi, J. N. Zhang, C. P. Sun, and S. Yi, Phys. Rev. A **82**, 033623 (2010).
- [62] M. Baranov, M. Dalmonte, G. Pupillo, and P. Zoller, Chem. Rev. **112**, 5012 (2012).
- [63] T. Shi, S. H. Zou, H. Hu, C. P. Sun, and S. Yi, Phys. Rev. Lett. **110**, 045301 (2013).
- [64] R. Qi, Z. Shi, and H. Zhai, Phys. Rev. Lett. **110**, 045302 (2013).
- [65] M. J. Lawler, D. G. Barci, V. Fernández, E. Fradkin, and L. Oxman, Phys. Rev. B **73**, 085101 (2006).
- [66] C. Wu, K. Sun, E. Fradkin, and S. C. Zhang, Phys. Rev. B **75**, 115103 (2007).
- [67] P. Fulde and R. A. Ferrell, Phys. Rev. **135**, A550 (1964).
- [68] A. I. Larkin and Yu. N. Ovchinnikov, Sov. Phys. JETP. **20**, 762 (1965).
- [69] M. Alford, J. A. Bowers, and K. Rajagopal, Phys. Rev. D **63**, 074016 (2001).
- [70] L. P. Pryadko, S. A. Kivelson, V. J. Emery, Y. B. Bazaliy, and E. A. Demler, Phys. Rev. B **60**, 7541 (1999).
- [71] A. van Otterlo, D. S. Golubev, A. D. Zaikin, and G. Blatter, Eur. Phys. J. B **10**, 131 (1999).
- [72] E. A. Yuzbashyan, M. Dzero, V. Gurarie, and M. S. Foster, Phys. Rev. A **91**, 033628 (2015).
- [73] K. D. Irwin and G. C. Hilton, Topics Appl. Phys. **99**, 63 (2005).
- [74] C. Gardiner and P. Zoller, *Quantum Noise: A Handbook of Markovian and Non-Markovian Quantum Stochastic Methods with Applications to Quantum Optics*. (Springer-Verlag Berlin Heidelberg)
- [75] C. Navarrete-Benlloch, E. Roldán, Y. Chang, and T. Shi, Optics express **22**, 24010 (2014).
- [76] G. Moore and N. Read, Nucl. Phys. B **360**, 362 (1991).
- [77] A. L. Cavalieri *et al.*, Nature (London) **449**, 1029 (2007).
- [78] L. Perfetti *et al.*, Phys. Rev. Lett. **99**, 197001 (2007).
- [79] J. Okamoto, A. Cavalleri, and L. Mathey, Phys. Rev. Lett. **117**, 227001 (2016).
- [80] R. Hoppner, B. Zhu, T. Rexin, A. Cavalleri, and L. Mathey, Phys. Rev. B **91**, 104507 (2015).
- [81] M. Knap, M. Babadi, G. Refael, I. Martin, and E. Demler, Phys. Rev. B **94**, 214504 (2016).

- [82] M. Babadi, M. Knap, I. Martin, G. Refael, E. Demler, arXiv:1702.02531.
- [83] M. A. Sentef, A. F. Kemper, A. Georges, and C. Kollath, Phys. Rev. B **93**, 144506 (2016).
- [84] E. A. Yuzbashyan, O. Tsypliyatyev, and B. L. Altshuler, Phys. Rev. Lett. **96**, 097005 (2006).
- [85] J. M. Tranquada, J. D. Axe, N. Ichikawa, A. R. Moodenbaugh, Y. Nakamura, and S. Uchida, Phys. Rev. Lett. **78**, 338 (1997).
- [86] E. Fradkin, S. A. Kivelson, and J. M. Tranquada, Rev. Mod. Phys. **87**, 457 (2015).
- [87] A. J. Leggett, Rev. Mod. Phys. **47**, 331 (1975).
- [88] J. G. Bednorz and K. A. Müller, Z. Phys. B. **64**, 189 (1986).
- [89] P. W. Anderson, Science **235**, 1196 (1987).
- [90] F. C. Zhang and T. M. Rice, Phys. Rev. B **37**, 3759R (1988).
- [91] W. C. Lee, S. C. Zhang, and C. Wu, Phys. Rev. Lett. **102**, 217002 (2009).
- [92] D. Pekker, M. Babadi, R. Sensarma, N. Zinner, L. Pollet, M. W. Zwierlein, and E. Demler, Phys. Rev. Lett. **106**, 050402 (2011).
- [93] D. H. Torchinsky, G. F. Chen, J. L. Luo, N. L. Wang, N. Gedik, Phys. Rev. Lett. **105**, 027005 (2010).
- [94] F. Marsiglio, A. E. Ruckenstein, S. Schmitt-Rink, and C. M. Varma, Phys. Rev. B **43**, 10882 (1991).
- [95] Z. Liu and E. Manousakis, Phys. Rev. B **45**, 2425 (1992).
- [96] A. Damascelli *et al.*, Rev. Mod. Phys. **75**, 473 (2003).
- [97] W. S. Lee *et al.*, J. Phys.: Condens. Matter **21**, 164217 (2009).
- [98] S. Lederer, Y. Schattner, E. Berg, and S. A. Kivelson, Phys. Rev. Lett. **114**, 097001 (2015).
- [99] H. J. Rothe, *Lattice Gauge Theories: An Introduction* (World Scientific Lecture Notes in Physics, 4th Edition).
- [100] J. Kogut and L. Susskind, Phys. Rev. D **11**, 395 (1975).
- [101] S. Diehl, A. Micheli, A. Kantian, B. Kraus, H. P. Büchler, and P. Zoller, Nat. Phys. **4**, 878 (2008).
- [102] E. M. Kessler, G. Giedke, A. Imamoglu, S. F. Yelin, M. D. Lukin, and J. I. Cirac, Phys. Rev. A **86**, 012116 (2012).